The Role of Vitamin D Receptor in Osteoblasts and Bone Mineralisation

Nga Ngoc Lam

University of Adelaide

Faculty of Health Science

School of Medical Sciences

Supervisors: Dr Peter O'Loughlin and Dr Paul Anderson

Musculoskeletal Biology Research Laboratory

SA Pathology, Adelaide

A thesis submitted for the degree of

Doctor of Philosophy to

The University of Adelaide

December 2012

TABLE OF CONTENTS

ABSTRACT

Age-related bone loss is associated with a change in bone remodelling characterised by decreased bone formation relative to bone resorption. It is well described that age-related bone loss is accelerated as a consequence of vitamin D deficiency, a process which can be replicated in rodent studies. While vitamin D has been shown to play important roles for adequate bone mineralisation and the prevention of osteoporosis, the exact mechanisms remain controversial. It is clear that vitamin D is necessary for the stimulation of intestinal calcium and phosphate absorption, maintenance of calcium homeostasis and supply of calcium and phosphate for bone mineralisation. However, vitamin D has also been shown to directly act on bone cells to promote mineralisation as well as regulate bone resorption. The question of the essential nature of the *in vivo* role for the direct actions of vitamin D on bone has proven to be difficult to resolve. The only published mouse model which addresses the direct actions of vitamin D in osteoblasts is the osteoblast-specific vitamin D receptor transgenic mouse, or OSVDR mouse. Using this transgenic mouse model, it has been reported that the enhanced vitamin D activity in osteoblasts promotes bone formation and mediates reduction in bone resorption most likely through reduced RANKL signalling of osteoclastogenesis. The reported overall bone phenotype of the OSVDR was increased vertebral trabecular bone as well as increased cortical bone volume leading to increased bone strength. In contrast to the findings in OSVDR mice, global VDR knockout mice can mineralise osteoid in the presence of high levels of dietary calcium and phosphate, therefore many have concluded that the role for direct vitamin D activity in bone cells is redundant. This view however, does not take into account the fact that vitamin D activity in bone cells may play a permissive role to optimise bone health by modulating mineralisation and bone resorption.

Thus, the studies conducted in this thesis are aimed to further address the role of osteoblastic VDR in bone remodelling and bone architecture. Specifically, these studies aimed to further

establish the phenotype of the OSVDR mouse model utilising 3D micro-CT analyses as well as establish the role of vitamin D activity in osteoblasts during vitamin D deficiency and dietary calcium depletion. The effects of these physiological interventions on OSVDR mice are described in terms of bone structure, cellular activities, biochemical parameters, and gene expression profiles of bone and other organs involved in calcium and phosphate homeostasis. The overall hypothesis is that VDR activity in mature osteoblast lineage is important to regulate processes of bone remodelling and maintenance of an optimal skeletal structure.

The data presented within these chapters showed that the phenotype of increased bone mineral volume is present in more regions of bone, which was not previously recognised. Furthermore, during vitamin D deficiency, while bone loss occurs in wild-type mice, OSVDR mice maintain both cortical and trabecular bone volume, indicating that bone loss due to vitamin D deficiency is due, at least in part, to reduced vitamin D activity in osteoblasts. In contrast to vitamin D deficiency, the effects of low calcium stress in OSVDR mice results in bone loss comparable to wild-type mice, which is likely to be due to a disruption of bone remodelling, since we observed lowered osteoblast, osteoclast and osteocytes activities. Intriguingly, low calcium fed OSVDR mice demonstrate a marked increase in serum fibroblast growth factor 23 (FGF23) levels, resulting in suppressed renal 1,25-dihydroxyvitamin D (1,25D) synthesis, and reduced expression of intestinal calcium absorption genes. Thus, the inappropriately low 1,25D-mediated intestinal calcium absorption in OSVDR mice, fed low calcium, may further contribute to the reduction in bone mineralisation and bone volume. These data suggest that in addition to the reported direct action of vitamin D activity in osteoblasts to regulate bone turnover, VDR-mediated activity in osteoblast also plays a role in the endocrine feed-back mechanism of renal 1,25D synthesis, which may contribute to the maintenance of bone mineral and the resulting bone phenotype.

In summary, the findings from this thesis implicate the essential role of vitamin D and VDR in osteoblasts either directly or indirectly impacts on bone homeostasis, including osteoclast

activity, osteoblast differentiation, osteocyte activity, bone FGF23 production and renal feed-back signalling.

DECLARATION

"This work contains no material which has been accepted for the award of any other degree or diploma in any university or other tertiary institution to **Nga Ngoc Lam** and, to the best of my knowledge and belief, contains no material previously published or written by another person, except where due reference has been made in the text"

"I give consent to this copy of my thesis when deposited in the University Library, being made available for loan and photocopying, subject to the provisions of the Copyright Act 1968."

"The author acknowledges that copyright of the published work contained within this thesis (as listed in the – Publications arising from this thesis) resides with the copyright holder(s) of those works."

"I also give permission for the digital version of my thesis to be made available on the web, via the University's digital research repository, the Library catalogue, the Australian Digital Theses Program (ADTP) and also through web search engines, unless permission has been granted by the University to restrict access for a period of time."

Nga Ngoc Lam

ACKNOWLEDGMENTS

Dr Paul Anderson

Thanks to my supervisor, Dr Paul Anderson who has provided me with support, enthusiasm and encouragement throughout my PhD study. It was a privileged to work in your laboratory and I have very much enjoyed the research project. Thank you for your advice, knowledge, guidance and reassurance, all of which have been invaluable.

*

Dr Peter O'Loughlin

Thanks to Dr Peter O'Loughlin for being my supervisor. I truly appreciate all your advice and help with my PhD project and the thesis.

*

Prof Howard Morris

Thank you for your enthusiasm, encouragement and invaluable intellectual advice and guidance throughout my studies and to the preparation of this thesis.

*

SA Pathology (IMVS)

To all the members of the Musculoskeletal Biology Research group, I offer sincere thanks for your advice and assistance, support and friendship throughout my PhD journey.

*

Garvan Institute

Thankyou to Dr Paul Baldock and Prof Edith Gardiner for providing the OSVDR transgenic mouse model

*

Family and friends

I would like to express everlasting gratitude to my family and friends. My parents Hoan and Oanh who have raised me into the person I am today, who have always offered encouragement, advice and unconditional love. Thanks to my sisters and brother, Tien, Hao

and Tra who have always been there for support and love. Thank you to my wonderful partner, Thien for all your patience, understanding, support and love throughout the years and for helping me fulfil my dreams and pursue happiness. I love you all.

INTERNATIONAL AND NATIONAL SCIENTIFIC MEETINGS AND AWARDS ARISING FROM WORK PRESENTED IN THIS THESIS

PRESENTATIONS

International

Oral: **Lam NN**, Sawyer RK, Anderson SR, Morris HA, O'Loughlin PD, Anderson PH. Skeletal effects of increased osteoblastic VDR during calcium-deprivation in a mouse model. **American Society for Bone and Mineral Research, Toronto, Canada, 2010**

Poster: **Lam NN**, Sawyer RK, Anderson SR, Morris HA, O'Loughlin PD, Anderson PH. Osteoblast-specific VDR over-expression protects against bone loss due to vitamin D-deficiency. **International Bone & Mineral Society combined with Australian & New Zealand Bone and Mineral Society conference, Sydney, Australia, 2009**

National

Oral: **Lam NN**, Sawyer RK, Anderson SR, Morris HA, O'Loughlin PD, Anderson PH. Increased bone VDR during low dietary calcium mediates renal negative feedback and impairs osteoclast and osteoblast activities in a mouse model. **Australian Health and Medical Research Congress, Melbourne, 2010**

Poster: **Lam NN**, Sawyer RK, Anderson SR, Morris HA, O'Loughlin PD, Anderson PH. Skeletal effect of increased osteoblastic VDR during calcium-deprivation in a mouse model. **Australian & New Zealand Bone and Mineral Society Conference, Adelaide, 2010**

Poster: **Lam NN**, Sawyer RK, Anderson SR, Morris HA, O'Loughlin PD, Anderson PH. Skeletal effect of increased osteoblastic VDR during calcium-deprivation in a mouse model. **6th Clare Valley Bone Meeting, McLaren Vale, 2010**

Poster: **Lam NN**, Sawyer RK, Anderson SR, Morris HA, O'Loughlin PD, Anderson PH. Osteoblast-specific VDR over-expression protects against bone loss due to vitamin D-deficiency. Australian Society for Medical Research Conference, Adelaide, 2009

Poster: **Lam NN**, Sawyer RK, Anderson SR, Morris HA, O'Loughlin PD, Anderson PH. The study of osteoblastic VDR in a mouse model. **Australian & New Zealand Bone and Medical Society Conference, Melbourne, 2008**

AWARDS

- **American Society for Bone and Mineral Research: *Young Investigator Travel Award*, 2010**
- **Molecular and Experimental Pathology Society of Australasia: *Travel Award*, 2010**
- **Australian Society for Medical Research: *Best Poster Award in Healthy Aging*, 2009**
- **Australian & New Zealand Bone and Medical Society: *Travel Awards*, 2008 and 2009**
- **Department of Physiology, University of Adelaide. *Travel awards*, 2008-2010.**

Chapter 1

LITERATURE REVIEW: VITAMIN D RECEPTOR AND BONE HOMEOSTASIS

1.1 INTRODUCTION

The maintenance of an adequate vitamin D status throughout life is essential to prevent the bone mineralising defect causing rickets in children and osteomalacia in adults, as well as osteoporosis and for fracture prevention in the elderly (Bischoff-Ferrari, et al., 2005; Chapuy, et al., 1992; Tang, et al., 2007). While the most widely accepted actions of the active vitamin D hormone, 1α,25-dihydroxyvitamin D3 (1,25D) via the vitamin D receptor (VDR) in the maintenance of healthy bone are their abilities to stimulate intestinal calcium and phosphate absorption, there is now substantial evidence to indicate that during metabolism of healthy, mineralised bones, 1,25D and VDR also play direct roles in regulating the activity of bone cells (Anderson, et al., 2007; Atkins, et al., 2003; Gardiner, et al., 2000; Matsumoto, et al., 1991; Owen, et al., 1991; Rickard, et al., 1995; van Driel, et al., 2006; van Driel, et al., 2004; van Leeuwen, et al., 2001). The fact that the osteomalacic bone phenotype observed in the vitamin D receptor knockout (VDRKO) mouse can be prevented by feeding a “rescue” diet containing high levels of calcium and phosphorus have led some to conclude that VDR-mediated activity in bone is redundant (Amling, et al., 1999; Erben, et al., 2002; Li, et al., 1998). However, it has been shown that while osteomalacia was prevented in the young VDRKO mice, the rescue diet did not entirely correct the bone microstructure and there were continuing bone volume deficiencies and growth defects in adult VDRKO animals (Panda, et al., 2004). Furthermore, the over-expression of osteoblast-specific VDR in a transgenic mouse (OSVDR) exhibits a high bone mass phenotype due to both increased bone formation and reduced bone resorption. While the molecular mechanisms for the role of VDR in osteoblasts are not entirely clear, it appears that the direct activity of vitamin D in osteoblasts plays a role in regulating bone remodelling. Thus, the main hypothesis of this thesis is that the direct activities of vitamin D in cells of the osteoblast lineage mediate bone formation and resorption for maintenance of a healthy skeletal structure. With the exception of the osteoblast-specific VDR transgenic (OSVDR) mouse, there is little data which describe the

bone cell-specific actions of vitamin D in an *in vivo* setting (Baldock, et al., 2006; Gardiner, et al., 2000). Thus, using the OSVDR transgenic mouse model, this thesis aims to address the mechanisms by which vitamin D, acting via the VDR in cells of the osteoblast lineage, regulates bone remodelling and bone architecture in response to physiological challenges such as vitamin D depletion and low dietary calcium. Establishing a direct role for vitamin D in the bone is important to clarify the significance of maintaining an adequate circulating vitamin D status for the prevention of bone loss.

1.2 BONE BIOLOGY

1.2.1 Function and composition of bone

Bone is a specialised and mineralised form of connective tissue. The main functions of bones are to serve as structural support, sites of muscle attachment for movement, protection of vital organs and the bone marrow, as well as functioning as a reservoir of calcium and phosphate for the maintenance of serum calcium and phosphate homeostasis. The majority (65%) of bone is made up of matrix, in which type 1 collagen accounts for approximately 90%, and (35%) hydroxyapatite mineral [$Ca_{10}(PO4)_6(OH)_2$]. Crystals of hydroxyapatite are formed on collagen fibres which make up the bone matrix. It is this association of hydroxyapatite with collagen fibres which is responsible for the hardness of bone, reviewed by (Downey and Siegel, 2006) and (Rey, et al., 2009).

There are two histological types of bones that can be identified by the pattern of collagen fibres and bone mineral, namely lamellar and woven bone. Lamellar or mature bone has a regular alignment of collagen, allowing the highest density of collagen per unit volume to be assembled with mineral and thus provide optimal bone strength. Lamellar bone can be arranged in parallel alignment if deposited along a flat surface (e.g. trabecular bone) or concentric if deposited on a surface surrounding a blood vessel (e.g. osteon in cortical bone). Woven bone or immature bone is characterised by irregular bundles of collagen fibres which are not as tightly packed rendering it mechanically weak. Woven bone is formed during rapid

bone formation or development, fracture healing and in some bone diseases. Woven bone however is progressively replaced by lamellar bone during the bone remodelling process (Buckwalter, et al., 1996).

1.2.2 Skeletogenesis

There are two distinct types of skeletogenesis of bone, intra-membranous ossification and endochondrial ossification, giving rise to flat bones (e.g. calvaria and scapula) and long bones (e.g. tibia and femora) respectively. The main difference between intra-membranous and endochondrial ossification is the involvement of the cartilaginous model in the latter. In intra-membranous ossification the bone is developed from a condensation of mesenchymal tissue to form an ossification centre. Mesenchymal cells differentiate directly into osteoblasts to synthesise osteoid and then undergoes calcification (Abzhanov, et al., 2007). In endochondrial ossification, the primary ossification centre is in the middle of the long bone and produces chondrocytes, which then undergoes hypertrophy and the cartilage matrix undergoes calcification. The chondrocytes are then invaded by primitive mesenchymal cells and blood vessels to differentiate into osteoblasts and bone marrow cells, recently reviewed by Marino (2011) and Karsenty, et al. (2009).

1.2.3 Structure of bone

The overall bone structure, in particular of long bones, is made up of cortical and trabecular bone, which can consist of either woven or lamellar bone, and although both are made up of the same cells and matrix elements, they are structurally and functionally different.

1.2.3.1 Cortical (compact) bone

Cortical bone forms approximately 80% of the mature skeleton and surrounds the marrow cavity and the trabecular plates. In long bones, cortical bone makes up the thick cortical wall of the diaphysis region, which becomes thinner and increases in diameter as they form the

metaphysis region (Cowin, 1990). Structurally, 80-90% of the cortical bone volume is calcified and therefore of a very low porosity, which ultimately results in cortical bone having a significant resistance to torsional and bending forces (compressive strength) (Currey, 2003; Winwood, et al., 2006). The cortical bone thus provides the mechanical and protective functions of bone. Detailed analysis of the cortical bone properties showed cylindrical units of mineralised matrix called osteons or Haversian systems. In the centre of each osteon is the Haversian canal, containing blood vessels, nerves and loose connective tissues (Buckwalter, et al., 1996). Surrounding each canal is concentric lamellae bone with osteocytes arranged in parallel with the lamellae bone structure. These are interconnected by osteocyte processes, which are important for nutrient and waste exchange between the osteocytes and the blood vessels (Klein-Nulend, et al., 2003).

1.2.3.2 Trabecular (cancellous/spongy) bone

Trabecular bone consists of thin, irregularly shaped plates called trabeculae, arranged in a latticework network. Unlike the structure of cortical bone, trabecular bone is highly porous (50-90%), thus providing greater resilience and shock absorption, such as in the metaphyseal and epiphyseal region of long bones (Kuhn, et al., 1990). Trabecular bone has a much greater surface area to volume ratio and thus more cells lining the trabecular bone surface and within the bones are able to be directly influenced by the adjacent bone marrow cells, which may account for the high metabolic rate of trabecular bone and the faster response to hormonal regulators as well as mechanical loading and unloading of bone (Marwan, et al., 2009). Trabecular bone, like cortical bone, contain osteocytes within the mineralised bone. Since trabecular structure are considerably thinner than cortical bone (Lozupone, 1985), each osteocyte is capable of exchanging nutrients with nearby blood vessels and thus no central canal is necessary such is found within osteons of human bone.

1.2.3.3 Surfaces of bone

The outer surface of bone or periosteum, is a thin vascularised membrane-like layer consisting of an outer fibrous layer of collagen fibres and fibroblasts, and an inner cambium layer composed of osteoprogenitor cells with the capacity to proliferate and differentiate into osteoblasts (Allen, et al., 2004; Orwoll, 2003). The internal surfaces of bone cortex, or endosteum, is composed of osteoprogenitor cells and a very small amount of connective tissue (Gong, 1978). The periosteum and endosteum provide a source of osteoprogenitor cells for repair and growth of bone (Arai, et al., 2009; Orwoll, 2003).

1.2.4 Cellular composition and activity in bone

Bone is a dynamic and metabolically active tissue containing a variety of specialised cells which either line the bone surfaces or are embedded within the bone mineral. Three of the most characterised bone cell types which contribute to bone remodelling are osteoblasts, osteoclasts and osteocytes.

1.2.4.1 The Osteoblast

Osteoblasts are specialised bone-forming cells that can produce bone matrix proteins and mediate bone mineralisation, as well as regulate other bone cell activities.

1.2.4.1.1 Osteoblast origin and differentiation

Osteoblast precursor cells originate from pluripotent mesenchymal stem cells which, given the right regulatory signals, undergo proliferation and differentiation into osteoblasts rather than adipocytes, myocytes or chondrocytes (Aubin, 1998; Jensen, et al., 2010). For instance, osteoblast differentiation requires the presence of the transcription factor RUNX2 (runt-related transcription factor 2 or also known as CBFA1 (core-binding factor A1)) (Ducy, et al., 1997). Runx2-knockout mice have complete failure of osteoblast maturation, which resulted

in a cartilaginous skeleton and completely lack of mineralised bone tissue (Komori, et al., 1997; Otto, et al., 1997). As the osteoblasts mature, they express high levels of alkaline phosphatase and osteocalcin, which are markers for bone mineralisation (Barragan-Adjemian, et al., 2006; Liu, et al., 1997). Towards the end of the matrix secreting period, through unknown mechanism, approximately 15% of the mature osteoblasts become entombed in the new bone matrix and mineral, and further differentiate into osteocytes. The remaining osteoblasts either reside on the bone surface as lining cells or undergo apoptosis (Jilka, et al., 1998).

1.2.4.1.2 Osteoblast structure

When osteoblasts mature, they form junctions with adjacent osteoblasts cells and conform to a cuboidal shape. Each osteoblast contains large quantities of rough endoplasmic reticula (RER), mitochondria and Golgi apparatus (Holtrop, 1975), reflecting their capacity for protein synthesis. Other microscopic components found within osteoblasts include microtubules, microfilaments, lysosomes, glycogen, and lipids (Holtrop, 1975).

1.2.4.1.3 Osteoblast function

Osteoblasts do not operate in isolation and are found in clusters of cells forming a monolayer lining the surface of bone. Osteoblasts attach to the bone surface with adhesion molecules including integrins (Doty, 1981; Jekir and Donahue, 2009). Active osteoblasts synthesise and secrete collagenous and non-collagenous bone matrix proteins, including high levels of the type 1 collagen, alkaline phosphase and osteocalcin, which are responsible for bone matrix formation as well as initiation for bone mineralisation (Harada and Rodan, 2003).

Central to osteoblastic function is the regulation of osteoclastogenesis (Asagiri and Takayanagi, 2007; Boyle, et al., 2003). Osteoblasts can secrete cytokines that are essential to the regulation of osteoclast formation and differentiation, including macrophage colony-stimulating factor (M-CSF), receptor activator of nuclear factor (NF)-κB ligand (RANKL)

and Osteoprotegerin (OPG). M-CSF is required for inducing the commitment of monocytes to the osteoclast lineage (Wiktor-Jedrzejczak, et al., 1990). Similarly RANKL promotes the differentiation and activity of osteoclasts via RANK receptor expressed on monocytes (Kong, et al., 1999). OPG is the decoy receptor for RANKL, preventing RANK-RANKL interaction, moderating osteoclastogenesis (Simonet, et al., 1997). Moreover, osteoblasts can produce a range of growth factors, including the insulin-like growth factors (IGFs), platelet-derived growth factors (PDGFs), basic fibroblast growth factor (bFGF) and transforming growth factor-β (TGFβ). Although the precise mechanisms for these factors in bone homeostasis are to be established, osteoblasts are also found to express receptors for these factors and thus could play a roles in regulating osteoblast activity in an autocrine or paracrine manner (Canalis, 2009). Furthermore, a range of endocrine receptors are found to be expressed on osteoblasts, including receptors for parathyroid hormone (PTH), growth hormone, insulin and progesterone, as well as receptors for nuclear steroid hormone, including estrogens, androgens and vitamin D receptor (Harada and Rodan, 2003; Martin, et al., 2006).

NOTE:
This figure/table/image has been removed to comply with copyright regulations.
It is included in the print copy of the thesis held by the University of Adelaide Library.

Figure 1.1: A schematic diagram of the osteoblastogenesis. Osteoblasts originate from pluripotent mesenchymal stem cells (MSC). With signalling from factors including Wnt10b and BMPs, cells differentiate to osteo/chondro-progenitor cells rather than adipocytes, expressing key genes such as Runx2. Osteoprogenitor cells continue to differentiate to preosteoblasts expressing genes such as Alp and Col1a1. The active matrix producing and mineralising osteoblast then acquire the expression of genes such as Opn and Ocn. Adapted from Andrea and colleges (Andrea, et al., 2012.), Frontiers in Bioscience, E4:2302-2321.

1.2.4.2 The osteoclast

Mature osteoclasts are giant, multinucleated mobile bone-resorbing cells that can secrete a wide range of enzymes and factors able to dissolve the bone minerals and matrix proteins.

1.2.4.2.1 Osteoclast origin and differentiation

Osteoclasts are derived from mononuclear hematopoietic precursor cells which can also give rise to macrophages and dendritic cells (Suda, et al., 1992). Osteoclast differentiation is dependent on two important cytokines, M-CSF and RANKL. M-CSF is essential to engage the cells in the monocyte lineage to become osteoclast precursors and ensure their survival and proliferation, as well as the expression of the RANK receptor (Wiktor-Jedrzejczak, et al., 1990). RANKL acting on the RANK receptor is essential for further progression of osteoclastic differentiation and fusion of mononuclear osteoclasts to form the multinucleated osteoclast (Kong, et al., 1999; Suda, et al., 1999). RANK signalling activates downstream signalling molecules, including TNF receptor-associated factor 6 (TRAF6), nuclear factor (NF)-κB ,c-Fos and nuclear factor of activated T cells c1 (NFATc1), which are all required for proper osteoclastogenesis (Zhao, et al., 2007). In contrast, osteoclast differentiation is inhibited by the osteoprotegerin (OPG) protein, a TNF receptor family member (Simonet, et al., 1997). OPG binds to RANKL preventing the binding of RANKL to its receptor RANK which is required for osteoclastogenesis (Hofbauer, et al., 2004). Notably, recent evidence has implicated the important role of the transcription factor NFATc1 as a key regulator for osteoclastogenesis. NFATc1 in cooperation with other transcription factors regulates osteoclast adhesion, migration, acidification and degradation of inorganic and organic bone matrix genes, including β3 integrin, cathepsin K, tartrate resistance acid phosphatase (TRAP) and calcitonin receptor (Takayanagi, 2007; Zhao, et al., 2010) .

1.2.4.2.2 Osteoclast structure

Osteoclast can be up to 100µm in diameter and contain up to 20 nuclei. It is usually found in contact with the calcified bone surface. It is possible to find up to five osteoclasts in the same resorptive site. Osteoclasts nuclei shape and size can vary within the same cells, reflecting the asynchronous fusion of mononuclear precursors (Holtrop, 1975). Osteoclasts contain many Golgi complexes around each nucleus, mitochondria, and extensive transport vesicles loaded with lysosomal enzymes, such as TRAP and cathepsin K, reflecting the capacity of osteoclasts to dissolve the bone mineral and matrix proteins (Halleen, et al., 1999). The most prominent features of the osteoclasts are the deep foldings of the plasma membrane (ruffled border) in the area facing the bone matrix and the specific membrane surrounding the zone of attachment (sealing zone) (Holtrop, 1975). At the sealing zone, attachment of the osteoclast to the matrix is performed via integrin receptors, which bind specifically to the Arginine-Glycine-Aspartate (termed RGD) sequences found in matrix proteins (Helfrich, et al., 1996). The ruffled border membrane is formed by fusion of intracellular acidic vesicles with the region of cell membrane facing the bone, where the intracellular vesicle membrane is transferred to the cell membrane and forms the finger-like projections of the ruffled border (Halleen, et al., 1999). The characteristics of the ruffled border resemble that of late endosomal membranes, providing optimal pH for lysosomal enzyme activity and bone resorption (Vaananen, et al., 1990).

1.2.4.2.3 Osteoclast function

The main function of osteoclasts is to degrade the mineralised bone matrix, which involves the dissolution of hydroxylapatite crystals and proteolytic cleavage of the collagen matrix. Dissolution of mineral occurs by acidification via targeted secretion of HCl and protons through the ruffled border into the resorption lacuna (space between the ruffled border and bone matrix) (Vaananen, et al., 1990). After dissolution of mineral, proteolytic enzymes are produce to degrade the organic bone matrix, including matrix metalloproteinases (MMPs)

(Tezuka, et al., 1994), cathepsin K (Drake, et al., 1996) and TRAP, which is a widely used osteoclast marker that can generate highly destructive reactive oxygen species able to destroy collagen (Halleen, et al., 1999). The degradation products are removed from the resorption lacuna through a transcytotic vesicular pathway which can either internalise, or transport the products across the cell and release to the extracellular space (Salo, et al., 1997). After the osteoclasts complete a resorptive cycle, they undergo cell apoptosis or become inactive osteoclasts (Vaananen and Laitala-Leinonen, 2008).

NOTE:
This figure/table/image has been removed to comply with copyright regulations.
It is included in the print copy of the thesis held by the University of Adelaide Library.

Figure 1.2: A schematic diagram of the process of osteoclastogenesis. Osteoclasts originate from mononuclear hematopoietic precursor cells. Osteoclast differentiation and fusion of mononuclear osteoclasts to form the multinucleated active osteoclast is dependent on the cytokines, M-CSF and RANKL. Signalling molecules, including TNF receptor-associated factor 6 (TRAF6), nuclear factor (NF)-κB ,c-Fos and nuclear factor of activated T cells c1 (NFATc1) are all key factors for osteoclastogenesis. Adapted from Henriksen and colleges (Henriksen, et al., 2011), Endocrine Reviews, 32:31-63.

1.2.4.3 The Osteocyte

Osteocytes represent approximately 90-95% of cells within the adult bone and have numerous functions, including mechanosensation, bone matrix mineralisation and hormone producing cell involved in feedback mechanism of phosphate homeostasis.

1.2.4.3.1 Osteocyte origin and maturation

Osteocytes originate from mesenchymal stem cells through osteoblast differentiation. Although the exact signalling and molecular mechanism(s) of how and why an osteoblast becomes an osteocyte (osteocytogenesis) is not yet understood, there exist a number of theories explaining this process. It was suggested that osteocytogenesis is a passive process where the osteoblast becomes trapped when its neighbour osteoblasts place osteoid on top of the embedding cell (Franz-Odendaal, et al., 2006). Others however have shown osteocytogenesis to be an active invasive process requiring cleavage of collagen matrix and regulation of mineralisation by the newly formed osteocytes (Barragan-Adjemian, et al., 2006; Holmbeck, et al., 2005). By unknown mechanisms, some designated osteoblasts form dendritic projections and become osteiod osteocytes, recently reviewed by (Dallas and Bonewald, 2010). These dendritic projections extend toward the mineralising front and into the vascular space and bone matrix, while keeping in contact with cells that were already embedded and cells on the bone surface. These osteoid osteocytes have been shown to express metalloproteinase (MT1-MMP) that can cleave collagen, fibrin, fibronectin and other matrix molecules (Holmbeck, et al., 2005). Embedding osteoid osteocytes also express high levels of E11/gp38 protein (or E11), also called podoplanin (Schulze, et al., 1999; Wetterwald, et al., 1996). E11 is an early osteiod osteocyte marker and is essential for dendritic formation, where knock-down using siRNA in osteocyte-like MLO-Y4 cells significantly reduced the number and length of dendritic processes and reduced response to fluid flow shear stress (Zhang, et al., 2006). These osteoid osteocytes have also been shown to initiate and regulate

mineralisation surrounding their dendritic projections as the cells are extending and transitioning into a mature osteocyte phenotype (Barragan-Adjemian, et al., 2006).

1.2.4.3.2 Osteocyte structure

Osteocytes reside within fluid-filled cavities called lacunae and possess long dendrite-like projections passing through the bone in tunnels with a diameter of 100 to 300 nm called canaliculi. These dendrite-like processes interact with other adjacent osteocytes within mineralised bone and also interact with cells on the bone surface and marrow. These connecting networks are extremely important for osteocyte responses to mechanical load, cellular communication as well as nutrition and waste exchange within the mineralised matrix (as reviewed in Bonewald, 2011).

1.2.4.3.3 Osteocyte function

Mechanical loading is essential for bone health and reduced loading can lead to bone loss, whereas increased mechanical loading can maintain or even increase bone volume (Burr, et al., 2002; Robling, et al., 2002). Osteocytes have been well recognised as the mechanical transducer cells (Bonewald, 2006; Santos, et al., 2009). Targeted deletion of osteocytes in mice results in bone loss and these mice are resistant to unloading-induced bone loss, implicating the important role of the osteocyte in mechano-transduction to regulate bone resorption (Tatsumi, et al., 2007). However, the precise mechanisms by which osteocytes sense the mechanical forces applied to the bone and transform these mechanical stimuli into biochemical signals, remains to be established. Evidence exists to indicate that osteocytes may sense the loading forces via the fluid shear stress that occurs along their dendritic processes and/or the cell body (Weinbaum, et al., 1994; Westbroek, et al., 2000). It has also been proposed that cilia may play a role in osteocyte mechanosensation (Xiao, et al., 2006; Xiao and Quarles, 2010). Nevertheless upon sensing the mechanical strains, osteocytes rapidly upregulate a variety of genes such as 6-phosphate dehydrogenase, a marker of cell

metabolism (Skerry, et al., 1989), c-Fos, TGF-β and IGF-1 (Raab-Cullen, et al., 1994; Santos, et al., 2009) for cellular growth and development. Additionally, osteocyte-specific markers, such as E11 (Zhang, et al., 2006) and dentin matrix protein 1 (DMP1) (Gluhak-Heinrich, et al., 2003), as well anabolic signals such as nitric oxide (NO), prostaglandins, and other small molecules such as ATP are also up-regulated during mechanical loading (Bakker, et al., 2002; Santos, et al., 2009). Another anabolic pathway in osteocytes that is involved in the response to mechanical loading is the canonical Wnt/β-catenin pathway and the Wnt co-receptor, LRP5. Mice with mutation of the Wnt co-receptor, LRP5 do not respond to mechanical load and have low bone mass (Sawakami, et al., 2006).

Osteocytes have also been shown to possess endocrine and paracrine activities by producing a range of factors important for bone matrix mineralisation and mineral homeostasis. One of these factors is sclerostin, which is a product of the *SOST* gene. Sclerostin, produced predominantly by mature osteocytes, is an inhibitor of osteoblast activity and bone formation (Kusu, et al., 2003; Poole, et al., 2005). Sclerostin inhibits the Wnt signalling pathway to reduce bone formation (Li, et al., 2005; Ott, 2005). *SOST* mutation in humans (Balemans, et al., 2002) and mouse deletion of the *SOST* gene lead to high bone mass (Li, et al., 2008). Mechanical loading has been shown to decrease sclerostin expression (Robling, et al., 2008), whereas unloading resulted in increased sclerostin levels (Lin, et al., 2009; Robling, et al., 2008). Osteocytes are also important for the regulation of blood phosphate homeostasis and bone mineralisation through their production of DMP1 (Feng, et al., 2006; Yang, et al., 2005), matrix extracellular phosphoglycoprotein (MEPE) (Gowen, et al., 2003; Nampei, et al., 2004), phosphate regulating gene with homologies to endopeptidases on the X chromosome (PHEX) (Thompson, et al., 2002) and fibroblast growth factor 23 (FGF23) (Liu, et al., 2006; Shimada, et al., 2004). Mutation of DMP1 (or PHEX) results in hypophosphatemic rickets, which is associated with increase circulating FGF23 level (Feng, et al., 2006; Liu, et al., 2006). DMP1 has been shown to have a nuclear localization sequence (Narayanan, et al., 2003), suggesting possible transcriptional role of DMP1. Furthermore, recombinant DMP1 is able to initiate

hydroxyapatite nucleation (He, et al., 2003), suggesting DMP1 could function to regulate mineralisation of osteoid. MEPE, a member of the SIBLING protein family, can be cleaved by cathepsin B to release a carboxy-terminal MEPE peptide (ASARM peptide) and the phosphorylated ASARM peptide have been shown to inhibit mineralization *in vivo* and *in vitro* (Rowe, et al., 2004; Boskey, et al., 2010), indicating another mechanism in which osteocytes are able to regulate mineralisation. FGF23 acts at the kidney both as a phosphaturic hormone (Shimada, et al., 2004) and regulator of the synthesis of 1,25D (Liu, et al., 2006; Shimada, et al., 2004). Excess FGF23 causes hypophosphatemia via inhibition of renal sodium phosphate co-transporter 2 (NaPi2a and NaPi2c) and suppresses 1,25D via inhibition of 25-hydroxyvitamin D-1α-hydroxylase (CYP27B1) and stimulation of 24-hydroxylase (CYP24) (Liu and Quarles, 2007; Shimada, et al., 2005) as is described in Section 1.3.2.2 in more detail below. In contrast, FGF23 deficiency (Bai, et al., 2003; Liu, et al., 2006; Shimada, et al., 2004) or mutations increasing FGF23 degradation (Larsson, et al., 2005) results in hyperphosphatemia, increased serum 1,25D levels, and can lead to soft tissue calcification. These findings indicate that osteocytes produce key factors which either act locally or act as endocrine regulators, targeting other tissue such as the kidney, to regulate mineral homeostasis, possibly as a feed-back mechanism.

NOTE:
This figure/table/image has been removed to comply with copyright regulations.
It is included in the print copy of the thesis held by the University of Adelaide Library.

Figure 1.3: A schematic diagram showing osteocyte differentiation and the molecules involved. Approximately 15% of osteoblasts are entrapped in the bone matrix, produced by osteoblasts, and differentiate to osteoid osteocytes before becoming a mineralising and mature osteocyte. Key genes such as PHEX, MEPE, DMP1, are expressed during osteocyte differentiation and sclerostin (Sost) and FGF23 are expressed primarly in mature osteocytes. Adapted from Bonewald (Bonewald, 2011), JBMR, 26:229-238.

1.2.5 Bone modelling and remodelling

Bone modelling (during growth) and bone remodelling (during homeostasis and repair) are required for the development and maintenance of skeletal health by optimising bone strength and minimising bone mass, serving the requirement for load tolerance and lightness for mobility.

1.2.5.1 Bone modelling

Bone modelling occurs mainly during growth and requires the processes of bone formation and bone resorption, and while globally coordinated, bone formation and resorption can occur independently at distinct anatomical locations. For instance, bone formation occurs during growth without prior bone resorption on the outer or periosteal surface of bone (Parfitt AM, 2000), as well as on the inner or endosteal surfaces of bone (endocortical, intracortical and trabecular) (Parfitt AM, 2000). In addition, bone modelling by bone resorption without subsequent bone formation can occur on the periosteal surface, particularly at metaphyseal regions of long bones, shaping the flask-like ends (Rauch, 2001).

1.2.5.2 Bone remodelling

Bone remodelling, often referred to as bone turnover, occurs predominantly on the endosteal surface and much less on the periosteal surface (Epker, et. al., 1965). Bone remodelling does not change the size or shape of the bone but is responsible for the removal and repair of damaged bone to maintain integrity of the adult skeleton and mineral homeostasis. Unlike bone modelling, bone remodelling by bone formation and bone resorption is a tightly coordinated/coupled process which requires synchronised activities of multiple cellular participants to occur at the same anatomical location. There are 3 major sequential phases of cellular activities at the remodelling site: activation, resorption and formation.

The *activation phase* of bone remodelling involves detection of an initiating remodelling signal to activate osteoclastogenesis, such as direct mechanical strain on the bone and

endocrine signal, such as PTH. Studies have demonstrated mechanical strain or damage on the skeleton results in osteocyte apoptosis and reduces the local TGF-β levels produced by the osteocytes, whose function is to inhibit osteoclastogenesis and thus allowing osteoclast differentiation to occur (Bonewald, 2006; Heino, et al., 2002). Moreover, PTH is secreted in response to low serum calcium levels and binds to PTH receptors on osteoblasts, activating a protein kinase signalling cascade and a wave of transcriptional responses that modulate the secretion of a range of factors, including those required for the recruitment of osteoclast precursor cells and osteoclast differentiation and activation (Swarthout, et al., 2002; Zajac, et al., 1992).

The *resorption phase* of bone remodelling involves the osteoclastic bone resorption as well as osteoblastic and osteocytic activity in terms of signalling the recruitment and promotion of osteoclastic proliferation and differentiation. In response to signals generated either by osteocytes or a direct endocrine activation signal such as PTH, osteoblasts produce M-CSF and RANKL (Li, et al., 2007; Ma, et al., 2001) to promote the recruitment, proliferation, survival and differentiation of osteoclasts. Osteoblasts also produce matrix osteoclastogenic cytokines, such as chemokine monocyte chemoattractant protein-1 (MCP-1), metalloproteinases (MMPs) which promote the degradation of the bone matrix and expose the RGD adhesion site necessary to facilitate osteoclasts attachment (Partridge, et al., 1987; Yang, et al., 2004).

The *formation phase* of bone remodelling involves paracrine signalling mechanisms to allow the transition from bone resorption to bone formation within the remodelling space. Recently the role of sub-class of an ephrin transmembrane receptor and its ligand (EphB4/ephrin-B2) to activate bone formation and inhibit bone resorption simultaneously at the formation phase of bone remodelling (Zhao, et al., 2006). EphB4 receptor is expressed by osteoblasts, whereas osteoclast expresses the ligand ephrin-B2. Binding of ephrin-B2 ligand to the EphB4 receptor in osteoblast enhances osteoblastic differentiation, and whereas signalling through ephrin-B2 into osteoclast suppresses osteoclastic differentiation by inhibiting the osteoclastogenic c-

Fos/NFATc1 cascade (Zhao, et al., 2006). In addition, osteoclasts have been shown to secrete the soluble molecule sphingosine 1-phosphate (S1P) and induce osteoblasts precursor recruitment as well as promote mature osteoblasts survival (Pederson, et al., 2008). Recently osteocytes have also been found to regulate bone formation during this critical phase of bone remodelling. Mechanical strain and PTH signalling, via PTH receptors on osteocytes (Fermor and Skerry, 1995) reduces sclerostin expression, removing inhibition of Wnt signalling, allowing Wnt-directed bone formation to occur (Robling, et al., 2008). When an equal quantity of resorbed bone has been replaced, the remodelling cycle concludes with no net gain or loss of bone mineral.

NOTE:
This figure/table/image has been removed to comply with copyright regulations.
It is included in the print copy of the thesis held by the University of Adelaide Library.

Figure 1.4: A schematic diagram showing the bone remodelling process, which consists of 3 phases: Phase 1: initiation/activation of bone remodeling at a specific site. Phase 2: bone resorption and Phase 3: osteoblast differentiation and formation and mineralisation of osteoid. In normal bone remodelling, there is no net change in bone mass after each remodelling cycle. However, abnormal bone remodelling such as in osteoporosis, causes reduced bone mass and strength. Abbreviation: BRC: bone-remodeling compartment. Adapted from Feng and McDonald (Feng and McDonald, 2011), Annual Reviews of Pathology Mechanisms of Disease, 6:121-45

1.3 VITAMIN D METABOLISM

Vitamin D can be obtained either from the diet or majority via UVB-irradiation of the skin, which initiates the conversion of 7-dehydrocholesterol in the skin to vitamin D_3. Vitamin D_3 in the circulation is bound to vitamin D-binding protein (DBP) (Haddad, 1995) and is transported to the liver where vitamin D_3 is hydroxylated to form 25-hydroxyvitamin D_3 (25D), via the 25-hydroxylase activity, which can occur by the CYP27A1 (Masumoto, et al., 1988), CYP2R1 and CYP3A4 enzymes with varying efficiencies (Shinkyo, et al., 2004). While 25D is the non-active form of vitamin m abolite, because of its high stability, its circulating levels is used to assess the vitamin D status of an individual (Holick, et al., 2007). 25D undergoes a second hydroxylation in kidney to produce 1,25 dihydroxyvitamin D_3 (1,25D), the active circulating metabolite of vitamin D (Boyle, et al., 1972; Holick, et al., 1972). While the synthesis of 25D by the liver is constitutive, the synthesis and catabolism of 1,25D in the kidney is tightly regulated by two cytochrome P450 enzymes, 25-hydroxyvitamin D-1-α-hydroxylase (CYP27B1) and 25-hydroxyvitamin D-24-hydroxylase (CYP24).

1.3.1 Renal vitamin D hydroxylases

The CYP27B1 enzyme is responsible for the bioactivation of 25D to 1,25D, which occurs predominantly in the kidneys (Jones, et al., 1987). On the other hand, CYP24 catabolises both 25D and 1,25D to 24,25-dihydroxyvitamin D_3 (24,25D) and 1,24,25 trihydroxyvitamin D_3 respectively (Holick, et al., 1973; Holick, et al., 1972) . It is the relative activities of these two enzymes in the kidneys that are largely responsible for the regulation of circulating levels of 1,25D (Omdahl, et al., 2001; Prosser and Jones, 2004). Inactivating mutations in the *CYB27B1* gene results in vitamin D-dependent rickets (VDDR) type 1, indicating the importance of the CYB27B1 enzyme in producing the active 1,25D (Kitanaka, et al., 1998). Notably the activity of CYP27B1 has also been reported in a variety of other tissues including the skin, intestine, brain, testis and bone, however local regulation of CYB27B1 activities in

these tissues appear to be different from that in the kidney (Anderson and Atkins, 2008; Anderson, et al., 2005; Bikle, 2004; Kato, et al., 1998).

The enzyme CYP24 is ubiquitously expressed, especially in vitamin D target tissues (Jones, et al., 1998; St-Arnaud, 1999). The renal CYP24 catalyses the inactivation of 1,25D, as well as clearance of excess 25D from the circulation. Extra-renal CYP24 activities catabolise cellular levels of 1,25D (Makin, et al., 1989; Prosser and Jones, 2004; St-Arnaud, 1999) and do not influence the circulating 1,25D or 25D levels. Studies have shown that CYP24-knockout mutant mice are unable to clear 1,25D from the bloodstream after both chronic and acute treatments with 25D and 1,25D (St-Arnaud, 1999; St-Arnaud, et al., 2000), demonstrating the important role for CYP24 in the catabolism of vitamin D metabolites.

1.3.2 Regulation of renal vitamin D hydroxylases

1.3.2.1 Calcium, Phosphate, PTH and 1,25D

The expression of renal vitamin D hydroxylases is regulated through a series of negative and positive feedback mechanisms. Low levels of dietary calcium and phosphate stimulates parathyroid hormone (PTH) secretion from the parathyroid gland, which potently up-regulates the transcription of renal CYB27B1 enzyme and down-regulates the mRNA levels and activity of the renal CYP24 enzyme (Brenza, et al., 1998; Murayama, et al., 1999). Elevated 1,25D in turn suppresses PTH transcription and production (Kim, et al., 2007). 1,25D also negatively regulates the CYB27B1 gene expression (Brenza and DeLuca, 2000; Bouillon, et al., 2005) while potently stimulates CYP24 expression via the two vitamin D responsive elements (VDRE) in the CYP24 promoter (Dhawan, et al., 2005; as reviewed in Christakos, et al., 2006). The marked induction of CYP24 by 1,25D results in suppression of 1,25D to protect against hypercalcemia and hyperphosphatemia.

1.3.2.2 FGF23

Recent studies have shown that fibroblast growth factor 23 (FGF23), which is a phosphaturic hormone that promotes renal phosphate excretion, is also a inhibitor of vitamin D metabolism (Liu, et al., 2006; Shimada, et al., 2004; Shimada, et al., 2001). FGF23 reduces 1,25D levels by inhibition of CYP27B1 and stimulation CYP24 expression (Liu, et al., 2006; Shimada, et al., 2004). Studies have shown that excess 1,25D can directly stimulate FGF23 expression in osteocytes, possibly via a putative VDRE in the FGF23 promoter (Liu, et al., 2006). Administration of 1,25D to mice results in increase serum levels of FGF23 prior to elevation in serum phosphate, suggesting that 1,25D induces FGF23 expression is independent of changes in serum phosphate (Liu, et al., 2006). In a feed-back loop, FGF23 in turn suppresses renal 1,25D synthesis, which in turn decreases FGF23 expression in bone (Shimada, et al., 2004). Conversely, during FGF23 deficiency and in FGF23 knockout mice elevated production of 1,25D and hyperphosphatemia occurs (Benet-Pages, et al., 2005; Sitara, et al., 2006). In FGF23-knockout mice this results in soft tissue calcifications, severe growth retardation, abnormalities of bone mineralisation and a shortened lifespan (Shimada, et al., 2004; Sitara, et al., 2004). Thus, the primary functions of FGF23 are to enhance phosphate excretion and suppress 1,25D production, which may have evolved to protect from vitamin D toxicity.

NOTE:
This figure/table/image has been removed to comply with copyright regulations.
It is included in the print copy of the thesis held by the University of Adelaide Library.

Figure 1.5: Photosynthesis of vitamin D and the metabolism of vitamin D to $25(OH)D_3$ and $1,25(OH)_2D_3$. In response to low serum calcium and phosphate, PTH is produced and stimulates 1αOHase (CYP27B1) expression in the kidney to increase $1,25(OH)_2D_3$ synthesis, promoting calcium and phosphate mobilization from the bone. $1,25(OH)_2D_3$ also induces calcium and phosphate absorption in the intestine. Adapted from McCullough and colleges (Mc Cullough, et al., 2009), Annual Reviews of Nutrition, 29:111-132.

NOTE:
This figure/table/image has been removed to comply with copyright regulations.
It is included in the print copy of the thesis held by the University of Adelaide Library.

Figure 1.6: A schematic diagram of FGF23 signalling and vitamin D metabolism. Osteocytes secrete FGF23 plus other osteocyte-related proteins. FGF23 binds to an FGF receptor:Klotho complex in the kidneys and inhibits sodium-dependent phosphate uptake and 1α-OHase activity. FGF23 have also been suggested to promote PTH release via the expression of FGF receptor:Klotho complex in the parathyroid gland. A rise in $1,25(OH)_2D_3$ level or phosphate level in turn stimulates FGF23 production. Adapted from Liu and Quarles (Liu and Quarles, 2007) JASN, 18:1637-1647.

1.4 VITAMIN D RECEPTOR

Majority of vitamin D's actions are mediated through binding to the nuclear hormone vitamin D receptor (VDR), which when ligand-bound, hetero-dimerises with the retinoid-X receptor (RXR) whereby it binds to DNA response elements (VDRE) on the promoter of target genes. Together with the co-regulatory complex the VDR-RXR hetero-dimer recruits, results in either the positive or negative transcriptional regulation of the gene in question (MacDonald, et al., 2001; Mangelsdorf and Evans, 1995). The VDR ubiquitously expressed, with significant expression in the kidneys, bone, parathyroid glands, small intestine, skin and the immune system (Demay, 2006). Activation of ligand binding of the VDR and activity regulates a wide range of tissue-specific responses, ranging from homeostatic control of mineral metabolism to local actions that control the growth, differentiation, and functional activity of numerous cell types, including those of the immune system, skin, the pancreas and bone (Bouillon, et al., 2008; Haussler, et al., 2008).

1.4.1 Structure of VDR

The human VDR gene has been localised to chromosome 12q13-14 (Baker, et al., 1988). The 4.6kb human VDR transcript contains a 1281 nucleotide open reading frame that codes for the full length VDR protein of 427 amino acids (Baker, et al., 1988). The human VDR coding sequence is highly homologous to the avian, amphibian, mouse and rat sequences, which range in molecular weight between 48-55kDa (Baker, et al., 1988). The full length VDR protein shows significant homology to other nuclear hormone receptor superfamily, including receptors for glucocoticoids, oestrogen, androgen, progesterone, thyroid hormone, retinoic acid, retinoic X and more than 150 orphan receptors (Mangelsdorf, et al., 1995; Ribeiro, et al., 1995). In general, all members of the nuclear hormone receptor superfamily possesses five functional domains: a short N-terminal domain, namely A/B domain, whose also contain an activation-factor (AF-1), a DNA binding domain (DBD), a hinge region and the C-terminal ligand binding domain (LBD), and an activation-factor (AF-2) domain (Kumar and

Thompson, 1999). The *A/B domain* of the VDR is 21 amino acids long, with known functions similar to that of most other nuclear hormone receptors, including the regulation of DNA binding, nuclear localisation and gene transcription (Freedman and Towers, 1991). The function of the AF-1 domain is unclear, although it has been suggested to be involved in regulation of the ligand-dependent function of the AF-2 region (Sone, et al., 1991). The *DNA binding domain* (DBD) of the VDR includes amino acids 22-114 and has been shown to contain many positively charged amino acids to facilitate the electrostatic interactions with the negatively charged phosphate backbone of the DNA helix (Freedman and Towers, 1991). The DBD contains two highly conserved zinc-finger DNA binding motifs (Freedman, 1992). In between the zinc-fingers there are five basic amino acids residues that have been implicated in the nuclear localisation of the VDR (Hsieh, et al., 1998). Phosphorylation of a serine residue 51 within the DBD by protein kinase C has been shown to affect DNA binding of the VDR protein (Haussler, et al., 1998). The hinge region confers flexibility to the VDR protein and changes in conformation upon ligand activation, which is a hallmark characteristic of the nuclear receptor family (Haussler, et al., 1998). The C-terminal ligand binding domain (LBD), contains 12 α-helices and 3 β-sheets both in the human (Rochel and Moras, 2006) and rat (Vanhooke, et al., 2004) form of the receptor. The LBD is the most complex and important region of the VDR structure, containing both the ligand binding pocket and ligand-dependent trans-activation function (AF-2). The LBD possesses large interaction surfaces for multiple partners, including the hetero-dimeric RXR partner, as well as co-repressors, co-activators and bridging factors involved in the VDR transcriptional machinery (Jurutka, et al., 2000; Rochel, et al., 2007). The ligand binding pocket of the VDR binds to the A ring containing the 1α-hydroxyl group of the 1,25D molecule with high affinity and nearly 1000 times less affinity to 25D and 24,25D (Brumbaugh and Haussler, 1973; Rochel, et al., 2007).

In response to ligand binding, LBD undergoes a conformational change (Rochel, et al., 2007). In particular, helix 12, containing the ligand-dependent AF-2, folds over top of the globular LBD and caps the ligand binding cavity, which ultimately creates a large hydrophobic cleft

(Feng, et al., 1998). The hydrophobic cleft serves as a docking surface for many nuclear receptor co-activators by interacting with a complementary hydrophobic domain in the co-activator containing the consensus LXXLL motif (Heery, et al., 1997). Phosphorylation at serine residue 208 by casein kinase II in the LBD has been shown to enhance transcriptional activation of VDR (Jurutka, et al., 1996).

1.4.2 Mechanism of actions

The conventional nuclear receptor superfamily mode of actions involve 1,25D enters the cell by transversing of the plasma membrane in a free form and binds strongly to the VDR inside the nucleus (K_d=2x10^{-10}M) (Haussler, et al., 1998). The liganded-VDR is then phosphorylated and its surface conformation is reconfigured, this allows the interaction of the VDR with its hetero-dimer partner, retinoid X receptor (RXR) (Haussler, et al., 2008). The VDR/RXR hetero-dimer binds specifically to DNA enhancer sequence termed vitamin D-responsive element (VDRE), which is present within the promoter region of vitamin D target genes (Haussler, et al., 2008; Jurutka, et al., 2001). The VDRE consensus sequence contain a tandem repeating oligonucleotide of six base pairs containing a 3-nucleotide spacer: 5'-(A/G)G(G/T)TCA-NNN-(A/G)G(G/T)TCA-3', where RXR binds to the 5' half site and the VDR occupies the 3' half site (Haussler, et al., 2008). The liganded VDR/RXR hetero-dimer complex can either positively or negatively modulate gene transcription, which is dependent upon the cell- and promoter-specific activities to interact with nuclear co-regulatory protein complexes.

1.4.2.1 Positive gene regulation

The ligand-induced conformational change of VDR releases the bounded co-repressors and allows co-activators to bind to VDR (Glass and Rosenfeld, 2000; McKenna and O'Malley, 2002). These co-activators include members of the p160/SRC family (Gill, et al., 1998) and CBP/p300 (Castillo, et al., 1999) that either have or can recruit histone acetyl transferase

activities to open up the chromatin structure, allowing transcription to occur. These co-activators are also essential for the formation of the initial transcriptional complex with RNA polymerase II (Jenster, et al., 1997). The opened chromatin template is then able to recruit the DRIP/TRAP co-activator complex which serves as a mediator between the VDR/RXR and the RNA polymerase II complex to induce target gene transcription (Rachez, et al., 2000). In addition to DRIP and SRCs, several other proteins involved in VDR-mediated transcription have been described. One example is NCoA62/ski-interacting protein (SKIP) which directly interacts with VDR and regulates VDR transcriptional activity (Baudino, et al., 1998). Furthermore, ATP-dependent chromatin remodelling complex, such as SWI/SNF has also recently been shown to be involved in VDR-regulated positive gene transcription (Villagra, et al., 2006).

1.4.2.2 Negative gene regulation

The process of transcriptional repression by VDR has been recognised as a more complicated and much less understood process. During transcriptional repression, such as that of the PTH gene, binding of the VDR-RXR complex to a negative VDRE recruits co-repressors of the family of histone deacetylases, which prevent chromatin exposure, and consequently, the binding of TATA binding protein required to initiate the transcription of the target gene by RNA-polymerase II (Haussler, et al., 2008; Jurutka, et al., 2001). Recent studies have suggested a bifunctional role for the VDR co-modulator NCoA62/SKIP to promote transcriptional activation as well as repression, in a cell-specific manner, depending on the expression of co-activator CBP/p300 and the co-repressors NCoR/SMRT (Leong, et al., 2004). It was shown that the CBP/p300 and NCoR/SMRT can interact directly with the same region on the NCoA62/SKIP molecule and thus the relative expression levels the co-activator or co-repressor will dictate whether NCoA62/SKIP activates or represses VDR/RXR-dependent transcription (Leong, et al., 2004).

1.4.2.3 Non-genomic effects of VDR

In addition to the genomic actions of VDR, it has also been shown to mediate biological responses via non-genomic actions or rapid responses. This activity of VDR includes activation of rapid and transient changes in transmembrane transport of ions such as calcium and chloride, as well as intracellular signalling pathways, such as cAMP, phospholipase C, phosphatidylinositol-3 kinase, protein kinase C and MAPK (Haussler, et al., 2011; Ordonez-Moran et al., 2009). In contrast to the genomic responses, which generally take hours, the rapid responses are generated within 1-2 minutes to 15-45 minutes. Interestingly, the structure of the 1,25D required to mediate the genomic effects of VDR differs to the one involved in the genomic actions. VDR binds specifically to a 6-s-*trans* shape of 1,25D to mediate genomic responses (Rochel et al., 2000), while a 6-s-*cis* shape is responsible for the rapid responses (Zanello et al., 2004). The mechanisms of how VDR of only one ligand binding pocket can bind ligands of different shapes to mediate two different biological responses are still under investigation.

1.4.3 VDR polymorphisms

In humans, multiple polymorphisms (allelic variants) of the VDR gene have been identified with substantial differences between race and ethnic groups (Fang, et al., 2005; Uitterlinden, et al., 2004). These polymorphisms are distributed throughout the complete VDR gene region and have been associated with changes to bone mineral density (Eisman, 1999; Wood and Fleet, 1998), hyperparathyroidism (Gomez Alonso, et al., 1998), susceptibility to infections, autoimmune diseases and cancer (Kostner, et al., 2009; Uitterlinden, et al., 2004). Among the VDR polymorphisms (greater than 60), there are several functional VDR polymorphisms and have been thoroughly studied. Three of these polymorphisms are ‘cluster’ polymorphisms in the intron separating exon 8 and 9, which were identified by restriction enzyme *BsmI*, *ApaI* and *TaqI* (Fleet, et al., 1995; Schmidt, et al., 1997). These *BsmI-ApaI-TaqI* VDR polymorphisms have been linked not only to bone specific parameters (Fang, et al., 2006;

Fleet, et al., 1995; Wood and Fleet, 1998), but also to greater occurrence of parathyroidism (Schmidt, et al., 1997) and prostate cancer (Taylor, et al., 1996). An additional allelic variation in the human VDR gene can be found in the 3'UTR, approximately 1 kb upstream of the poly-A tail in the form of a microsatellite poly-A repeat with variable lengths (Ingles, et al., 1997). Given that this variable poly-A repeat sequence occurs in the 3'UTR of the messenger RNA, it may therefore able to affect either message stability or translatability, although the exact function is unclear. Interestingly microsatellite poly-A repeat polymorphisms has been reported to be tightly linked to the *BsmI-ApaI-TaqI* cluster in certain ethnic populations, but not in others (Ingles, et al., 1997), possibly leading to differences in bone density association studies of VDR polymorphisms (Cooper and Umbach, 1996; Garnero, et al., 1995). Moreover, a polymorphism in the VDR promoter is located on the recognition site for the intestinal specific transcription factor homeodomain protein Cdx-2, resulting defective binding of Cdx-2 (Arai, et al., 2001), decreased intestinal VDR expression levels and reduction in 1,25D-mediated calcium absorption (Fang, et al., 2003). While the majority of VDR polymorphisms do not affect structural alteration in the VDR protein, the *FokI* single nucleotide polymorphism located at the translation start site results in a VDR protein shortened by three amino acids (Arai, et al., 1997; Gross, et al., 1998; Harris, et al., 1997). Epidemiological studies suggest an association between the shorter form of *FokI* VDR polymorphism protein and increased bone mineral density in humans (Ames, et al., 1999; Ferrari, et al., 1998; Harris, et al., 1997), although the functional mechanism of this association remains unclear and controversial (Gross, et al., 1998; Uitterlinden, et al., 2004).

1.5 BIOLOGICAL ACTIONS OF 1,25D-VDR AND BONE HOMEOSTASIS

Vitamin D is essential for the maintenance of a healthy skeleton. Vitamin D deficiency in animals and humans can result in reduced bone mineralization, such as that occurs in the bone diseases of rickets and osteomalacia. Ablation of the genes for VDR or CYP27B1 results in a similar reduction in bone mineralisation, which will be discussed in detail in the next section.

The most widely studied action of vitamin D on bone homeostasis is with respect to the ability of vitamin D to maintain serum calcium and phosphate at physiological levels, which is vital for normal cellular processes and for skeletal integrity. However, vitamin D has also been shown to affect many aspects of bone cell biology, directly regulating each of the major bone cell types resulting in changes in the bone remodelling process.

1.5.1 1,25D-VDR actions on calcium homeostasis

1.5.1.1 Intestine

Arguably the most pronounced effect of 1,25D is to regulate serum calcium levels via the stimulation of the absorption of dietary calcium in the small intestine. Studies in mice lacking either the VDR (Li, et al., 1997; Yoshizawa, et al., 1997) or CYB27B1 (Dardenne, et al., 2001; Panda, et al., 2001) showed marked hypocalcaemia as the result of calcium mal-absorption, indicating that both 1,25D and VDR are required for optimal calcium absorption. 1,25D acting via VDR in intestinal enterocytes induces a number of specific genes required for calcium entry across the brush border membrane, intracellular calcium diffusion, and extrusion of calcium across the plasma membrane. The cytosolic calcium-binding protein, calbindin-D9k, is thought to act as an intracellular calcium ferry and translocate calcium across the enterocyte (Christakos, et al., 1992). 1,25D is able to up-regulate the expression of calbindin-D9k through the VDRE in the proximal promoter of the gene (Darwish and DeLuca, 1996). VDR knockout mutant mice exhibit a 50% reduction in intestinal calbindin-D9k mRNA and impaired intestinal calcium absorption (Li, et al., 1997). Moreover, recently it has been confirmed that 1,25D is able to induce the expression of the epithelial calcium channels TRPV6 (also known as CaT1 or ECaC2) and TRPV5 (CaT2 or ECaC1) (Song, et al., 2003; Van Cromphaut, et al., 2001) and facilitate calcium entry across the brush border membrane. In VDR knockout mice, TRPV6 mRNA was found to be even more markedly decreased in the intestine than calbindin-D9k mRNA (Van Cromphaut, et al., 2001). Calcium extrusion at the basolateral membrane of the intestine is an active process, requiring a calcium

ATPase. Previous studies have shown that the intestinal plasma membrane calcium pump (PMCA) mRNA is also stimulated by 1,25D (Wasserman, et al., 1992), although no classical VDRE have been yet been identified for the promoter of this gene (Wasserman and Fullmer, 1995).

1.5.1.2 Kidney

While perhaps the most important effect of 1,25D in the kidney is the negative feedback on its own production through the suppression of CYP27B1 activity and the stimulation of CYP24 activity, 1,25D can also increase renal reabsorption of calcium in the distal tubules. Similar to studies in the intestine, the brush border membrane calcium channel protein, TRVP5 was found to be induced by 1,25D via multiple VDRE identified in the promoter of this gene (Hoenderop, et al., 2001). 1,25D also enhances the expression of the renal calcium transport protein, calbindin D-28k and extrusion of calcium across the plasma membrane via a PMCA transporter (Sooy, et al., 2000), as well as PTH-depended calcium transport in the distal tubule (Friedman and Gesek, 1993).

1.5.1.3 Parathyroid gland

Vitamin D is a potent modulator of parathyroid function. It is well established that PTH gene promoter contains a negative VDRE, which allows for the direct repression of PTH gene transcription by the 1,25D-VDR complex (Liu, et al., 1996). In addition to direct repression of the PTH gene, the 1, -25D VDR complex regulates both parathyroid cell growth (Szabo, et al., 1989) and responses of the parathyroid gland to extracellular calcium. 1,25D modulation of the parathyroid gland in response to calcium involves the direct 1,25D-VDR induction of calcium sensing receptor (CaSR) gene transcription (Brown, et al., 1996) mediated by two VDREs located in the CaSR promoter (Canaff and Hendy, 2002). Notably, the rescue diet containing high levels of calcium and phosphorous fed to VDR and CYB27B1 knockout mice

corrects the high serum PTH levels (Panda, et al., 2004), suggesting that neither the VDR or 1,25D is essential but are working cooperatively with calcium in controlling PTH synthesis.

1.5.2 1,25D-VDR direct actions on bone cells

1.5.2.1 Osteoblast

1,25D acting via the VDR regulates a wide array of osteoblastic gene transcription responsible for proliferation, differentiation and mineralisation (Atkins, et al., 2003; Matsumoto, et al., 1991; Rickard, et al., 1995; Stein, et al., 1996). Human primary osteoblasts respond to exogenous 1,25D by decreasing the rate of cell proliferation, and increasing the expression of vitamin D-responsive genes, including osteocalcin (Ocn), alkaline phosphatase (ALP), collagen type 1 (Col1) and osteopontin (OPN) (Atkins, et al., 2003; Beresford, et al., 1986). Consistent with the central role of vitamin D in maintaining osteoblastic function, the generation of colony forming units from cultured bone marrow-derived osteoblasts from VDR and CYB27B1 knockout mice were impaired compared to wild-type cells (Panda, et al., 2004), suggesting that 1,25D and VDR is important for osteoblast formation and activity. In addition to responding to exogenous 1,25D, osteoblasts express CYP27B1, synthesise detectable levels of 1,25D (Anderson, et al., 2005; Howard, et al., 1981) which was shown to inhibit cell proliferation and stimulate osteoblast differentiation in model of primary human bone cells and the human bone cell line, HOS (Anderson, et al., 2010; Atkins, et al., 2007).

Another prominent action of 1,25D-VDR on osteoblasts is to regulate the expression of the TNF-ligand family member, RANKL, a classical VDRE-containing promoter (Kitazawa, et al., 1999). As discussed earlier in chapter 1.2, osteoblast produced RANKL binds to its receptor, RANK, expressed by differentiation and survival osteoclast precursors, which promotes osteoclastic development, (Kearns, et al., 2008). 1,25D has been shown to stimulate osteoclastogenesis by increasing RANKL production as well as decreasing the expression of the RANKL decoy receptor, OPG by osteoblasts (Horwood, et al., 1998). 1,25D preferentially up-regulates RANKL expression in immature primary human osteoblasts, as defined by their

expression of the immature osteoblastic marker, STRO-1 (Atkins, et al., 2003). Similarly, the ability of mouse primary osteoblasts to express RANKL in response to 1,25D decreases with their osteogenic maturation (Thomas, et al., 2001). In contrast, osteoblasts isolated from transgenic mice which over-express VDR specifically in mature osteoblasts and osteocytes have reduced ability to support osteoclastogenesis in co-culture experiment, which was due to a decreased RANKL:OPG ratio (Baldock, et al., 2006). While the current view is that 1,25D maintains normocalcaemia by stimulating bone resorption and increasing the extent and rate of osteoblast-mediated osteoclastogenesis, these findings implicate that 1,25D can also directly regulate osteoblastic function and mineralisation, suggesting that 1,25D may be important for both the initiation and continuation of bone remodelling.

1.5.2.2 Osteoclast

Although the role of 1,25D-VDR on osteoclast formation is best described from the indirect effects via the osteoblasts, 1,25D has been shown to directly effect osteoclast precursors by increasing the expression of the osteoclast adhesion molecule, αVβ3 integrin, both in avian osteoclast precursor cells (Mimura, et al., 1994) and in the human myelomonocytic cell line, HL-60 (Andersson and Johansson, 1996). In HL-60 cells, 1,25D also increases the expression of the RANK and osteoclast maturation (Kido, et al., 2003). A direct positive effect of 1,25D on RANKL-induced osteoclast formation from the mouse osteoclast precursor cell line, RAW 264.7 have also been reported, where 1,25D increases the number of multinucleated TRAP-positive osteoclasts (Vincent, et al., 2009), indicating the direct effect of 1,25D on osteoclast activity. Intriguingly, osteoclasts have also been shown to express CYP27B1 and produce detectable levels of 1,25D (Kogawa, et al., 2010; van Driel, et al., 2006). Recent data indicate that the metabolism of 25D into 1,25D by human osteoclast precursors results in the increased mRNA expression encoding key regulators of osteoclastogenesis, NFATc1, and c-Fos as well as osteoclast marker genes, such as OSCAR, a co-regulator of osteoclast differentiation, and

TRAP (Kogawa, et al., 2010). Together these findings indicate that 1,25D is an important regulator of osteoclastic formation and activity.

1.5.2.3 Osteocyte

Although osteocytes *in situ* have been known to express VDR (Boivin, et al., 1987), the direct actions of 1,25D-VDR signalling in osteocytes remain largely unknown. 1,25D has been shown to act on mature osteoblast/osteocyte and increases FGF23 mRNA and protein levels via the putative VDRE in the FGF23 promoter (Kolek, et al., 2005; Liu, et al., 2006). Elevated FGF23 in turn suppresses renal 1,25D production and renal phosphate reabsorption (Liu, et al., 2006; Shimada, et al., 2004) forming a feed-back loop. Our laboratory have shown that the osteocyte cell line, MLO-A5, express both VDR and CYP27B1 mRNA, which increase with maturation of the osteocyte and is positively correlated with the osteocytic expression of Dmp1 and Phex (unpublished data). Moreover, the osteocyte-specific gene *SOST* (which encodes for Sclerostin, a potent inhibitor of bone formation as discussed previously) is directly regulated by 1,25D in human primary osteocyte-like cells by virtue of a unique VDRE in *SOST* promoter (unpublished data). Furthermore, recent unpublished data in a rodent model indicate that osteocyte density declines as a function of decreased circulating 25D levels, which is associated reduced bone strength in the tibia, suggesting that low vitamin D activity may contribute to the loss of osteocytes and bone integrity. Intriguingly, the OSVDR transgenic mouse with increased sensitivity of 1,25D-VDR signalling in mature osteoblasts and osteocytes (as driven by the osteocalcin promoter) are more sensitive to mechanical loading, by markedly enhancing bone formation, mineralising surface and bone formation rate on the periosteal surface when compared to wild-type controls (manuscript in preparation). Collectively, these new findings indicate that direct actions of 1,25D-VDR in osteocytes regulate gene expression and key bone formation events, such as mechanical loading.

1.6 CLINICAL SKELETAL EFFECTS OF VITAMIN D DEFICIENCY

Vitamin D deficiency can lead to the bone mineralisation defects of rickets in children and osteomalacia in adults as well as contribute to the onset of osteoporosis. However, the blood level of 25D required to prevent either of these diseases is controversial, which is due partly to the invasive nature of collecting histological evidence from patients to demonstrate the nature of the bone defect. Osteomalacia and osteoporosis are distinguished by unique changes in microscopic bone architectures. Osteomalacia occurs as a result of a mineralisation defect (increased osteoid volume and a delay in mineralisation lag time) (Bronner, 1976). Osteoporosis is often associated with a decrease in intestinal calcium absorption and increase in bone resorption leading to loss of trabeculae, reduced cortical bone and increased risk of fracture (Gallagher, 1990).

It is well established that vitamin D and dietary calcium supplementation are effective preventative strategies for reducing the risk of fractures in the elderly (Chapuy, et al., 1992), which has also been confirmed by a meta-analyses of clinical trials when vitamin D supplementation is 800 IU per day or greater (Bischoff-Ferrari, et al., 2005; Tang, et al., 2007). However, there has been confusion in the field because the level of 25D required to optimise intestinal calcium absorption and maintain plasma calcium homeostasis is considerably lower than that required to prevent fractures (Dardenne, et al., 2004; Fraser, et al., 1973). Clinical studies have demonstrated that 25D levels below 20 nmol/L result in hypocalcaemia, hypophosphateamia, secondary hyperparathyroidism and osteomalacia (Need, et al., 2008). At these frankly low levels of 25D, substrate depletion resulting in reduced renal synthesis of circulating 1,25D and intestinal calcium malabsorption (Anderson, et al., 2007; Need, 2007; Need, et al., 2008). With mean serum 25D levels around 40 nmol/L, while osteomalacia does not occur, the incidence of osteoporosis (Arnala, et al., 1997; Bell, et al., 1999) hip fracture increase, particularly in the elderly (Lidor, et al., 1993; Morris, et al., 1984). For reasons that are not entirely clear, this bone loss occurs without a change in circulating neither 1,25D levels nor impairment of intestinal calcium absorption (Lidor, et al.,

1993; Meller, et al., 1985). Only when 25D levels exceed 75 nmol/L, does the risk of hip and non-vertebral fractures reduce (Bischoff-Ferrari, et al., 2005). Given that the majority of the general population have levels of 25D below 80 nmol/L (Mithal, et al., 2009), there is a concern by some to recommend vitamin D supplementation to achieve such 25D levels. The difficulty in changing current recommendations of vitamin D status is, in part, due to our incomplete understanding of mechanisms by which 25D levels above 80nmol/L improve bone volume and reduce fracture risk.

1.7 ANIMAL STUDIES FOR THE ACTIONS OF VITAMIN D ON BONE HOMEOSTASIS

The majority of our understanding for the role of vitamin D in bone health has been derived from studies of dietary manipulations and from the analyses of disorders of rickets and osteomalacia in human and animal models. The development of techniques for genetic manipulation in mice have allowed in depth analyses of the molecular basis for the phenotypes observed when vitamin D activity is impaired and highlight the essential role of 1,25D-VDR in maintaining bone mineral homeostasis. A major question, which has been proven difficult to answer, is the relative importance of vitamin D activity in regulating mineral homeostasis and the direct actions of vitamin D on bone cells.

1.7.1 Vitamin D receptor knock-out (VDRKO) mice

There are two VDRKO strains with targeted deletion of the DNA binding domain of the VDR gene in either exon 2 (encoding the first zinc-finger) (Erben, et al., 2002; Yoshizawa, et al., 1997) or exon 3 (second zinc-finger) (Li, et al., 1997). Both the VDRKO mice have no detectable VDR protein and display all the features of the human disease: hereditary vitamin D-resistance rickets (HVDRR) (Hughes, et al., 1988; Malloy, et al., 1999). VDRKO mice are phenotypically normal at birth but in from the third week of life develop alopecia and growth retardation, accompanied by hypocalcaemia, hypophosphatemia, and compensatory secondary

hyperparathyroidism (Li, et al., 1997; Yoshizawa, et al., 1997). The expression of renal CYP27B1 mRNA is markedly elevated and CYP24 mRNA is virtually absent in VDRKO mice, resulting in high circulating 1,25D concentrations. Largely due to the hypocalcaemia and hypophosphatemia, severe skeletal defects occur in VDRKO mice, including decreased bone mineral density, thinned bone cortex, under-mineralized bone and widening of growth plates consistent with osteomalacia (Li, et al., 1997; Yoshizawa, et al., 1997). However, when VDRKO mice were fed a diet enriched in calcium, phosphorus and lactose, termed the 'rescue diet', serum calcium and phosphate levels were normal. This indicated that calcium supply from the intestine is essential for developing a normal secondary hyperparathyroidism. Under these conditions, VDRKO mice developed largely normal bone structures with no evidence of osteomalacia (Amling, et al., 1999; Li, et al., 1998) skeleton. Moreover, restoration of the VDR expression with the intestine rescued VDRKO mice from hypocalcemia, hypophosphatemia and osteomalacia (Xue and Fleet, 2009). It has therefore been generally concluded that the main effect of vitamin D on bone homeostasis D within the skeleton is via its action in the intestine to maintain serum calcium levels and not due to any direct effect of vitamin

However, the notion that the role of vitamin D in bone mineralisation and homeostasis is dispensable has been challenged studies conducted by Panda and colleagues (Panda, et al., 2004). In their studies, VDRKO mice were fed the rescue diet until 17 weeks of age, 7 weeks longer than had been previously reports. In these 17 week old VDRKO adult mice, bone volume was marked reduced when compared to WT mice deficiencies in these VDRKO mice (Panda, et al., 2004). These mice exhibited significant reduction in osteoblast number, mineral apposition rates, alkaline phosphatase activity and trabecular bone volume compared to wild-type mice (Panda, et al., 2004). In addition, bone sections stained for the osteoclastic markers, RANKL and tartrate resistant acid phosphatase (TRAP) were all reduced, demonstrated a reduction in osteoclastic activity in the VDRKO mice (Panda, et al., 2004). Taken together, these findings indicate that bone volume deficiencies in the older VDRKO mice was not due

to the increase of osteoclastic activity but rather a failure of osteoblastic activity and suggest that the 1,25D-VDR system may be important in cells of the osteoblast lineage to promoter bone mineralisation, particularly as mice age.

Consistent with these *in vivo* findings, *in vitro* studies with osteoblasts derived from the bone marrow of VDRKO mice demonstrated impaired mineralisation and reduced production of mineralised colonies (Panda, et al., 2004). Furthermore, the number of bone marrow osteogenic progenitors (colonies forming units) also markedly declined in normocalcemic aging VDRKO mice compared with WT mice (Panda, et al., 2004). However, other studies have shown contrasting findings with regards to VDR activity osteoblastogenesis. Calvarial osteoblasts isolated from VDRKO mice exhibited enhanced osteoblast differentiation with increased in the number of osteoblast colony forming units, alkaline phosphatase activity and mineralised matrix formation (Sooy, et al., 2005). These divergent data which may explained in part by the site of origin for which the cells are derived, suggest that the actions of 1,25D via VDR on osteoblasts, may be dependent upon stage of osteoblast differentiation or the conditions in which cells are treated, as indicated by studies investigating 1,25D treatment of osteoblasts culture (Owen, et al., 1991; Stein, et al., 1996).

1.7.2 CYP27B1 knock-out (CYP27B1KO) and VDR double knock-out mice

To address the question of whether the effects observed in VDRKO mice are due to the absence of the receptor or the lack of 1,25D ligand-dependent receptor action, CYP27B1KO mice were generated (Dardenne, et al., 2001; Panda, et al., 2001). The phenotype of CYP27B1KO mice is indistinguishable to that of VDRKO mice, including hypocalcemia, hypophosphatemia, hyperparathyroidism, growth retardation and osteomalacia. However unlike the VDRKO mice, CYP27B1KO mice have undetectable 1,25D levels and do not exhibit alopecia, resembling the human disease of pseudo vitamin D deficiency rickets (PDDR) (Dardenne, et al., 2001; Panda, et al., 2001). Although feeding the CYP27B1KO animals the rescue diet restores normal mineral ion homeostasis and corrects the skeletal

abnormalities, normal growth is observed only when the mice are treated with 1,25D, suggesting that the VDR-dependent actions contribute to bone growth (Dardenne, et al., 2001; Panda, et al., 2001).

Generation of the double knockout of both CYP27B1 and VDR mutant mice have conclusively demonstrated that normalization of serum calcium cannot entirely substitute for a defective 1,25D-VDR system in skeletal homeostasis, particularly for the normal coupling of bone remodelling (Panda, et al., 2004). Both osteogenesis and osteoclastogenesis were impaired in 1,25D-VDR-defective mutants, which were revealed after correction of hypocalcaemia and secondary hyperparathyroidism with the rescue diet. The 'rescued' phenotypes continue to exhibit reduced osteoblastic number, mineral apposition rates and bone volume compared to wild-type mice, despite achieving normalcalcemia and normal PTH levels (Panda, et al., 2004). Interestingly, despite the high PTH levels in the VDR knockout mice, osteoclast numbers were not able to be induced to greater levels than that observed in normocalcemic wild-type mice whose PTH levels were normal (Panda, et al., 2004). These data indicated that bone turnover in the knockout animals impaired and an intact 1,25-VDR system is necessary for an appropriate osteoclastic response to increased PTH. Moreover, neither the rescued diet nor 1,25D administration could correct either osteoclast size or osteoblastic RANKL levels in the absence of the VDR (Panda, et al., 2004).

1.7.3 Mature osteoblast-specific vitamin D receptor transgenic (OSVDR) mice

A direct role for 1,25D-VDR activity in bone has been demonstrated with the osteoblast-specific VDR over-expression mouse model (OSVDR). In this transgenic model, the human osteocalcin promoter drives the expression of human VDR transgene (hVDR) within mature osteoblastic lineage and osteocytes (Gardiner, et. al., 2000). The OSVDR line#3 contained 10 inserted copies of the hVDR transgene, VDR protein expression in the bones of these transgenic mice is 4-fold greater compared to wild-type controls. While no changes to serum biochemical measurements were observed, OSVDR mice exhibited a 25% increase periosteal

bone formation, a 20% increase in cortical cross-sectional area and a 15% increase in trabecular bone volume, leading to an overall 15% increase in the force required to break the mid-shaft of the OSVDR tibia (peak load) (Gardiner, et al., 2000). Furthermore, it was determined that the bone mineral of OSVDR mice contained a greater calcium concentration as measured by quantitative backscattered electron imaging, without affecting the structural properties of the mineral crystals (Misof, et al., 2003). Dynamic histomorphometric analyses demonstrated that both an increase in osteoblastic activity and a decrease in osteoclastic numbers were responsible for the changes in the OSVDR's bone architecture as measured by double-labelled fluorescence and TRAP-positive respectively (Baldock, et al., 2006; Gardiner, et al., 2000). Interestingly, by increasing the sensitivity of mature osteoblasts and osteocytes to 1,25D, the author observed an decreased in the local synthesis of RANKL:OPG ratio in the bone of the OSVDR mice, as well as reduced ability for OSVDR's osteoblasts to support osteoclastogenesis in *in vitro* co-culture experiments (Baldock, et al., 2006). Collectively, these data demonstrated an important interaction between the mature osteoblasts and osteoclasts that is mediated by 1,25D-VDR activity. Intriguingly, while the mechanisms are unclear, when OSVDR mice were maintained on a low 0.1% calcium diet, the OSVDR's anabolic bone phenotype was reduced and no changes to either 1,25D or PTH were observed (Baldock, et al., 2006). Furthermore, when OSVDR mice were subjected to mechanical loading using the tibial 4-point loading technique adapted for mice, a markedly enhanced level of periosteal woven bone formation, mineralisation surface and bone formation rate occurred when compared to levels in wild-type mice. These data suggest that the OSVDR mice are more sensitive to mechanical loading and that increased sensitivity of mature osteoblasts and osteocytes to 1,25D results in enhanced bone-forming activity due to mechanical strain (Anderson, et al., unpublished data).

Although it is clear that the OSVDR mice exhibit an overall anabolic bone phenotype, there remain a number of outstanding physiological questions regarding the role of vitamin D activity in the mature osteoblasts and osteocytes. Firstly, can OSVDR animals be protected

from bone loss due to vitamin D deficiency? Secondly, what are the mechanisms involved in the bone loss observed in the OSVDR animals when subjected the low calcium stress? Is there a role for osteoblastic/osteocytic VDR in calcium homeostasis?

1.8 AIMS AND HYPOTHESES

The general aim of this thesis is to investigate the role of VDR within osteoblasts and osteocytes and the impact on bone homeostasis. Our hypothesis is that VDR in osteoblasts and osteocytes play essential roles in the bone remodelling process and the maintenance of an optimal skeletal structure.

1.8.1 Specific aims

Accordingly, the OSVDR mouse model will be used to address the following specific aims of the project:

a) Establish the OSVDR's transgene bone-specific over-expression, as well as structural, cellular and biochemical analyses of the OSVDR mouse phenotype

b) Determine the effect of vitamin D deficiency on the OSVDR's bone structure, cellular activities, biochemical parameters, and gene expression

c) Characterise the structural, biochemical, cellular and molecular mechanisms which underpin the influence of low calcium stress in determining the OSVDR bone phenotype.

1.8.2 Significance of project

Currently, the role of vitamin D on bone health is thought to be primarily in regulating calcium and phosphate homeostasis through its actions on the intestine. Although roles for direct activity of vitamin D have been proposed, there is little *in vivo* evidence to demonstrate this. Hence, the proposed studies are needed to clarify the direct involvement of vitamin D in the regulation of skeletal homeostasis. The structural, cellular and molecular findings from this project may confirm the recent view of a fundamental role for vitamin D and VDR to directly regulate bone cell activities and bone mineralisation.

Chapter 2

2.1 MATERIALS

All chemicals and consumables used in the experiments were purchased from Sigma Aldrich Chemical Company (Castle Hill, NSW, Australia), unless otherwise stated.

2.2 ANIMALS

All animals used in the experiments were female FVB/N (wild-type) and OSVDR mice (OSV3 line) on the FVB/N background. All FVB/N wild-type mice were bought from Animal Resources Centre (Murdoch, Perth, Australia). Homozygous OSVDR transgenic mice (line 3) (Gardiner, et al., 2000) were kindly provided by Dr Edith Gardiner at the Garvan Institute (Darlinghurst, NSW, Australia) and were subsequently bred and maintained in the Institute of Medical and Veterinary Science (IMVS) Animal Care Facility. OSVDR hemizygous mice were generated by breeding OSVDR homozygous male mice with FVB/N female mice. All genotypes of OSVDR mice were confirmed by real-time PCR with primers spanning specifically the human VDR transgene (see primer table 2.3 below). All animal experimentations were approved by the IMVS Animal Ethics Committee.

2.3 HOUSING

All animals were housed at 24°C with a 12-hour light/dark cycle and were exposed to standard lighting. Animals involved in experimentation were caged with the same number of animals/cage and with the same conditions (including toys, boxes, etc).

2.4 DIET

All animals were fed a commercial chow diet containing 0.80% calcium, 0.71% phosphorus and 2000IU/Kg vitamin D from Specialty feeds (Glen Forrest, WA, Australia) and tap water *ad libitum* after weaning (3 weeks of age), unless specified otherwise. Animals in the studies involving changes to dietary vitamin D and calcium were fed 8g/animal/day of a modified

AIN-93-VX semi-synthetic diet from ICN Biochemicals (Cleveland, Ohio, USA) in which the levels of dietary calcium and vitamin D were modified for the different experimental procedures as specified in method section of each study.

2.5 SEMI-SYNTHETIC DIET

The semi synthetic diets were prepared in the laboratory according to a standard formula (Refer to Table 2.1). The components of the mineral mix (Table 2.2) were weighed, crushed and thoroughly mixed in a plastic container. Corn starch, casein and cellulose were mixed for 30 minutes in a dough mixer. The remaining dry ingredients were added slowly and the mixture combined for a further 30 minutes. The ingredients of the mineral mix were weighed and crushed then manually mixed for 5 minutes before adding with the rest of the dry ingredients. Subsequently, the corn oil was drizzled into the mixture during mixing and combined for another 30 minutes. Finally distilled water was added to form a thick paste which was poured into trays to a thickness of approximately 3cm and allowed to partially solidify before being cut into blocks and frozen at -20°C.

Table 2.1 Components of the Semi-Synthetic Diet

Ingredient	(g/Kg mix)
Casein	200
Corn Starch	650
Cellulose	50
DL-Methionine	3
Choline Bitartrate	2
Mineral Mix*	35
AIN-93-VX Vitamin Mix#	10
Calcium Carbonate (0.1%-1%)	25-250
Corn oil	50

Table 2.2 Components of the Mineral Mix*

Ingredient	(g/Kg mix)
Sodium di-hydrogen phosphate ($2H_20$)	197
Potassium di-hydrogen phosphate	275
Potassium sulphate	52
Magnesium oxide	24
Manganous carbonate	3.5
Ferric citrate	6
Zinc carbonate	1.6
Cupric carbonate	0.3
Potassium iodate	0.01
Sodium selenite	0.01
Chromium potassium sulphate	0.55
Sucrose (finely powdered)	440.03

2.6 BLOOD BIOCHEMISTRY

2.6.1 Blood sample collection

Food was withdrawn from mice 16 hours prior to bloods being collected by cardiac puncture while the animals were under isoflourane anaesthesia. Approximately 800µl of blood was collected for each mouse and immediately placed in ice. Serum was collected by centrifugation at 13,000 rpm for 10 minutes. Approximately 400µl of serum was collected for each animal. A 50µl aliquot of serum from each sample collected was stored separately for parathyroid hormone analysis. All serum samples were frozen at –80°C until required for analysis.

2.6.2 Serum calcium and phosphate

Serum calcium and phosphate was measured according to the method of Moorehead and Biggs (Moorehead and Biggs, 1974) on a clinical chemistry analyser Cobas Bio 4000 series (Roche, Indianapolis, Indiana, USA), using reagents manufactured by Trace Scientific (Victoria, Australia).

2.6.3 Serum 1,25-dihydroxyvitamin D_3

Serum 1,25-dihydroxyvitamin D_3 (1,25D) was measured by a ^{125}I radioimmunoassay (RIA) (Immunodiagnostic Systems Ltd, Bolden, UK). The assay was performed in accordance with the manufacturer's instruction. In brief: serum samples were delipidated and 1,25D extracted from potential cross-reactants by incubation with a highly specific, solid phase, monoclonal anti-1,25D antibody. The purified 1,25D elute is incubated with a highly specific sheep anti-1,25D antibody. Separation of the antibody-bound tracer from the free tracer is achieved by a short incubation with anti-sheep IgG cellulose. The bound radioactivity is inversely proportional to the concentration of 1,25D. The minimum detectable concentration of the assay was 5pmol/L and at 118pmol/L, the inter-assay coefficient of variation was 5%.

2.6.4 Serum 25-hydroxyvitamin D_3

Serum 25-hydroxyvitamin D_3 (25D) was measured by a ^{125}I radioimmunoassay (RIA) from Immunodiagnostic Systems (Bolden, Tyne & Wear, UK). This method involves the extraction of 25D, followed by incubation with both ^{125}I-25D and a highly specific sheep anti-25D-antibody. Separation of the antibody-bound tracer from the free tracer is achieved during a short incubation step with anti-sheep IgG cellulose. The bound radioactivity is inversely proportional to the concentration of 25D. The minimum detectable concentration of the assay was 3.0nmol/L and at 136nmol/L and the inter-assay coefficient of variation was 5%.

2.6.5 Serum parathyroid hormone

Serum parathyroid hormone (PTH) was measured using a rat-specific, two-site immunoradiometric assay (IRMA) from Immutopics Inc. (San Clemente, California, USA). Both intact PTH (1-84 amino acids) and N-terminal PTH (1-34 amino acids) are immunologically bound by an immobilised antibody and a radiolabelled antibody, to form a sandwich complex. The levels of the radioactively bound complex are then measured in a gamma counter, Crystal II, Multidetector RIA System from Packard Instruments Inc. (Downers Grove, Illinois, USA). The minimum detectable concentration of the assay was 1.0 pg/mL and at 50pg/mL, the inter-assay coefficient of variation was 4%.

2.6.6 Serum Fibroblast Growth Factor 23

FGF23 was measured using a two-site enzyme-linked immunosorbent assay kit from Kainos Laboratories (Bunkyo-ku, Tokyo, Japan) according to manufacturer's instructions. In brief: the assay uses two specific murine monoclonal antibodies bind to full-length FGF-23. One antibody is immobilized onto the microtiter plate well for capture, the other antibody is conjugated to HRP (horseradish peroxidase) labelled antibody to form a "sandwich" complex. The sandwich complex immobilized on the well is incubated with a substrate solution and

then measured by a spectrophotometric microtiter plate reader from Bio-TeK (Burleigh, QLD, Australia). The enzymatic activity of the complex bound to the well is directly proportional to the amount of FGF-23 in the sample. A standard curve is generated by plotting the absorbance versus each concentration of FGF-23 standards. The concentration of FGF-23 in the sample is determined from this curve.

2.7 BONE HISTOLOGY

All bones collected at time of death were dropped straight into tubes and immediately frozen in dry-ice and stored at -80°C until required.

2.7.1 Fluorochrome labelling injections

Demeclocycline hydrochloride and calcein were used as the two flurochrome agents to label bone forming surfaces. Demeclocycline hydrochloride (Lederle, NSW, Australia) was prepared by adding 300 mg of demeclocycline hydrochloride to 10 mL of 0.9% saline for a final concentration of 30mg/ml and then stirred for 2 hours prior to centrifugation to spin down any precipitants. A 10mg/kg injection of demeclocycline hydrochloride was performed intraperitoneally 6 days prior to killing mice. Calcein was prepared by adding 0.1g of calcein and 0.1g of sodium bicarbonate to 10 mL of 0.9% saline to achieve a final concentration of 10mg/ml, and then stirred for 1 hour to allow dissolution. Intraperitoneal injection of calcein label was performed 2 days prior to killing mice at the dose of 10mg/kg.

2.7.2 Bone preparation for dynamic histomorphometry

Tibiae were de-fleshed before being placed in 10% formalin at 4°C for 2 hours. The proximal end of the tibia was then sliced using a slow speed saw from Beuhler Ltd. (Lake Bluff, Illinois, USA) equipped with a diamond tipped blade bathed in 70% ethanol (van Moppes, Gloucester, UK) to expose the epiphyseal and metaphyseal regions. Bone samples were dehydrated in graded ethanol (70%, 90%, 2 x 100%) for 1 hour each, then transferred into two

changes of methylmethacrylate (MMA) and 10% w/v K-Plast plasticiser (Medim, Giessen, Germany) each for 10-14 days. 4mL of the final embedding mixture containing MMA, 10% w/v plasticiser and 0.9% (w/v) K-Plast initiator (peroxydicarbonate – perkadox 16) (Medim, Giessen, Germany) was poured into 25mL polypropylene tubes and the cut bone surface facing down. The tubes were tightly capped and transferred to a 37°C water bath for 24 hours polymerization in the fume hood. The embedded samples were cut from the tubes using a band saw and fixed to aluminium block holders (Bio-Rad, Gladesville, NSW, Australia) with araldite glue (Selleys, Padstow, NSW, Australia).

Following embedding, the samples were trimmed to expose the sample area by removing and discarding 10µm sections with a motorised microtome (Reichert-Jung, Holly, Michigan, USA). To expose the maximal epiphyseal and metaphyseal area, the samples were trimmed to the midline of the tibia. The exposed sample area was then moistened with demineralised water and three consecutive 5µm sections were cut and placed onto glass slides. Sections were flattened onto the slides following immersion in a 30:70 mixture of ethylene glycol mono-ethyl ether (Merck, Kilsyth, Victoria, Australia) and 70% ethanol (spreading solution) heated to 65-70ºC. Polyethylene plastic was dipped into the spreading solution before clamping to the slide with the catridge paper. The slides were placed in the 37°C oven overnight. Prior to staining, MMA was removed by 15 minute immersions in 100% acetone. Sections were then dehydrated in ethanol (2 x 100%), cleared in xylene (2 x 100%) and mounted in xylene-based moutant Eukill (Kinder GmbH and co., Freiburg, Germany). Unstained sections were used to measure the inter-label distance of demeclocycline hydrochloride and calcein flurochrome agents to calculate mineral apposition rate (MAR) and bone formation rate (BFR).

2.7.3 Tartrate resistant acid phosphatase (TRAP) staining of osteoclasts

Sections were immersed 3 times in histolene for 10 minutes and rehydrated in graded ethanol (100%x2, 95%, 90%, 75%, 50%) and demineralised water for 3 minutes each. Fixative solution was prepared in a glass bottle by adding 25mL of citrate solution, 65mL of acetone, 8mL of 37% Formaldehyde. Slides were fixed by immersion in fixative solution for 30 seconds and rinsed thoroughly in pre-warmed demineralised water. Diazotised Fast Garnet GBC solution was prepared by adding 0.5mL of Fast Garnet GBC base solution to 0.5mL of sodium nitrite solution and inverted for 30 seconds. The tartrate acid phosphatase solution was prepared by adding 1mL of the diazotised fast garget solution to a 100mL beaker with 45mL of prewarmed demineralised water, 0.5mL of naphthol AS-BI phosphate solution, 2mL of acetate solution and 1mL of tartrate solution. The mixed solution was then transferred to coplin jars. Fixed slides were immersed and incubated in the staining solution for 1 hour at 37°C in water bath protected from light. Slides were then rinsed thoroughly in demineralised water and counterstained in Hetamoxylin solution for 2 minutes and rinsed in alkaline tap water for several minutes until the nuclei turned blue. Slides were then air dried. Images were captured microscopically using an Olympus BH-2 microscope (Olympus, Bunkyo-ku, Tokyo, Japan) interfaced with a Quantimet 520 Image Analysis System (Cambridge Instruments, Middlesex County, Massachusetts, UK). The TRAP positive osteoclasts were evaluated using ImageJ software analysis.

2.8 BONE MICRO-COMPUTED TOMOGRAPHY

Tibiae and vertebrae were removed from the -80°C freezer and were packed tightly into plastic micro-CT tubes with soaked 70% ethanol gauze and tissue paper prior to scanning. Tibial and vertebral micro-architecture were analysed using a high resolution micro-CT system (Skyscan 1174, Kartuizersweg, Kontich, Belgium) to obtain multiple x-ray transmission images at scanning resolution of 6.5µM/pixel. Cross sectional images of the bones were then reconstructed by a modified Feldkamp cone-beam algorithm, creating a

complete 3-D representation of internal microstructure with ring artefact reduction set at level 12 and beam hardening set to 20%. For tibial total bone mineral content, trabecular bone volume (BV/TV), trabecular number and trabecular thickness analysis, a 3mm proximal metaphyseal region, measured from 1mm below the growth plate, was selected. For tibial cortical bone volume, cortical width, periosteal surface perimeter and endosteal surface perimeter, a 3mm diaphysis region, measured from 4mm below the growth plate was selected. These regions have been selected as standard operating procedure for our laboratory for cortical and trabecular bone analyses. Importantly, we have excluded all trabecular bone for diaphyseal cortical bone analysis and that all epiphyseal bone was excluded for metaphyseal trabecular bone analysis For vertebral total bone mineral content, trabecular bone volume, thickness and number, the complete lumbar spine (L1) was selected. Global threshold method was used in the cortical bone analysis, while adaptive threshold with the radius of 7, constant of 10 and pre-smoothing of 1 were used in the trabecular bone analysis. These thresholding methods were performed as standard recommendations for cortical and trabecular bone analyses as described in Skyscan manuals 2008. Tibia length was measured using digital callipers.

2.9 TISSUE MESSENGER RNA ANALYSES

All tissues collected at time of death were dropped straight into tubes and immediately frozen in dry-ice and stored at -80°C until required. For kidney and liver, 1mm portions were excised approximately at the same position for each animal. For intestine, the first 5cm proximal section and for bone (femur), the complete tissue was used. All tissues were homogenised in 1mL of Trizol in a 2mL sterile eppendorf tube. For soft tissues, a micro-pestle was used to homogenise the samples. For bones, IKA T10 basic electric homogeniser (IKA, Staufen, Baden-Wurttemberg, Germany) was used.

2.9.1 Extraction of total RNA

Total RNA was isolated from whole tissues using the Trizol extraction reagent (Invitrogen, Australia). The lysate in each tube was mixed by inversion with 200uL of Chloroform for 15 seconds and incubated at room temperature for 3 minutes. The aqueous phase, containing the RNA was removed after centrifuging the mixture at 13,000 rpm at 4ºC for 15 minutes and mixed in a new tube with 500uL of isopropanol to precipitate the RNA. The samples were left at room temperature for 10 minutes before centrifuging again at 13,000rpm at 4ºC for 15 minutes. The supernatant was removed and the RNA pellet washed with 1mL of 75% ethanol. The RNA pellet was air-dried at room temperature and finally dissolved in 100µL of diethylpyrocarbonate (DEPC)-treated water.

2.9.2 Quantification of messenger RNA

Purified RNA was quantified on a Nanodrop spectrophotometer (Beckman Instruments, Fullerton, California, USA). 1uL of the RNA samples were measured at wavelengths of 260 and 280nm. The RNA was considered to be adequately pure when the ratio between A_{260} and A_{280} was 1.8 or higher.

2.9.3 Synthesis of cDNA

Messenger RNA was reverse-transcribed to generate first strand cDNA. 1ug RNA was incubated with 1uL of 200ng oligo-dT primer (Geneworks, Adelaide, SA, Australia) 1uL of reaction mixture of 1nM of dATP, dTTP, dGTP and dCTP (Geneworks, Adelaide, SA, Australia) and deionised H_2O in a total volume of 12µL. The mixture was flickspin and placed on the PCR machine at 65ºC for 5 minutes, after which it was mmediately placed on ice until the machine has reached 4ºC. The volume of RNA and deionised H_2O was added to reaction buffer (250mM Tris-HCL, pH 8.3, 375mM potassium chloride, 15mM $MgCl_2$), 10nM DTT and Superscript III reverse-transcriptase enzyme were added and heated at 50°C for 60 minutes followed by 70°C for 5 minutes.

2.9.4 Quantitative Real Time Polymerase Chain Reaction (qRT-PCR)

The mRNA of interest was analysed by real-time RT-PCR using the SYBR Green incorporation technique. All PCR reactions were carried out using the RotorGene software (QIAGEN, Flemington, Victoria, Australia) in a final volume of 10 μL and were performed in duplicate for each cDNA sample. The reaction mix consisted of 5 μL of iQ SYBR Green Supermix (Bio-Rad Laboratories, Hercules, California, USA), gene-specific forward and reverse primers (0.5 μL) (Geneworks, Adelaide, SA, Australia), and dH2O (3μL) and cDNA template (1 μL). Included in each PCR run was a no template negative control for each primer set and a known positive control where applicable. Except for the human VDR primer sequence, which we obtained from Gardiner et al., 2000, the other PCR primers were designed in-house. Primers were designed using GenBank NIH genetic database sequences, Primer-BLAST and BLAST web-based software (NCBI, Bethseda, MD, USA) to achieve mRNA specific amplification at a consistent annealing temperatures and constant PCR conditions across all primer sets. Primer sets used are summarised in Table 2.3. PCR conditions were as follows: 95°C for 15 min; 35 cycles of 95°C for 30 sec, 60°C for 30 sec and 72°C for 30 sec, followed by 72°C for 4 min and a melt-curve analysis where temperature gradually rose from 72°C to 95°C over 5 min. All PCR reactions were validated by the presence of a single predicted peak in the melt curve analysis. Relative expression of mRNA was determined using the RotorGene software comparative cycle threshold (CT) method and was normalised to the house-keeping gene of β-actin or Gapdh. β-actin and Gapdh were chosen as housekeeping genes in our experiments, were in accordance with the previously published work by our laboratory (Anderson et al., 2005; Anderson et al., 2008; Anderson et al., 2010) in RNA extracted from bone samples and cell culture. Importantly, both β-actin and Gapdh remained stable (unregulated) with the different diets and treatments. Note the use of β-actin on some occasions (chapter 4 and 5) and Gapdh on other (chapter 3) was due to the CT value of the housekeeping gene in relative to the genes of interest in the study (the house

keeping gene that would have a CT value similar to the gene of interest), to reduce the variations in the PCR reaction.

Table 2.3: Primer sequences of Forward (F) and Reverse (R) for each messenger RNA species of interest.

Species/target gene	**F/R**	**Primer sequence (5'→3')**
Human VDR	F	TCATTCTGACAGATGAGGAAGTGC
	R	TCCTGGTATCATCTTAGCAAAGCC
Mouse *Vdr*	F	CTGAATGAAGAAGGCTCCGAT
	R	AAGCAGGACAATCTGGTCATCA
Mouse *β-actin*	F	AGGGTGTGATGGTGGGAAT
	R	GCTGGGGTGTTGAAGGTCT
Mouse *Gapdh*	F	TGCACCACCAACTGCTTA
	R	GGATGCAGGGATGATGTT
Mouse *Ocn*	F	AGACCTAGCAGACACCATGA
	R	GAAGGCTTTGTCAGACTCAG
Mouse *Alp*	F	TCCTGACCAAAAACCTCAAAGG
	R	TGCTTCATGCAGAGCCTGC
Mouse *Col1*	F	AGGCATAAAGGGTCATCGTG
	R	CGTTGAGTCCGTCTTTGCCA
Mouse *Cyp24*	F	GTCACCATCATCTTCCCAAAT
	R	TTGAAAGCATCTGCCTTGTGT
Mouse *Cyp27b1*	F	GACCTTGTGCGACGACTAA
	R	TCTGTGTCAGGAGGGACTTCA
Mouse *Napi2a*	F	GCTGTCCTCTACCTGCTCGTGTG
	R	GCGTGCCCACTCCGACCATAG
Mouse *Napi2c*	F	TTGCTGCCGCTGGAGAGTGC
	R	ACTGCTTCCCTGGGGCGTCT
Mouse *Cabp9k*	F	ATGTGTGCTGAGAAGTCTCCTGCAGAAATG

	R	CATTGTGAGAGCTTTTTGAAGAAAGCTTCG
Mouse *Trvp6*	F R	TGGGGTGGTCCCTGCCCAAG GCAGCTTGCTCAGAGCCTGGA
Mouse *Rankl*	F R	TGAAGACACACTACCTGACTCCTG CTGGCAGCATTGATGGTGAG
Mouse *Opg*	F R	GTCCCTTGCCCTGACCACT GGTAACGCCCTTCCTCACAC
Mouse *Nfatc1*	F R	AGGACACCCCATTGTGCAGCT CGTCAGCCGTCCCAATGAACA
Mouse *Fgf23*	F R	GGAAGCCTGACCCACCTGT CGGCGTCCTCTGATGTAATC
Mouse *E11*	F R	AAACGCAGACAACAGATAAGAAAGAT GTTCTGTTTAGCTCTTTAGGGCGA
Mouse *Sost*	F R	CCACCATCCCTATGACGCCAA TGTCAGGAAGCGGGTGTACT
Mouse *Dmp-1*	F R	GAAAGCTCTGAAGAGAGGACGGG TGTCCGTGTGGTCACTATTTGCCT
Mouse *Phex*	F R	GAAAAGCTGTTCCCAAAACAGAG TAGCACCATAACTCAGGGATCG

2.10 WESTERN IMMUNOBLOTTING

2.10.1 Protein extraction

Proteins were extracted by a modified method from Pierce (Pierce, et al., 1987). For protein extraction from bone, the whole femur was used. For soft tissue extraction, approximately 100mg of the tissue was used. Tissues were washed 3 times in PBS then homogenised in 200uL of TKED buffer, containing; 50 mM Tris-hydrochloride (pH 7.4), 1.5 mM EDTA, 5 mM dithiothreitol (DTT), 300 mM potassium chloride (KC1) and complete protease inhibitor cocktail solution at 50uL/mL (Invitrogen, Mulgrave, Victoria, Australia). Separation of the protein fraction and the crude pellet was achieved by centrifugation at 13,000rpm for 30 mins at 4°C. Upon completion of the centrifugation, the supernatant containing the protein fraction was immediately transferred to a new tube. Concentration of the protein extracted was analysed using the Biorad-protein assay system according to manufacturer's instruction (Biorad, Australia). Protein samples were quick-frozen in dry ice to prevent protein degradation and then immediately stored at -80°C until required.

2.10.2 VDR protein immunoblotting

To determine the tissue-specific expression level of total VDR proteins in OSVDR and WT mice, 5ug of the protein extracted was separated by 10% NuPAGE Bis-Tris gel (MES-SDS, Invitrogen, Mulgrave, Victoria, Australia) at 150V for 1hour and then transferred to nitrocellulose membrane at 200mA for 1 hour. To prevent non-specific immuno-binding to the membrane, 5% skim milk powder (SMP) dissolved in Tris-buffered saline with 0.1% Tween20 (TBST) was used to block membrane overnight at 4°C. VDR protein was detected using a rat anti-VDR monoclonal primary antibody (Affinity Bioreagent, Golden, Colorado, USA) of 1:2000 dilutions in TBST+5% SMP for 2 hours at room temperature with gently rocking. Non-specific binding of the VDR antibody was removed by washing in TBST for 3×10mins with gently rocking. The VDR immuno-complex was detected using a secondary goat anti-rat polyclonal antibody with conjugated alkaline phosphatase (Millipore, Kilsyth,

Victoria, Australia) of 1:2000 dilutions in TBST/5%SMP for 1 hour at room temperature. Non-specific binding of the secondary antibody was removed by washing in TBST for 3×10mins with gently rocking. The presence of the VDR protein was visualised by adding 500uL of alkaline phosphate substrate onto the membrane and immediately identify the immuno-reactive proteins using the Typhoon PhosphoImager (GE Life Sciences, Rydalmere, NSW, Australia) at setting of 488nm (blue), 550V. The VDR protein was detected at approximately 50kDa in molecular weight.

β-actin immunoblotting was subsequently performed on the same membrane as the house-keeping protein. Since β-actin molecular weight is detected at 42 kDa, no antibody stripping of the membrane was required and membrane was washed in TBST for 3x10mins with shaking. For detection of the β-actin protein, membrane was probed with a mouse anti-β-actin monoclonal antibody (Sigma-Aldrich, Castle Hill, NSW, Australia) at 1:10,000 dilutions in TBST (no SMP) for 1hour at RT with gentle rocking, followed by washing in TBST for 3×10mins. The β-actin immuno-complex was detected using a secondary rat anti-mouse polyclonal antibody with conjugated alkaline phosphatase activity (Sigma, Australia) at 1:10,000 dilutions in TBST for 1 hour at RT, followed by washing in TBST for 3×10mins. The presence of the β-actin protein was visualised by adding 500uL of alkaline phosphate substrate onto the membrane and immediately identify the immuno-reactive proteins using the Typhoon PhosphoImager at setting of 488nm (blue), 550V.

The intensity of the detected VDR and β-actin protein bands were quantified by the ImageQuant (GE Life Sciences, NSW, Australia) software and expressed as ratio of VDR:β-actin expression.

2.11 PRIMARY BONE CELL CULTURES

2.11.1 Cell preparation and culture

The long bones of one mouse were used for each preparation, which consisted of two tibiae, two femora and two humeri were dissected and de-fleshed. The method for isolation of primary cells from long bones was a modified version from Bakker, et al., 2003. Briefly, the periosteum layer was gently scraped away and ends of bones were removed before bone marrow was flushed out with phosphate buffered saline (PBS) until the bones appeared translucent. Cleaned bones were then crushed into small pieces (0.3mm^2) and were vigorously washed 3 times in PBS to remove remaining muscle fibres. Bone chips were then incubated in 1 mL of collagenase-1 solution at 2 mg/mL (Sigma, Australia) at 37°C for 1 hr to remove remaining collagen fibers. After collagenase treatment, bone chips were washed 2x with 50 mL HANKS+10mM HEPES (Media unit, SA Pathology) by vigorous shaking before plating onto culture flasks.

Primary bone cells were cultured in osteogenic medium containing α-MEM (Media unit, SA Pathology) supplemented with 10% fetal bovine serum (FBS) (Thermo Scientific, Victoria, Australia), 100 U/mL penicillin, 100 mg/mL streptomycin, 10 mM HEPES, 2 mM L-glutamine and 100 mM ascorbate (Media unit, SA Pathology) in a humidified atmosphere of 95% air, 5% CO_2 at 37°C . Media was refreshed every third day.

2.11.2 Cell preparation for mineralisation assays

Cells were removed from flasks by incubating in 1 mL of collagenase-1 solution (2mg/mL) at 37°C for 30 min. Cells were gently washed with 2x 10 mL of HANKS+10mM HEPES and pelleted by centrifugation at 1,200 rpm for 5 mins. Cells were then resuspended in 10 mL of α-MEM supplemented with 10% FBS, 100 U/mL penicillin, 100 mg/mL streptomycin, 10 mM HEPES, 2 mM L-glutamine and 100 mM ascorbate (Complete α-MEM 10% FBS). Cell count procedure was performed by adding 10 uL of cell with 10 uL trypan blue and cells on all 5 squares were counted. The formula for total cell number was calculated as follow:

Total cell counted in 5 squares / 5 = Cells/square

Cells/square x 2 (since it was diluted ½) = Cells counted

Cells counted x 10,000 = Cells/mL

(Thus if resuspended in 10 mL, then multiply by 10x)

Cells were seeded onto 24 well-plate at 40,000 cells/well (this gives an approximate 70% confluent well) in 500 uL of the media of Complete α-MEM 10% FBS. Media was changed on the 3rd day (or when 100% confluent). To promote maturation and differentiation, FBS was reduced to 2% and supplemented with 10 mM BGP and 0.1 nM of Dexamethasone. Media was refreshed every third day.

2.11.3 Alizarin red – calcium staining

Mineralised colonies were stained for calcium deposition by firstly washed with PBS then fixed with 10% buffered formalin for 1 hr at RT. After fixation, cells were washed 3 times with RO water (Media unit, SA Pathology), followed by staining with 1% Alizarin red mixture (George T. Gurr LtD, London, England) for 5 min at RT. To remove non-specific staining, cells were washed 3 times with RO water. Alizarin red stained colonies were air dried O/N then eluted from cultures into eppendorf tubes and prepared for calcium quantification as described in 2.11.5.

2.11.4 Von Kossa – Phosphate staining

Mineralised colonies were stained for phosphate deposition by firstly fixed cells with 10% buffered formalin for 5 min at RT, followed by a gentle wash with RO water. Cells were then stained with 1% silver nitrate solution (Sigma, Australia) in bright light for 1 hr at RT. Cells were then washed gently 3 times with RO water before sodium thiosulphate (2.5%) (Sigma, Australia) were added for 5 min at RT. To remove non-specific staining, cells were washed 3 times with RO water. Von Kossa stained colonies were air dried O/N then eluted from cultures and quantified using a spectrometer.

2.11.5 Calcium quantification

To quantify the calcium concentration presented in the mineralised culture, 500µl 10% acetic acid was added to dissolve the minerals for 30 min at RT, followed by heating at 85ºC for 10 min and then chilled on iced for 5 min. Undissolved minerals and solid impurities were collected by centrifugation at 13,000rpm for 15 mins at $4^{o}C$ and the supernatant containing the dissolved calcium ions was transferred to a new tube. The supernatant pH was neutralised with 10% ammonium hydroxide to 4.1 - 4.5 by adding 150uL of the supernatant to 96-well plate with 30µL 10% ammonium hydroxide. The pH of the supernatant was checked with the pH strip. Absorbance of the calcium ion was immediately read at OD_{405}.

2.12 STATISTICAL ANALYSES

2.12.1 Two-way analysis of variance

Two-way analysis of variance was used to analyse the interactions of the effects of dietary calcium and vitamin D treatment. One-way analysis of variance was used to assess the effect of OSVDR homozygous and hemizygous animals. The data were analysed in Statistical Package for the Social Sciences (SPSS) (version 9.0.2720). A value of $p<0.05$ was considered to be statistically significant

2.12.2 Tukey's post-hoc test

A Tukey's post-hoc test was used to identify the values that were significantly different from each other within data sets. The data were analysed in SPSS program.

Chapter 3

CHARACTERISATION OF THE OSVDR TRANSGENIC MOUSE

3.1 INTRODUCTION

Although there have been numerous *in vitro* studies to implicate the important role of 1,25D in the regulation of both osteoblastic and osteoclastic activity (Atkins, et al., 2007; Horwood, et al., 1998; Rickard, et al., 1995; Takeda, et al., 1999; van Leeuwen, et al., 2001), there are limited *in vivo* studies to understand the direct actions of 1,25D in the bone (Panda, et al., 2004; Song, et al., 2003). Currently the only *in vivo* data for the direct action of vitamin D signalling in osteoblast is the transgenic mouse model, OSVDR, where expression of the human vitamin D receptor (VDR) transgene is specifically over-expressed primarily in mature cells of the osteoblastic lineage expressing osteocalcin (Gardiner, et al., 2000). The 3.3 kb human VDR transgene was reported to be expressed specifically in the bones of the OSVDR transgenic animals and was not expressed in any other tissues and that total VDR protein was 4-fold greater in the bones of OSVDR (OSV3 line) compared to wild-type FVB/N (WT) animals. By two-dimensional histomorphometric analysis, OSVDR mice demonstrated site-specific anabolic bone effects, such that they have increased trabecular bone volume only in the vertebra and not in the femora or tibia, however femoral and tibial cortical bone volume were significantly greater, which consistent with a 15% overall increased tibial bone strength compared to WT animals (Gardiner, et al., 2000). The increase in bone volume is attributed to increased mineral apposition and decreased osteoclast formation, due to reduced RANKL-mediated osteoclastogenesis, while no significant effects of biochemical homeostastic hormones were observed (Baldock, et al., 2006). These results indicate that activities of vitamin D via the VDR are important in directly regulating bone cell activities. Notably, the studies previously conducted in the OSVDR animals were performed in hemizygous animals and no studies have examined the homozygous OSVDR animals.

We have obtained the OSVDR animals (OSV3 line) from Dr Edith Gardiner and Dr Paul Baldock of the Garvan Institute with the major aim to address the physiological question:

What is the role of osteoblastic VDR on bone homeostasis during challenges of low dietary vitamin D and calcium? However before we can ultilise the OSVDR animals to study the effects of calcium and vitamin D deficiencies in osteoblasts, we aim to further characterise the OSVDR animals' transgene expression, biochemistry and bone morphometry, using the more sensitive analytical methods of micro-computed tomography scan (Micro-CT) and quantitative real time RT-PCR (qRT-PCR). Moreover, we aim to examine the biochemistry, bone morphometry and age effects of WT versus hemizygous versus homozygous OSVDR transgenic animals and also to examine the direct effect of increased 1,25D and VDR signalling in OSVDR osteoblast *in vitro* mineralisation. The findings from this study will provide us with important information and guidelines to design subsequent experiments to address our major aims.

3.2 METHODS

3.2.1 Animal housing

Age matched female FVB/N wild-type, homozygous and hemizygous OSVDR animals were randomly allocated into groups of 6 animals/cage. Female mice were chosen for the study to directly compare with the previous published studies (Gardiner et al., 2000, Baldock et al., 2006) and for other studies in this thesis. Our previous data has shown that osteoclast surface is the most variable parameter. The average osteoclast surface we observe in control mice is 3% with a standard deviation of 0.8%. In order to detect a difference of 20% increase in osteoclast surface in our experimental mice at a significance level of = 0.05 with 80% power requires 6 mice per group. Hemizygous OSVDR animals were bred by mating homozygous males to FVB/N wildtype females. All FVB/N animals studied were bought age-matched from Animal Resources Centre (ARC, Perth, Australia). All animals were fed a semi-synthetic diet beginning at 6 weeks of age, which contained replete levels of vitamin D of 1000 IU $VitD_3$ per kg of diet as recommended by the American Institute of Nutrition, AIN (ref AIN93). Since mice were fed 8g/mouse/day, this was equivalent to 8 IU $VitD_3$/mouse/day, plus 1 % calcium and 0.65% phosphorus was contained in the vitamin D replete diet. Animals were sacrificed at 6 and 18 weeks of age for analyses. These ages were chosen to represent growing (young) and non-growing (adult) groups of animal. All animal procedures were approved by the Institute of Medical and Veterinary Science Animal Ethics Committee.

3.2.2 Micro-computed Tomography

The micro-architecture of the tibia was evaluated using a high resolution micro-CT system at 6.5µm/pixel. A 2mm diaphysis region and 3mm metaphysis region of the left proximal tibia was used for cortical bone volume and trabecular bone volume (BV/TV) analyses respectively as described in chapter 2.8.

3.2.3 Serum Biochemistry

16-hour fasting blood samples were collected at time of death for analyses. Serum calcium and phosphate were measured using a chemistry analyser (Chapter 2.6.2). Serum 1,25D was measured by a ^{125}I radioimmunoassay (RIA) (Chapter 2.6.3). Serum PTH was measured using immunoradiometric assay (IRMA) (Chapter 2.6.5)

3.2.4 Quantitative Real-Time Reverse Transcription PCR

Total RNA was isolated from brain, intestine, kidney and femur using the Trizol extraction method as described in chapter 2.9.1. RNA was reverse transcribed from 1µg of total RNA from each sample using the Geneworks cDNA synthesis kit (Chapter 2.9.3). Human VDR, mouse Vdr, Ocn and Gapdh mRNA expression were analyzed by real-time RT-PCR using the SYBR Green incorporation technique as previously described in chapter 2.9.4. Relative gene expression was calculated using the comparative cycle threshold (ΔCT) method, using Gapdh as a house keeping gene. Sequences of the oligonucleotide primers are shown in Table 2.3.

3.2.5 Western blot of VDR proteins

Total nuclear proteins were extracted from the femurs of three homozygous OSVDR and three WT animals at 18 weeks of age as described previously in chapter 2.10.1. Western immunoblotting of VDR and β-actin proteins were performed as described in chapter 2.10.1 and 2.10.2. The intensity of the detected VDR and β-actin protein bands were quantitively analysed by ImageQuant system and expressed as ratio of VDR:β-actin expression level.

3.2.6 Primary osteoblast cell culture

Long bones of 6 week old FVB/N wild-type and hemizygous OSVDR female mice were dissected out and defleshed as described in chapter 2.11.1. Briefly, the periosteum layer was gently removed and bone marrow was flushed out with PBS. Bones were then crushed into

small pieces and cultured in 5 mL of osteogenic proliferative media of α-MEM supplemented with 10%FBS. Media was refreshed every third day until cultures were 100% confluent.

3.2.7 Preparation of cell for mineralisation assays

Osteoblast cells were collagenased from culture plates as described in chapter 2.11.2. Cells were seeded onto 24 well-plate at 40,000 cells/well (this gives an approximate 70% confluent well) in 500 uL of the media of α-MEM+10% FBS. Media was changed every third day, until 100% confluence was reached. To promote maturation and differentiation of the osteoblasts, the FBS was reduced to 2% and supplemented with 10 mM BGP and 0.1 nM dexamethozone. Media was refreshed every third day. At day 6 and day 15, cultures were ceased and analysed for mineralisation.

3.2.8 Detection of mineralisation

Mineralised colonies were stained for calcium deposition (Alizarin red) and phosphate deposition (Von Kossa) as described in chapter 2.11.3 and 2.11.4. Calcium quantification **of** the minerals were subsequently analysed by dissolving the minerals in 10% acetic acid as described in chapter 2.11.5. Absorbance of the calcium ions was read at OD_{405}.

3.2.9 Statistical analysis

One-way analysis of variance was use to assess the effect of OSVDR homozygous and hemizygous animals. Significance was set at $P \leq 0.05$.

3.3 RESULTS

3.3.1 Analysis of transgene expression by quantitative real time RT-PCR

Human VDR (hVDR) mRNA was detected in the brain, kidney, intestine and bones of the OSVDR transgenic animals and was undetectable in wild-type FVB/N (WT) animals. hVDR transgene level was 4-fold higher in the bone compared to all other tissues ($p<0.01$), followed by the intestine, brain and kidney (Figure 3.1). Mouse Vdr (mVdr) mRNA was detected in the OSVDR and WT animals. The mVdr expression was detected 3-4 fold higher in the intestine compared to all other tissues for both genotypes ($p<0.01$), followed by the kidney and the bone in both animals (Figure 3.2). To determine the regulation of the osteocalcin (Ocn) promoter and to shed light onto why hVDR transgene was also detected in non-osseous tissues, endogenous mouse Ocn mRNA was measured. Ocn was detected in the bones of both OSVDR and WT animals, with 50% higher in WT compared to OSVDR bones ($p<0.01$). Low level (50-fold less than bone) was also detected in the intestine of both animals (Figure 3.3). It is uncertain as to why endogenous mouse osteocalcin gene expression in OSVDR animal is lower than WT, I think it may be related to sample size as I only had 3 animals in each group. Importantly this did not change the protein expression of the transgene in OSVDR's bone sample (Figure 3.4).

3.3.2 Expression of the VDR protein in bones

To determine whether the mRNA expression of the human VDR transgene translates to VDR protein levels, western blot was performed on bone samples of WT and OSVDR animals using a VDR-specific monoclonal antibody that detects both human and mouse VDR protein expression. Results showed that total VDR level in bone samples of OSVDR mice were detected more intense than WT samples (Figure 3.4A). Quantification of the individual bands showed total VDR protein level was 2-3 fold higher in OSVDR compared to WT bone samples ($p<0.001$) (Figure 3.4B). Although there were low levels of the human VDR mRNA

present in kidney and brain tissues of OSVDR mice, there were no differences in the levels of VDR protein in these tissues between OSVDR and WT animals (Figure 3.5).

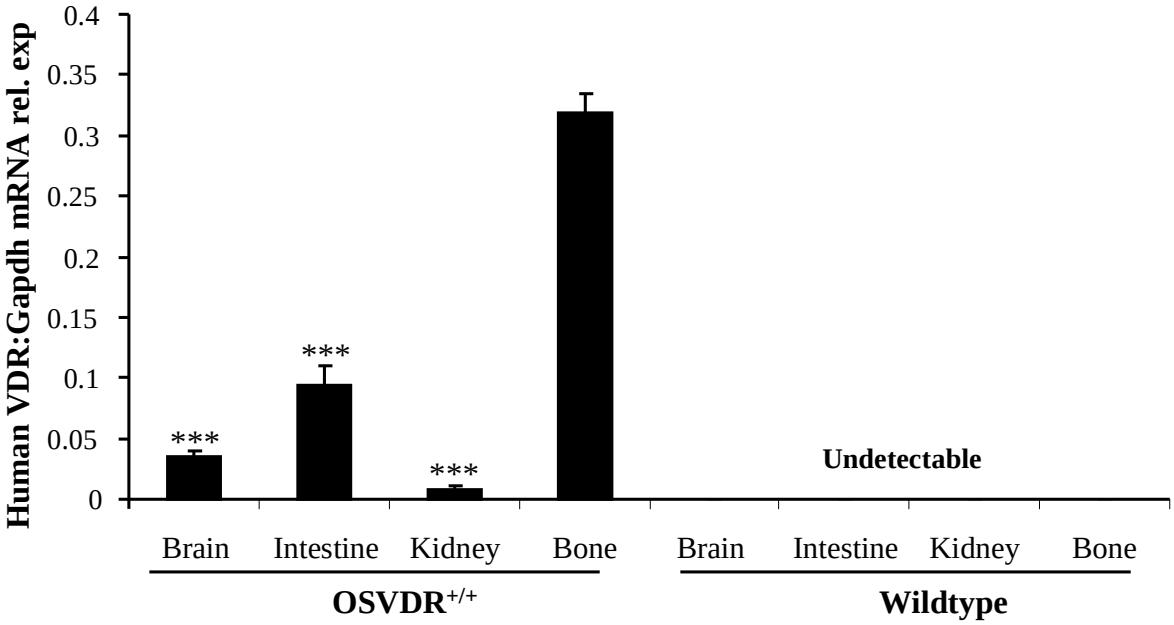

Figure 3.1 *Expression levels of the OSVDR transgene*. Total RNA was extracted from bone, kidney, intestine and brain of WT and OSVDR homozygous animals as described previously. Human VDR (hVDR) mRNA transgene was measured by quantitative real-time RT-PCR and expressed as relative expression with *Gapdh* as a house-keeping gene using the formula: $2^{\wedge -(Ct\ [gene\ of\ interest]-Ct\ [Gapdh])}$. Values are mean ± SEM of 3 animals; each animal sample was done in triplicate; ***p <0.0001 versus OSVDR bone.

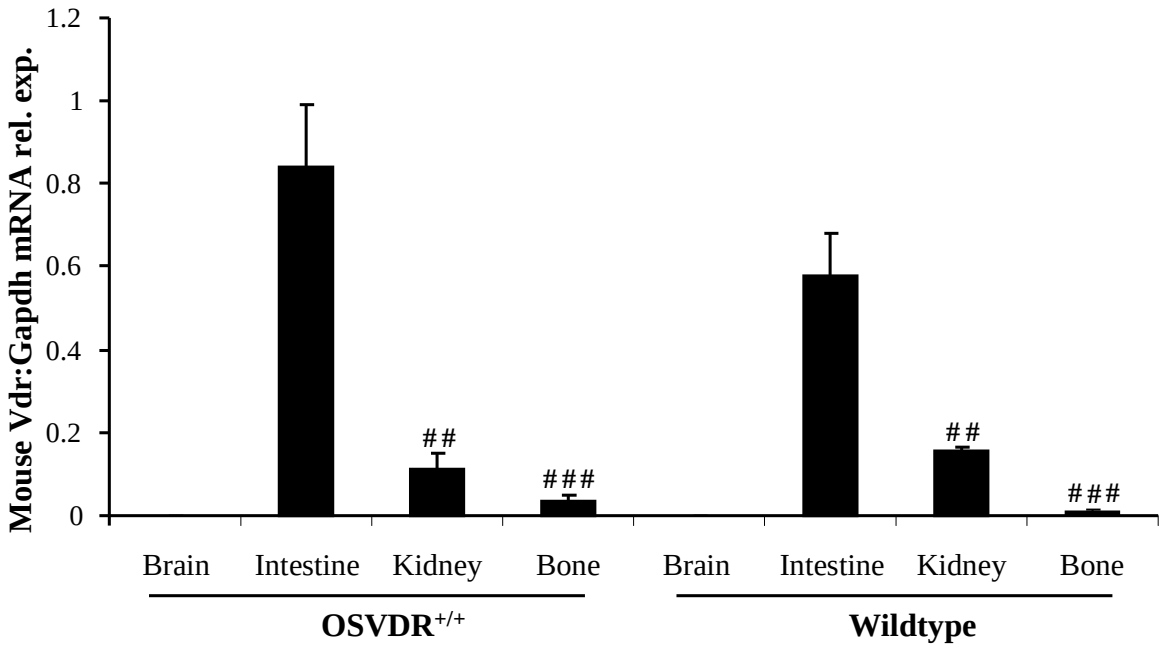

Figure 3.2 *Expression levels of the mouse Vdr mRNA in OSVDR and WT tissues.* Endogenous mouse *Vdr* mRNA expression was measured by quantitative real-time PCR and expressed as relative expression with *Gapdh* house-keeping gene using the formula: $2^{\wedge -(Ct\ [gene\ of\ interest]-Ct\ [Gapdh])}$. Values are mean ± SEM of 3 animals; each animal sample was done in triplicate; ##p<0.001 and ###p<0.0001 versus intestinal sample of the same genotype.

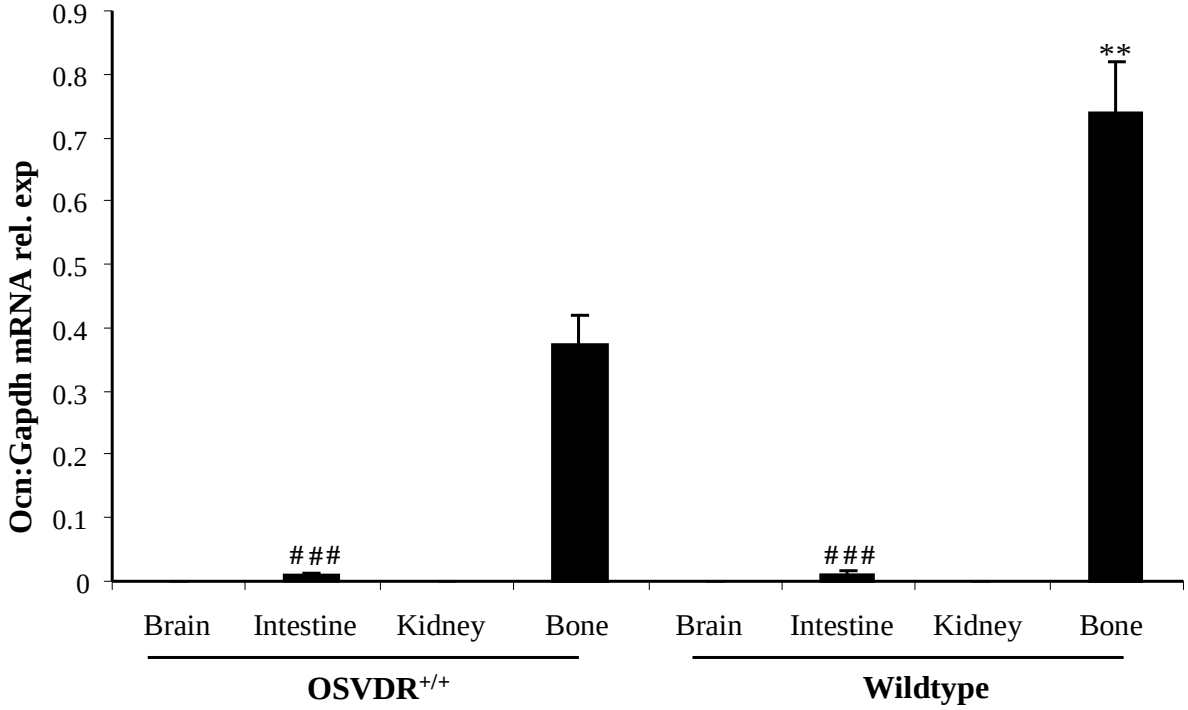

Figure 3.3 *Expression of osteocalcin mRNA in osseous and non- osseous tissues.* Osteocalcin (*Ocn*) mRNA expression was measured by quantitative real-time RT-PCR and expressed as relative expression with *Gapdh* as a house-keeping gene using the formula: $2^{-(Ct\ [gene\ of\ interest]-Ct\ [Gapdh])}$. Values are mean ± SEM of 3 animals; each animal sample was done in triplicate; **p<0.01 versus OSVDR bone; ###p<0.0001 versus bone sample of the same genotype.

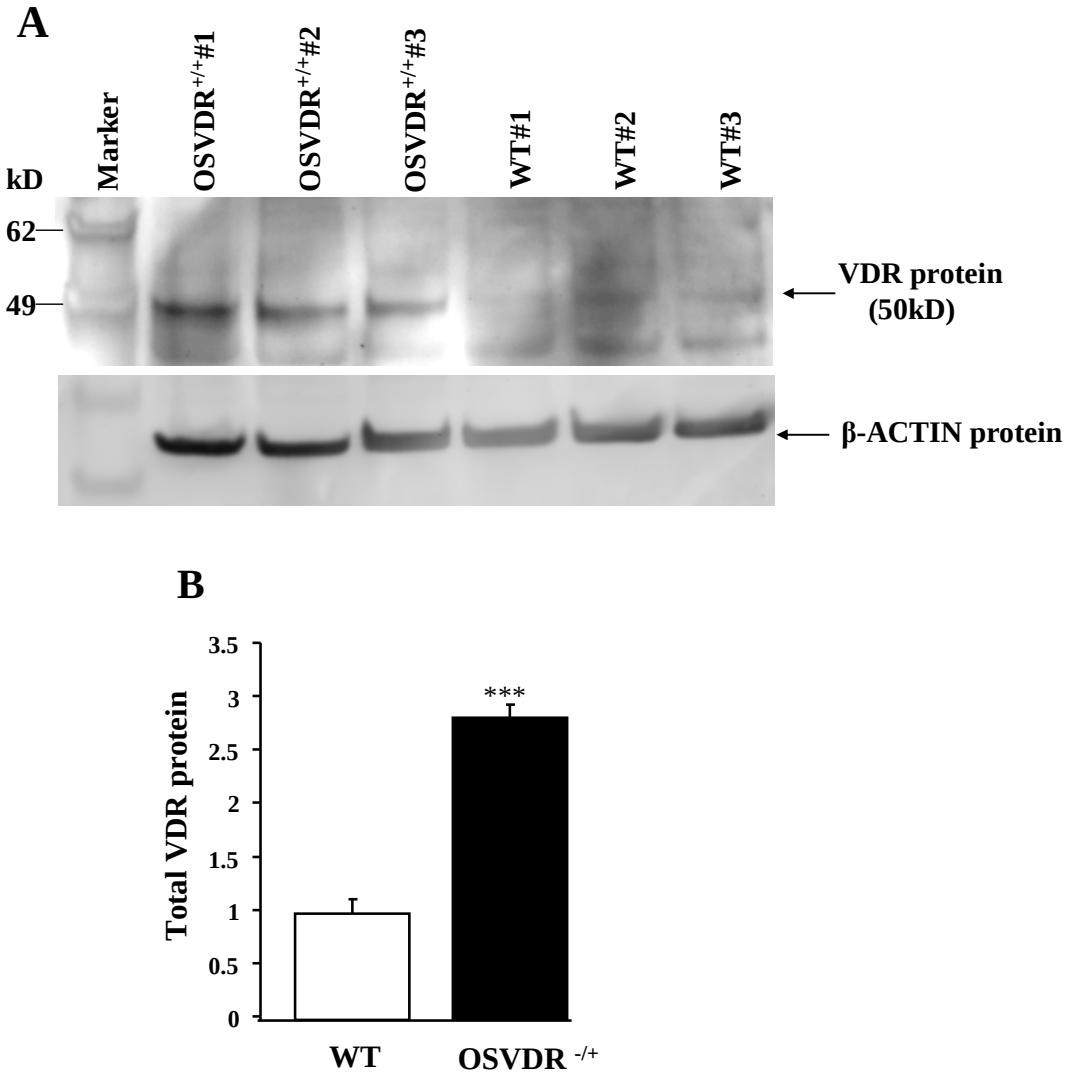

Figure 3.4 *Expression of VDR proteins in OSVDR and WT bone samples*. Total VDR protein (human and mouse) was extracted from long bones of WT (white bar) and OSVDR (black bar) homozygous animals as described previously. (**A**) VDR protein was measured by western blot using anti-VDR antibody, which cross-reacted with both mouse and human VDR protein. Three OSVDR and three WT bone samples were shown on blot. β-ACTIN expression was included as a house-keeping protein. (**B**) Expression of the VDR and β-ACTIN proteins were quantitatively analysed using ImageQ volume report method and expressed as VDR:β-ACTIN ratio. Values are mean ± SEM. ***p <0.0001 versus WT.

A

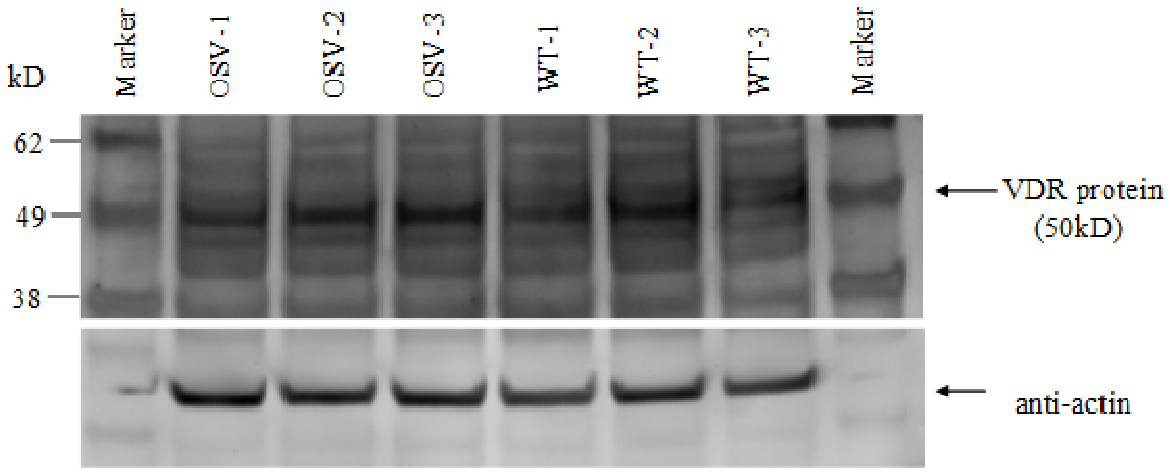

B

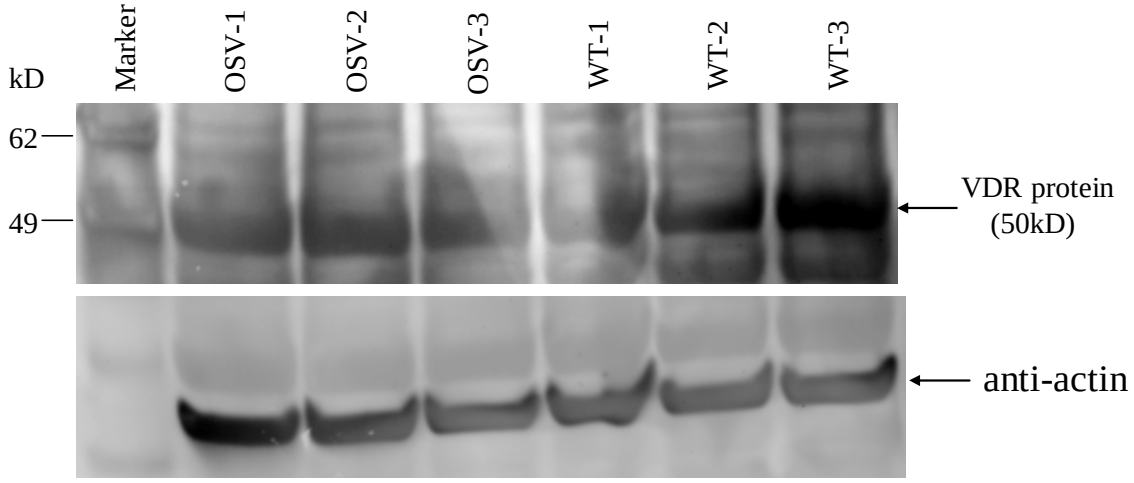

Figure 3.5 *Expression of VDR proteins in OSVDR and WT kidney and brain samples*. Total VDR protein (human and mouse) was extracted from kidney (**A**) and brain (**B**) of WT and OSVDR homozygous animals. VDR protein was measured by western blot using anti-VDR antibody, which cross-reacted with both mouse and human VDR protein. Three OSVDR and three WT samples were shown on blot. β-ACTIN expression was included as a house-keeping protein.

3.3.3 Effects of OSVDR transgene on serum biochemistry measurements

No statistical differences were observed between WT, hemizygous and homozygous OSVDR transgenic animals for serum 1,25D, phosphate and PTH at 18 weeks of age (Table 3.1). Serum calcium levels were significantly greater in homozygous compared to WT animals (2.57 ± 0.10 versus 2.12 ± 0.10, $p<0.05$). Notably, all the biochemical parameters measured were within the appropriate range for mice and they were all phenotypically comparable.

3.3.4 Characterisation of the OSVDR tibial bone volume at 6-weeks of age

Tibial cortical bone volumes were respectively 12% and 10% higher in hemizygous and homozygous OSVDR compared to WT animals of 6 weeks old ($p<0.001$) (Table 3.2). Tibial proximal metaphyseal trabecular bone volumes were respectively 30% and 25% higher in hemizygous and homozygous OSVDR compared to WT animals ($p<0.001$). The greater trabecular bone volume was associated with greater trabecular number (2.12 ± 0.11 and 2.08 ± 0.10 versus 1.58 ± 0.06: WT, $p<0.05$) for both genotype, and greater trabecular thickness in OSVDR hemizygous (39.1 ± 0.4 versus 36.7 ± 0.5: WT, $p<0.05$) compared to WT. No transgene-associated effects were seen on body weight or tibia length (Table 3.2).

3.3.5 Characterisation of the OSVDR tibial bone volume at 18-weeks of age

At 18 weeks of age the tibial cortical bone volume of hemizygous and homozygous OSVDR was approximately 12% greater over WT animals ($p<0.001$) (Table 3.3). Tibial proximal metaphyseal trabecular bone volume was approximately 30% higher in the hemizygous and homozygous OSVDR compared to WT animals at 18 weeks of age ($p<0.001$) (Table 3.3). Trabecular thickness was significantly greater in hemizygous and homozygous OSVDR compared to WT animals (51.2 ± 0.9 and 49.6 ± 0.9 versus 45.6 ± 0.9: WT, $p<0.05$) and not trabecular number (Table 3.3).

Table 3.1 Comparison of OSVDR hemizygous versus homozygous mice on serum 1,25D, calcium, phosphate and PTH at 18 weeks of age fed a regular diet.

	WT	**OSVDR$^{-/+}$**	**OSVDR$^{+/+}$**
1,25D pmol/L	76.3 ± 22.5	91.8 ± 23.7	126.3 ± 15.6
Ca mmol/L	2.12 ± 0.10	2.24 ± 0.07	2.57 ± 0.10 *
Pho mmol/L	2.04 ± 0.25	2.15 ± 0.22	2.61 ± 0.13
PTH pmol/L	10.9 ± 1.3	15.3 ± 1.8	14.1 ± 1.9

Hemizygous OSVDR, OSVDR$^{-/+}$; Homozygous OSVDR, OSVDR$^{+/+}$; 1,25-dihydrixyvitamin D3, 1,25D; Calcium, Ca; Phosphate, Pho; Parahyroid hormone, PTH; Values are mean ± SEM, n = 6; *$p<0.05$ OSVDR homozygous versus WT animals.

Table 3.2 Comparison of OSVDR hemizygous versus homozygous mice for tibial bone morphometry at 6 weeks of age.

	WT	**OSVDR$^{-/+}$**	**OSVDR$^{+/+}$**
Cort. BV (mm^3)	1.44 ± 0.04	1.63 ± 0.03**	1.58 ± 0.02**
BV/TV (%)	5.88 ± 0.29	8.49 ± 0.50**	7.67 ± 0.35**
Tb.Th (µm)	36.7 ± 0.5	39.1 ± 0.4 *	36.8 ± 0.2
Tb.N (#/mm)	1.58 ± 0.06	2.12 ± 0.11*	2.08 ± 0.10 *
Bone length (mm)	16.5 ± 0.1	16.6 ± 0.2	16.5 ± 0.2
Body weight (gram)	19.4 ± 0.3	20.2 ± 0.5	20.0 ± 0.5

Hemizygous OSVDR, (OSVDR$^{-/+}$); Homozygous OSVDR, (OSVDR$^{+/+}$); Cortical bone volume, (Cort. BV); Trabecular bone volume, (BV/TV); Trabecular thickness, (Tb. Th); Trabecular number, (Tb. N); Values are mean ± SEM, n=5. **$p<0.001$ and *$p<0.05$ of OSVDR hemizygous and homozygous versus WT animals.

Table 3.3 Comparison of OSVDR hemizygous versus homozygous mice for tibial bone morphometry at 18 weeks of age.

	WT	**OSVDR$^{-/+}$**	**OSVDR$^{+/+}$**
Cort. BV (mm^3)	1.68 ± 0.03	1.92 ± 0.05**	1.93 ± 0.05**
BV/TV (%)	6.32 ± 0.28	8.11 ± 0.65**	8.09 ± 0.70**
Tb.Th (µm)	45.6 ± 0.9	51.2 ± 0.9*	49.6 ± 0.9*
Tb.N (#/mm)	1.39 ± 0.08	1.58 ± 0.12	1.64 ± 0.15
Bone length (mm)	17.5 ± 0.1	17.4 ± 0.1	17.2 ± 0.1
Body weight (gram)	22.9 ± 0.5	21.9 ± 0.6	22.5 ± 0.6

Hemizygous OSVDR, (OSVDR$^{-/+}$); Homozygous OSVDR, (OSVDR$^{+/+}$); Cortical bone volume, (Cort. BV); Trabecular bone volume, (BV/TV); Trabecular thickness, (Tb. Th); Trabecular number, (Tb. N); Values are mean ± SEM, n=5; **$p<0.001$ and *$p<0.05$ of OSVDR hemizygous and homozygous versus WT animals.

3.3.6 In vitro mineralisation of OSVDR osteoblast

To determine whether the OSVDR transgene could directly affect osteoblast activity, osteoblasts from the long bones of WT and hemizygous OSVDR animals were isolated and cultured in pro-differentiation media and allowed to mineralise. At 6 and 15 days, the cultures were stopped and prepared for calcium and phosphate staining. In OSVDR cultures, both calcium, as measured by Alizarin red (Figure 3.6A a, b, e, f) and phosphate as measured by Von Kossa (Figure 3.6B c, d, g, h) showed greater staining, which were more distinct at 6 days of culture compared to WT osteoblasts. There was no significant difference in the ability of osteoblasts isolated from OSVDR animals to deposit calcium compared to WT osteoblasts at 6 days ($p=0.09$) and 15 days culture ($p=0.28$) (Figure 3.6C).

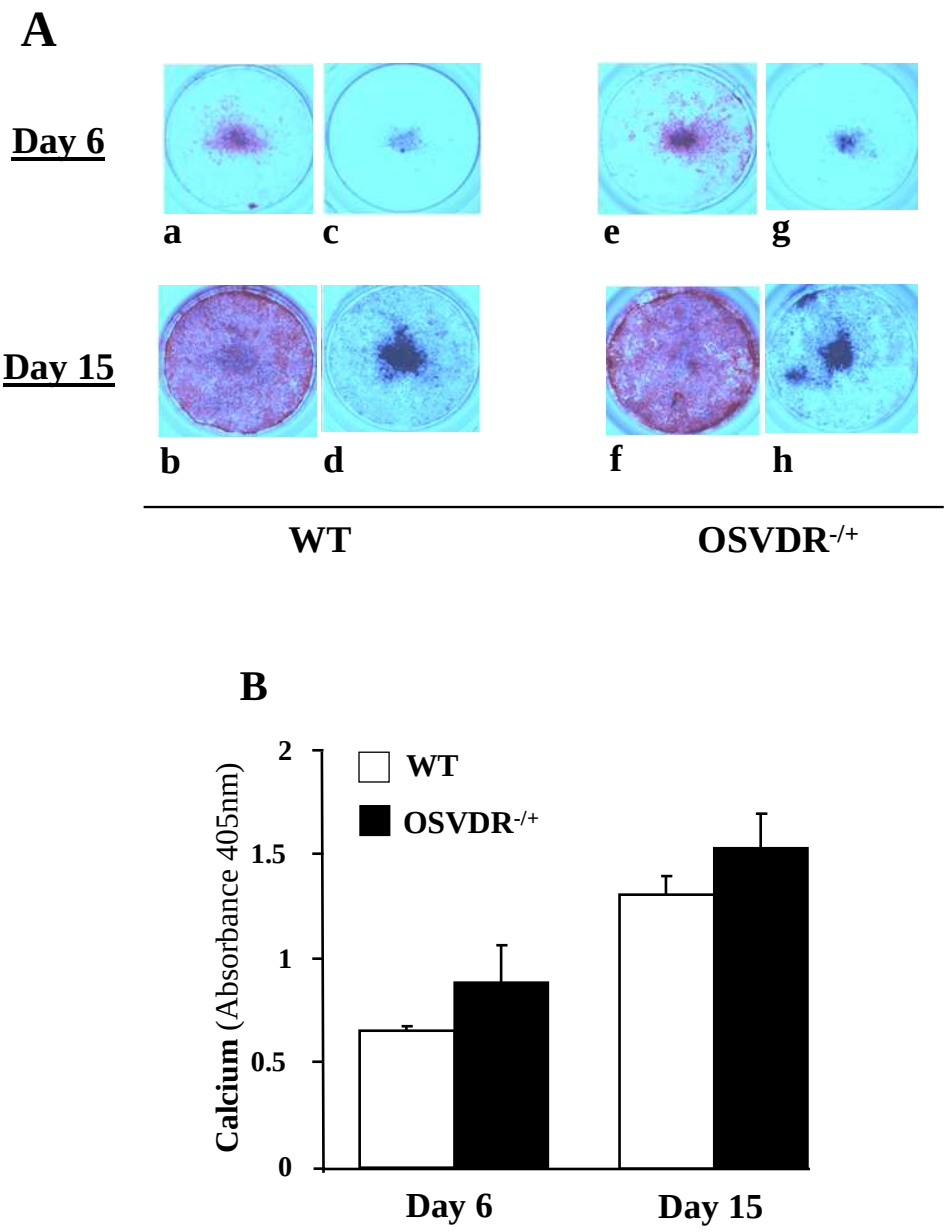

Figure 3.6 *The effect of increased VDR in mature osteoblasts on mineralisation.*

Long bones of 6-weeks old WT (white bar) and OSVDR (black bar) hemizygous animals were prepared for primary osteoblast cell cultures. (**A**) The osteoblasts were cultured in osteogenic differentiation medium for 15 days and examined for ability to mineralise by Alizarin red stains (a,e,b,f) and Von Kossa stains (c,d,g,h). (**B**) Calcium quantification by absorbance analysis as described previously. Values are the mean ± SEM, n=3 animals of each genotypes; each animal was done in triplicate; experiment repeated 2 times.

3.4 DISCUSSION

3.4.1 Validation of human VDR transgene specific expression

In this study, we have successfully validated that the human VDR transgene expressed specifically in OSVDR tissues and was not present in WT tissues. Furthermore, mouse VDR expression was not affected by the transgene expression since both WT and OSVDR tissues achieved comparable expression levels. However using the sensitive quantitative real-time RT-PCR method, we were able to detect low levels of human VDR transgene in other tissues of the OSVDR animals. The real-time PCR method offers greater sensitivity over other techniques of mRNA analysis, such that of the Northern blot analysis, which was used to analysed the OSVDR human VDR transgene expression in the earlier Gardiner *et al.,* study (Gardiner, et al., 2000). One obvious advantage is the sensitivity of real-time PCR for the detection of low abundance mRNA species and therefore significantly smaller amounts of starting material are required than that in the Northern blot procedure. This would explain why low expression of the human VDR transgene in other tissues was not previously detected by Northern blot (Gardiner, et al., 2000). Furthermore, the expression of human VDR transgene in other OSVDR tissues may reflect the low level of induction of the osteocalcin promoter used to drive the OSVDR transgene in tissues other than bone. Studies have shown that osteocalcin is expressed in non-osseous tissues such that of the brain, lungs, liver, kidney and intestine (Sims, et al., 1997). However, the highest expression of osteocalcin resides within the bones and more primarily within mature and mineralising osteoblast cells (Bilic-Curcic, et al., 2005; Lian, et al., 1998). Consequently the relative expression of the human VDR mRNA was 4-fold greater than that found in other tissues, which translated to a 3-fold greater VDR protein level. There was no difference in VDR protein levels in the kidney nor brain of WT when compared to OSVDR animals (Figure 3.5A and B). These findings provided us with confidence that the effects associated with the OSVDR transgenic animals are due primarily to the increased VDR activity within the bone.

3.4.2 Characterisation of the hemizygous and homozygous OSVDR transgenic animals

Important considerations should be taken when working with transgenic mice formed by micro-nuclear injection which was the technique used to generate the OSVDR transgenic mouse, such as the random insertion of the transgene potentially could cause disruption of endogenous functioning genes thus inducing unanticipated effects. Also, a transgene may be inserted in front of an endogenous enhancer which can stimulate inappropriate gene activity. These effects may not show if the genes disrupted are recessive, i.e disruption of only one allele in the case of hemizygosity, but may be present in homozygous transgenic animals. There have been no studies which have established whether the homozygous OSVDR transgenic animals are comparable to hemizygous animals that were previously published (Baldock, et al., 2006; Gardiner, et al., 2000; Misof, et al., 2003). Furthermore, the question of whether the homozygous genotype causes transgene-dose dependent effects of increased VDR expression in mature osteoblast and osteocytes remains unanswered. It appeared that in terms of the biochemical and histomorphometric results, the effect of over-expression of VDR does not provide a dose-dependent effect on bone volume. While this suggests that hemizygous mice provide maximal effects of increased VDR, the precise reasons for the lack of dose-dependency are worth further investigation.

Since previous studies have shown that the tibia is a significant site for the anabolic bone effects of OSVDR transgene, we have sought to use this site to establish the characterisation of the OSVDR homozygous bone phenotype. Using the more sensitive method of Micro-CT scan (Barou et al., 2002; Muller et al., 1997; Thomsen et al., 2005), the transgene anabolic effect is observed in tibial trabecular bone as well as cortical bone volume, consistent with published results in hemizygous OSVDR animals (Gardiner, et al., 2000). Furthermore, with the present quantitative method, we have also shown at 6 weeks of age the OSVDR anabolic bone phenotype could be observed in both the hemizygous and homozygous animals. This suggests that increased levels of VDR in mature osteoblastic allowed early growth advantages, suggesting that even during periods of increased cell activities of modelling,

VDR-mediated activities are important. Exactly how this process occurs will be an interest for future investigation and whether this is also evident *in utero* remains to be established. Study in chondrocyte-specific CYP27B1KO mice embryos showed an increased in the hypertrophic zone of the mouse growth plate at embryonic 15.5 day (Naja, et. al., 2009). By contrast, chondrocyte-specific CYP27B1 transgenic embryos have reduced width of the hypertrophic zone (Naja, et. al., 2009), suggesting a role for extra-renal metabolism of vitamin D in mediating the skeletal effects *in utero*. Moreover, studies in humans showed children born to mothers with vitamin D deficiency (less than 25nM) during pregnancy exhibit defects in bone mineral content at 9 years of age (Javaid, et. al., 2006). Pregnant mothers who have sufficient vitamin D (greater than 75nM) have been shown to have foetuses that were associated with increased femur metaphyseal cross-sectional area and femur splaying index at 19 and 34 weeks of gestation as shown by a high-resolution 3D ultrasound system (Mahon, et. al., 2009).

Our study showed at 6 weeks of age the increased OSVDR trabecular bone volume phenotype was associated with greater trabecular number, however at 18 weeks of age the increased bone volume in OSVDR animals was associated with increased trabecular thickness, suggesting that as the animal matures, vitamin D activity in osteoblasts mediates processes of bone resorption as well as bone formation. These findings are supported by Baldock et al., they showed that OSVDR osteoblasts in co-culture experiments had reduced capacity to support osteoclastogenesis via reduced RANKL:OPG ratio and that mineral apposition was increased in OSVDR animals (Baldock, et al., 2006). Future investigation into osteoblast and osteoclast numbers in these OSVDR animals will be necessary to establish the relative role of formation and resorption in early and late stages of development.

With regards to serum biochemical analyses, we observed no transgene dose-dependent effects on serum 1,25D, phosphate and PTH. Interestingly OSVDR homozygous animals fed a regular diet have significantly higher serum calcium compared to WT animals. Although a direct effect of increased VDR levels in osteoblasts has been proposed for the OSVDR

transgenic animal (Baldock, et al., 2006; Gardiner, et al., 2000), an indirect effect of OSVDR cannot be ruled out since we also observed the human VDR transgene to also be expressed in tissues other than the bone, such as the intestine and kidney (Figure 3.1), suggesting that increased vitamin D activity in these tissues may contribute to the anabolic effects seen in OSVDR transgenic animals and affecting calcium homeostasis.

3.4.3 Effects of increased VDR in mature osteoblasts and mineralisation

In vitro studies in osteoblasts suggest that 1,25D acting via the VDR can inhibit osteoblastic cell proliferation, while stimulating differentiation and mineralization (Atkins, et al., 2007; Matsumoto, et al., 1991), however some contradictory effects have been described (Owen, et al., 1991; Sooy, et al., 2005). These differences could be attributed to various causes such as origin of the osteoblasts e.g. bone marrow, long bone or calvaria-derived, the absence of regulatory hormones and cytokines, mechanical loading, interactions with other cells, differentiation status of the osteoblasts and *in vitro* culture conditions, all may play a significant role in the ultimate response to 1,25D. Our investigation using the *in vitro* mineralisation assay demonstrates that increased 1,25D-VDR signalling osteoblasts have no statistically significant effect on mineralisation compared to WT osteoblasts.

Technically it was difficult to isolate pure primary osteoblasts, which created problems for accurate comparison across different cell culture preparations. Additionally, the cultures contained osteoblasts of different differentiation status, such as osteoblast precursors, immature osteoblast, mature osteoblasts, pre-osteocytes and osteocytes. Thus, as discussed above, since 1,25D can regulate these osteoblastic cells differently at different stages, it is difficult to measure the effects of 1,25D on proliferation and differentiation in our cultures. Whether this mild increase in OSVDR mineralisation was due to enhancement of osteoblasts proliferation or differentiation warrants future investigation. Furthermore, whether the levels of 1,25D in the media were sufficient to induce observable changes in this study is questionable. Therefore future experiments to include isolation of pure population of

osteoblasts which are of the same differentiation status and treatment with higher doses of 1,25D to OSVDR osteoblasts should be included. To isolate a pure osteoblast progenitor cell population, an experiment such as dual-colour fluorescence activated cell sorting (FACS), utilising the specific expression of osteoblastic markers such as alkaline phosphatase and parathyroid hormone-related protein receptor as described previously (Purpura, et al., 2003), or alternatively the method of magnetic cell sorting using STRO-1 antibody can also be employed (Oyajobi, et al., 1999). However these experiments were out of the scope for this thesis. *In situ* hybridisation and immunohistochemistry showed that the human VDR transgene and protein are present in osteocytes as well as in osteoblasts (Gardiner, et al., 2000), furthermore using osteocalcin-promoter driven GFP expression, osteocalcin expression was shown to be expressed in osteoblasts on the bone surface as well as osteocytes within the bone (Bilic-Curcic, et al., 2005), therefore the possibility that the OSVDR animal is an osteocytic model could not be excluded. Indeed in unpublished data (Anderson, unpublished findings), OSVDR mice respond to mechanical bone loading by markedly enhancing woven bone formation, mineralising surface and bone formation rate, which presumably is due to increased osteocyte activity. Furthermore, OSVDR microarray data using cortical bone mRNA, demonstrate that the bone expression of the osteocyte genes Dkk1 and Mepe are more than 2-fold lower in OSVDR mice when compared to WT levels (Anderson, unpublished findings). Recently, SOST and FGF23, which are osteocyte specific markers (Moester, et al., 2010; Ubaidus, et al., 2009) have been found to contain putative VDRE and can directly reponse to 1,25D treatment ((Liu, et al., 2006) unpublished data for SOST) were found to be increased in OSVDR bones (Atkins, unpublished findings). Additionally, osteocytes have been shown to regulate osteoblast and osteoclast formation and activation (as recently reviewed by Henriksen, et al., 2009), indicating the important of osteocytes in regulating bone cell activities. The direct and indirect effects of enhancing 1,25D signalling for osteocytic function, density and apoptosis are the subjects of ongoing investigation in our laboratory.

In summary, we have shown that OSVDR animals when fed sufficient levels of vitamin D and calcium have greater trabecular and cortical bone volume compared to WT animals. The anabolic bone effects of the homozygous OSVDR animals were consistent with hemizygous animals. Unlike what had previously published, the OSVDR transgene was also found to be expressed in tissues other than the bone such as the intestine and the kidney, therefore we cannot rule out the possibility that the anabolic bone effect in OSVDR mice may also involve the intestine and kidney, possibly contributing to calcium homeostasis. We thus anticipate that the OSVDR transgene exhibits wider effects on non-osseous tissues and also on osteocytic activity. Importantly, we have provided further evidence that 1,25D-VDR activity in the bone is important for bone cell activities and for skeletal homeostasis.

Chapter 4

THE ROLE OF VITAMIN D RECEPTOR IN OSTEOBLASTS DURING VITAMIN D DEFICIENCY

4.1 INTRODUCTION

Vitamin D is an important regulator of calcium and phosphate homeostasis. Activation of vitamin D activity occurs in response to hypocalcemia, where the major form of vitamin D metabolite in the circulation, 25-hydroxyvitamin D (25D) is hydroxylated by the renal activity of 25-hydroxyvitamin D 1-α hydroxylase (CYP27B1) enzyme to form the active hormone 1,25 dihydroxyvitamin D (1,25D). 1,25D mediates up-regulation of intestinal calcium absorption and restores serum calcium to normal levels, 1,25D also up-regulates the transcription of the 25-hydroxyvitamin D 24-hydroxylase (CYP24) enzyme, which catalyses the catabolism of 1,25D reducing its level in serum (Christakos, et al., 2010; Omdahl, et al., 2001). It is well established that maintaining an adequate vitamin D status throughout life is required to prevent the bone mineralisation defects of osteomalacia and osteoporosis. In humans and rodents, serum 25D levels below 20 nmol/L result in hypocalcaemia, hypophosphateamia, secondary hyperparathyroidism and osteomalacia (Bronner, 1976; Dardenne, et al., 2004). Although the level of 25D required to prevent osteoporosis is still controversial, it is generally accepted that patients with levels around 40 nmol/L develop osteoporosis rather than osteomalacia (Gallagher, 1990; Lore, et al., 1981) and it is only when levels of above 80 nmol/L are achieved that optimal bone mineral content is maintained in both humans and rodents (Anderson, et al., 2008; Bischoff-Ferrari, 2008).

1,25D mediates the majority of its actions via binding to vitamin D receptor (VDR) which is located in cells and tissues throughout the body, including the bone (Anderson and Atkins, 2008; Valdivielso, 2009). In addition to its well described roles in the regulation of intestinal calcium absorption, 1,25D also has recognised roles in the bone, regulating both osteoblast and osteoclast activities (Atkins, et al., 2007; Kogawa, et al., 2010; Kogawa, et al., 2010; Tang, et al., 2010; van Leeuwen, et al., 2001). Recently, it has been shown that osteoblasts are also capable of converting 25D to 1,25D via the activity of bone CYB27B1 making local

1,25D, which can directly regulate osteoblastic proliferation, differentiation and mineralisation (Anderson, et al., 2010; Anderson, et al., 2005; Atkins, et al., 2007; van Driel, et al., 2006) suggesting that vitamin D has autocrine and paracrine roles within the skeleton. Interestingly studies from our laboratory have shown that the major source of 1,25D for osteoblasts is the locally produced 1,25D and not the 1,25D from the circulation (Anderson, et al., 2005). Furthermore, serum 25D levels of less than 25nmol/L in rodents have been shown to be substrate limiting (Anderson, et al., 2008) for osteoblast to induce bone CYP27B1 mRNA expression, unlike the kidney, where CYP27B1 is able to be induced at levels below 20nmol/L (Anderson, et al., 2007). However, the questions of the relative importance of vitamin D stimulation of intestinal calcium absorption and the direct actions of vitamin D in osteoblasts whether via the locally produced 1,25D or 1,25D from the circulation to maintain a healthy skeleton have not yet been addressed. Furthermore, the question of what roles does vitamin D activity play in bone cells during conditions of vitamin D depletion is unanswered.

With the exception of the OSVDR mouse there have been no published data on vitamin D osteoblast cell-specific activity in an *in vivo* setting. OSVDR animals with transgenic elevation of VDR in mature osteoblasts exhibited cortical bone that was 5% wider and 15% stronger, due to a doubling of periosteal mineral apposition rate without altered body weight or calcium homeostatic hormonal levels (Gardiner, et al., 2000). Furthermore, a 20% increase in vertebral trabecular bone volume was observed in the transgenic animals, which was associated with 30% reduction in resorption surface and greater mineral apposition (Gardiner, et al., 2000). It was latter discovered that OSVDR osteoblasts have reduced OPG levels both *in vivo* and *in vitro*, resulting in reduced RANKL:OPG ratio and inhibition of osteoclastogenesis in OSVDR animals compared with WT animals (Baldock, et al., 2006). These findings provided important evidence that vitamin D activity via the VDR in cells of the mature osteoblastic lineage, regulate bone remodelling, bone architecture and bone strength.

In this study we aim to use the OSVDR transgenic mouse to investigate the role of vitamin D in osteoblasts during vitamin D deficiency. We hypothesised that vitamin D activity in the bone is essential for osteoblastic function and that increase sensitivity of vitamin D signalling in mature osteoblastic lineage cells will protect the skeleton from bone loss due to vitamin D deficiency. Understanding the activities of vitamin D within the skeleton which is independent of other recognised roles for vitamin D, may resolve the controversy regarding its role in the prevention of osteoporosis, and provide the molecular basis for health recommendations for vitamin D supplementation to reduce the risk of fractures.

4.2 METHODS

4.2.1 Mice and dietary vitamin D restriction

Age matched female FVB/N wild-type and homozygous OSVDR animals were randomly allocated into groups of 5 animals/cage. All FVB/N animals studied were bought age-matched from Animal Resources Centre (ARC, Perth, Australia). All animals were fed a semi-synthetic diet beginning at 4 weeks of age, which contained either replete levels of vitamin D+ of 1000 IU $VitD_3$ per kg of diet (ref AIN93) or deplete levels of vitamin D-, which contained 0 IU $VitD_3$ per kg of diet (recommended by the American Institute of Nutrition, AIN), plus 1 % calcium and 0.65% phosphorus was contained in both the vitamin D replete and deplete diets. The vitamin D+ and D- dietary amounts have been shown in rats to achieve circulating 25D levels above 80 nmol/L and below 20nmol/L respectively, representing vitamin D sufficient and deficient amount (Anderson et al., 2008). Animals were selected at 4 weeks of age to represent a young and growing metabolic state. We hypothesised that increase VDR activity in mature osteoblasts has early growth advantages and will protect the skeleton from bone loss due to vitamin D deficiency. Female homozygous animals were chosen for this study to directly compare with the previous published studies of OSVDR animals (Misof et al., 2003, Gardiner et al., 2000). Our previous data has shown that osteoclast surface is the most variable parameter. The average osteoclast surface we observed in control mice is 3% with a standard deviation of 0.8%. In order to detect a difference of 20% increase in osteoclast surface in our experimental mice at a significance level of = 0.05 with 80% power requires 6 mice per group. Unfortunately at the beginning of the study, there was an unexpected death of one mouse in one of the groups, therefore the number was reduced to 5 mice per group to minimise variation due to housing conditions. Animals were sacrificed at 20 weeks of age for analyses.

4.2.2 Micro-computed Tomography

The micro-architecture of the tibia (left) and vertebra (L1) was evaluated using a high resolution micro-CT system at 6.5um/pixel. A 2mm diaphysis region and 3mm metaphysis region of the left proximal tibia was used for cortical bone volume and trabecular bone volume (BV/TV) analyses respectively as described in chapter 2.8. The same 2mm region of cortical bone volume was used to determine cortical width and periosteal and endosteal surface perimeters. The complete lumbar vertebra 1 (L1) was used for vertebral trabecular bone volume analysis.

4.2.3 Dynamic histomorphometry

Mice were injected with the fluorescent tetracycline compounds calcein and demeclocycline at 10mg/kg, 6 days and 2 days prior to sacrifice respectively. The proximal end of the tibiae (right) was used to prepare sections for the analysis of mineralizing surface, mineral apposition rate and for tartrate-resistant acid phosphatase (TRAP) activity as described in chapter 2.7.2 and 2.7.3. Images were captured microscopically and evaluated as described in chapter 2.7.

4.2.4 Serum Biochemistry

16-hour fasting blood samples were collected at time of death for analyses. Serum calcium and phosphate were measured using a chemistry analyser (chapter 2.6.2). Serum 1,25D and 25D were measured by a radioimmunoassay (RIA) (chapter 2.6.3 and 2.6.4). Serum FGF23 was measured using an ELISA-kit method (chapter 2.6.6). Serum PTH was measured using a rat-specific, two-site immunoradiometric assay (IRMA) (chapter 2.6.5).

4.2.5 Messenger RNA analyses

Total RNA was isolated from whole femurs using the Trizol extraction method as described in chapter 2.9.1. RNA was reverse transcribed from 1µg of total RNA from each sample using

the Geneworks cDNA synthesis kit (Chapter 2.9.3). Mouse Cyp27b1, Cyp24, Alp, Col1, Ocn, Dmp1 and β-actin mRNA expression were analyzed by real-time RT-PCR using the SYBR Green incorporation technique as previously described chapter 2.9.4. Relative gene expression was calculated using the comparative cycle threshold (ΔCT) method, using β-actin as a house keeping gene. Sequences of the oligonucleotide primers are shown in Table 2.3.

4.2.6 1,25D and osteoblast mineralization

Osteoblasts from long bones of 6-week old FVB/N wild-type and hemizygous OSVDR female mice were dissected out and defleshed as described in chapter 2.11.1, and seeded onto 24 well-plates at 40,000 cells/well in 500 uL of the media α-MEM+10% FBS. Media was changed every the 3rd day until 100% confluent. Fresh differentiated α-MEM media (2% FBS, 10 mM BGP and 0.1 nM of dexamethozone) was added containing a 1,25D concentration of either 0.1nM or 1nM. The basis for 0.1nM of 1,25D as low level was based relative to 1nM 1,25D as 'functional' level. A previous study showed treatment of human primary osteoblasts with 1nM of 1,25D induced the expression of genes known to be vitamin D responsive, such as OCN, RANKL and OPG (Atkins et al., 2007). The same media was refreshed every 3rd day until day 18, the culture was ceased and cells were treated with alizarin red (chapter 2.11.3) and harvested on ice for messenger RNA analyses. Calcium quantification was performed as described in chapter 2.11.5.

4.2.7 Statistical analysis

The effects of dietary vitamin D and the transgene were statistically analysed using a 2-way ANOVA, where the p-value significance was set at ≤ 0.05. If significance of the interaction between diet and genotype were found, then Tukey's post-hoc test was performed to determine where the significance occurred and values were reported under each figure and table where appropriate. If however the interaction p-value was >0.05 then no further statistical analysis was performed.

4.3 RESULTS

4.3.1 Serum Biochemistry

There was a significant effect of the vitamin D- diet (0IU) on serum 25D. Both WT and OSVDR animals fed vitamin D+ (1000IU) diet achieved circulating 25D level to approximately 150nmol/L, while vitamin D- fed WT and OSVDR animals had markedly reduced serum 25D levels to approximately 25nmol/L ($p<0.01$) (Table 4.1). Circulating serum 25D levels was not affected in OSVDR animals compared to WT animals fed either D+ or D- diets (Table 4.1).

Serum 1,25D remained unchanged within each of the genotypes (WT or OSVDR) regardless of dietary vitamin D intake. There was however a trend to reduced serum 1,25D in OSVDR fed D+ compared to WT D+ animals, which did not reache statistically significance (Table 4.1).

Serum calcium and phosphate levels were not different between WT and OSVDR animals fed vitamin D+ diet. However, WT fed the vitamin D- diet recorded the lowest level of serum calcium compared all other groups ($p<0.05$). Interestingly, serum PTH levels were significantly lower in OSVDR compared to WT animals in both dietary vitamin D conditions ($p<0.05$), while no effects on PTH levels were observed as a result of dietary vitamin D-. There were no effects on the weights or tibia lengths (Appendix Figure 4.3) as a result of diet or transgene (Table 4.1).

Table 4.1: Serum 25D, 1,25D, calcium, phosphate, PTH and body weights of WT and OSVDR animals at 20 weeks of age fed vitamin D+ (1000 IU $VitD_3$/kg) and D- (0 IU $VitD_3$/kg) diet.

		Vitamin D+	**Vitamin D-**
25D nmol/L	Wild-type	150 ± 9	26 ± 1 ##
	OSVDR	157 ± 5	29 ± 2 ##
1,25D pmol/L	Wild-type	72 ± 30.3	55.4 ± 9.0
	OSVDR	28 ± 6.5	43.0 ± 12.5
Ca nmol/L	Wild-type	2.31 ± 0.02	2.14 ± 0.03#
	OSVDR	2.39 ± 0.02	2.34 ± 0.04*
Pho nmol/L	Wild-type	2.13 ± 0.12	1.79 ± 0.10
	OSVDR	1.87 ± 0.04	1.96 ± 0.18
PTH pmol/L	Wild-type	24.4 ± 4.5	21.2 ± 2.7
	OSVDR	14.3 ± 3.6*	12.7 ± 2.8*
Weight grams	Wild-type	25.8 ± 0.9	22.6 ± 1.7
	OSVDR	24.7 ± 0.8	25.7 ± 2.1

Values are mean ± SEM, n = 5; *p <0.05 versus WT in the same dietary group; # p <0.05; ## p <0.01 versus vitamin D+ group of the same genotype.

4.3.2 The role of osteoblastic VDR during vitamin D deficiency on cortical bone parameters

Vitamin D- fed WT animals have significantly lower tibial cortical bone volume when compared to vitamin D+ fed WT animals ($p<0.01$, Figure 4.1A). This was due to a significant decrease in cortical diameter ($p<0.01$, Figure 4.1B) and periosteal surface perimeter ($p<0.05$, Figure 4.1C). In contrast, OSVDR animals fed vitamin D- diet maintained tibial cortical bone volume comparable with levels in the vitamin D+ fed OSVDR animals, indicating that OSVDR osteoblasts respond to vitamin D- environment (vitamin D insufficiency: 25nmol/L serum 25D) differently to WT osteoblast cells. Moreover, OSVDR animals demonstrated 20% greater tibial cortical bone volume when fed vitamin D+ (1000 IU $VitD_3$/kg) and vitamin D- (0ng/day) compared to WT animals ($p<0.001$, Figure 4.1A), consistent with significantly greater cortical diameter ($p<0.001$) and periosteal perimeter in these OSVDR animals ($p<0.05$) (Figure 4.1B and 4.1C).

4.3.3 The role of osteoblastic VDR during vitamin D deficiency on trabecular bone volume and bone cell activities

There was no effect of vitamin D- on the tibial and vertebral trabecular bones of both wild-type (WT) and OSVDR animals (Figure 4.2). Significant increases of both tibial (35%) and verterbral (20%) trabecular bone volume was observed in OSVDR compared to WT animals fed either vitamin D+ (1000 IU) or D- (0 IU) diets ($p<0.0001$). This was due to the increase of both trabecular thickness and number, which was consistence with previous findings (Gardiner, et al., 2000).

To determine whether osteoblast and osteoclast cells were affected by the D- diet, tibial metaphyseal trabecular bone was measured for bone formation rate (BFR) and osteoclast surface number (Oc.N). No effects of D- diet on BFR and Oc.N were recorded in WT and OSVDR animals. OSVDR animals have a significant increase in BFR due to increased in mineralising surface rather than mineral apposition rate, and a decrease in Oc.N compared to WT in both vitamin D+ and D- diets ($p<0.05$, Figure 4.3) consistent with the increase of trabecular bone effects in OSVDR animals.

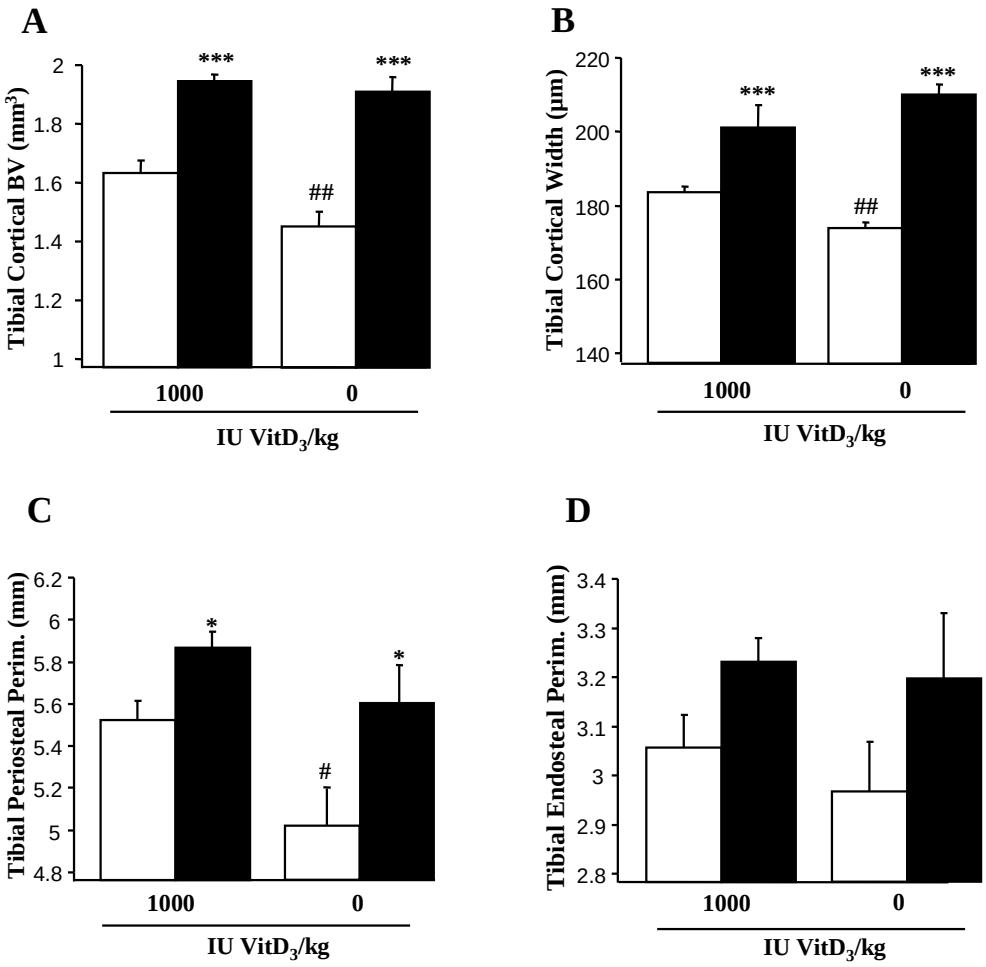

Figure 4.1: *The effect of vitamin D deficiency on tibial cortical bone*. (**A**) Tibial cortical bone volume, (**B**) cortical diameter, (**C**) cortical periosteal surface perimeter and (**D**) cortical endosteal surface perimeter in WT (white bar) an OSVDR animals (black bar) fed either 1000IU or 0IU $VitD_3$ per kg of diet. Values are mean ± SEM, n=5;*p <0.05 and ***p <0.001 versus WT in the same dietary group; # p <0.05; ## p <0.01 versus 1000IU group of the same genotype. Note: truncated axis was used for this figure.

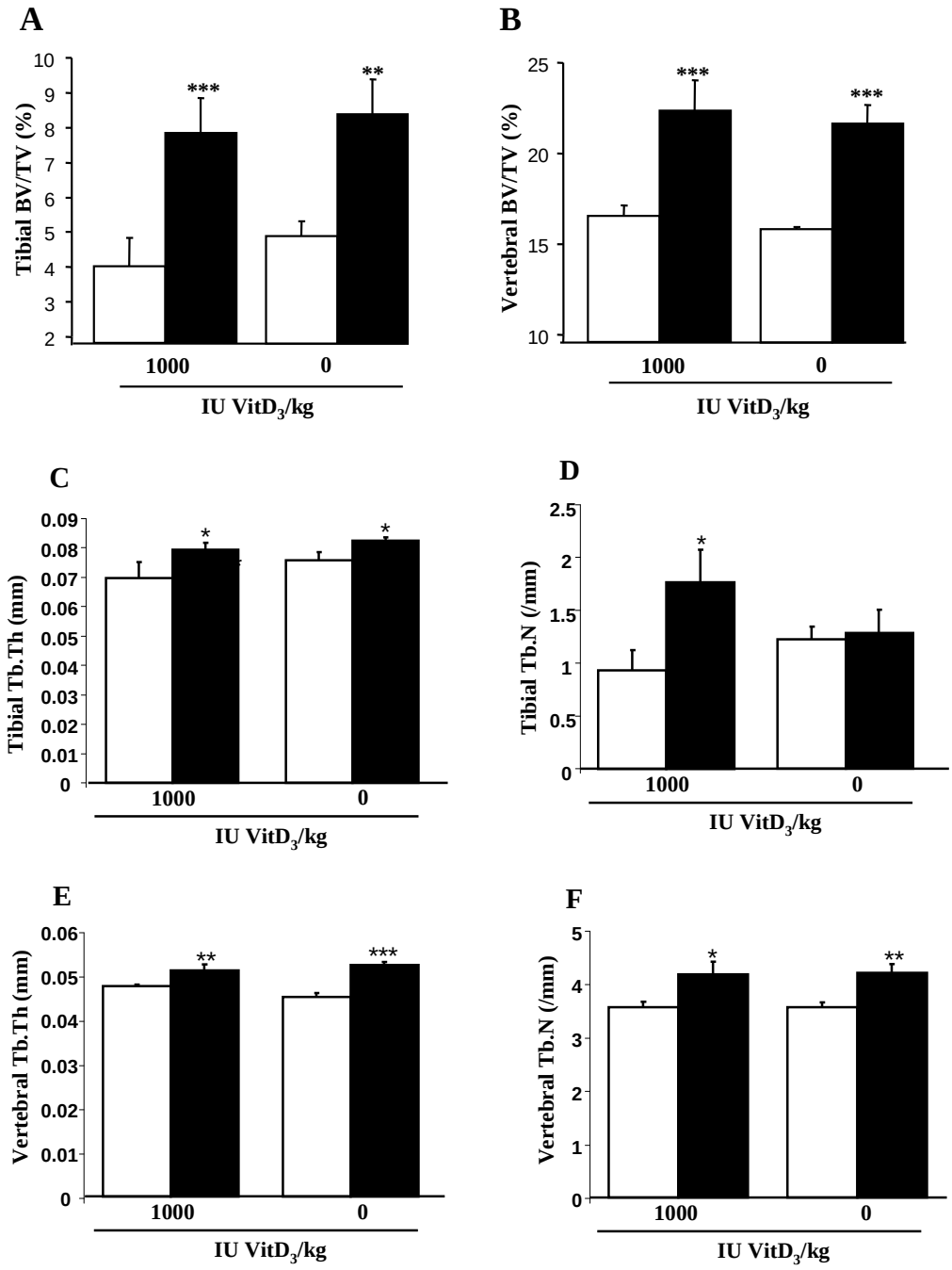

Figure 4.2*: The effect of vitamin D deficiency on tibial and vertebral trabecular bone parameters*. (**A**) Tibial trabecular BV/TV, (**C**) Thickness, (**D**) Number and (**B**) Vertebral trabecular BV/TV, (**E**) Thickness, (**F**) Number in WT animals (white bar) compared to OSVDR animals (black bar) fed with either 1000IU or 0 IU $VitD_3$ per kg of diet. Values are mean ± SEM, n = 5; * $p<0.05$, **$p<0.01$; ***$p<0.001$ vs. WT in the same dietary group; BV/TV, bone volume/total volume.

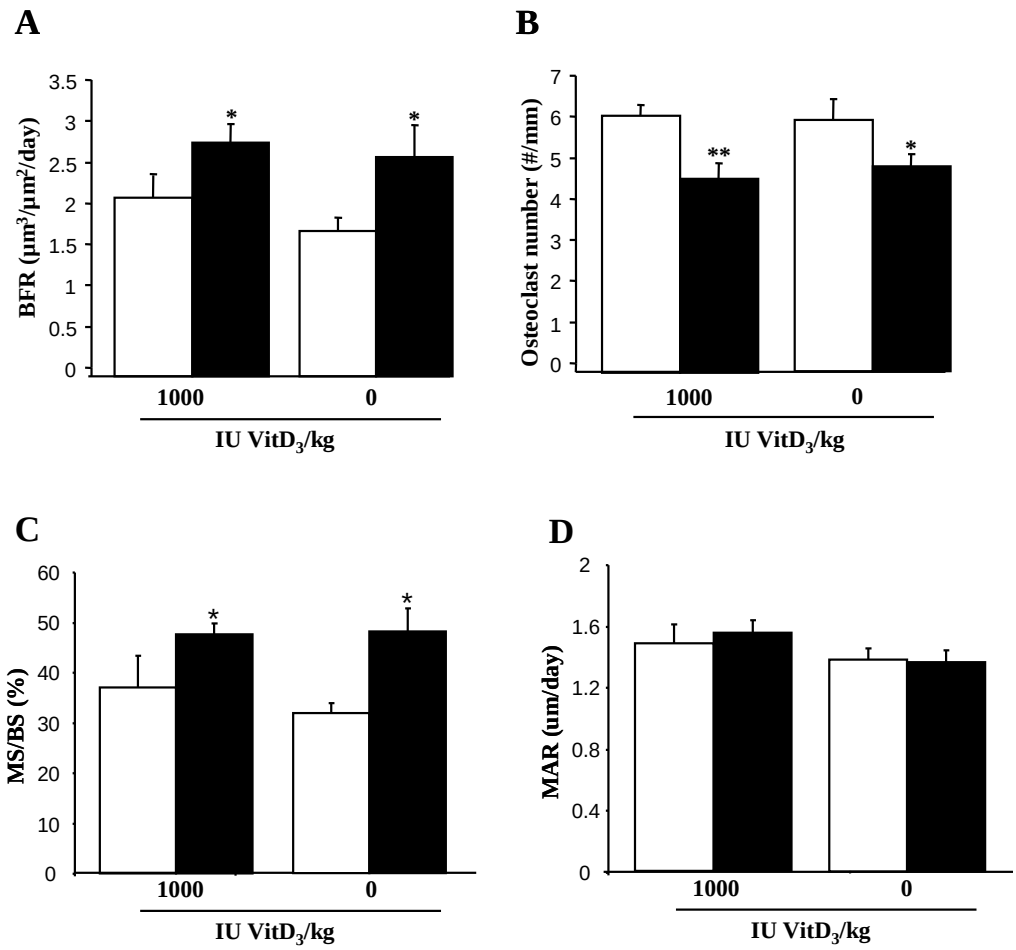

Figure 4.3: *The effect of vitamin D deficiency on bone cell activities*. (**A**) Bone formation rate, (**B**) Osteoclast number per millimetre of bone surface, (**C**) Mineralised surface percentages over total bone surface and (**D**) Mineral apposition rate in WT animals (white bar) and OSVDR animals (black bar) fed either 1000IU or 0IU $VitD_3$ per kg of diet. Values are mean ± SEM, n = 5; *p <0.05 and **p <0.01 versus WT in the same dietary group.

4.3.4 Effects of enhanced osteoblastic VDR on FGF23 production and renal activity

Serum FGF23 levels were measured to assess whether increased VDR in the mature osteoblast lineage cells contributed to the regulation of FGF23 production. Serum FGF23 levels were significantly elevated in OSVDR animals (approximately +40%) compared to WT animals levels fed either vitamin D+ (1000 IU $VitD_3$/kg) or D- (0 IU $VitD_3$/kg) diets ($p<0.01$, Figure 4.4A). Increased FGF23 levels did not result in hypophosphatemia, however serum 1,25D levels were marginally reduced in these OSVDR animals, although this did not reach statistical significance (Table 4.1). In WT animals, vitamin D- diet caused a significant reduction in serum FGF23 levels ($p<0.05$), which did not occur in OSVDR animals (Figure 4.4A). The greater serum FGF23 levels in OSVDR animals were strongly consistent with higher renal CYP24 mRNA levels in OSVDR animals fed either vitamin D diet ($p<0.01$, Figure 4.4B), which may explain the low 1,25D in these animals (Table 4.1).

Dietary vitamin D restriction led to induction of the renal CYP27B1 in both WT and OSVDR mice ($p<0.001$, Figure 4.4C). Notably the greater serum FGF23 levels in OSVDR had no effect on renal CYP27B1 mRNA, suggesting that vitamin D-mediated up-regulation of renal CYB27B1 levels dominates under conditions of vitamin D restriction. Interestingly the greater serum FGF23 levels in the OSVDR animals is consistent with lower serum PTH levels (Table 4.1), suggesting serum FGF23 is having physiological effects in OSVDR animals.

4.3.5 Effects of increased osteoblastic VDR and 1,25D treatment on mineralisation

To determine the effects of extracellular stimulus of 1,25D in OSVDR and WT osteoblastic functions, osteoblasts from the long bones of WT and hemizygous OSVDR animals were isolated and cultured in pro-differentiating media containing either extra 0.1nM or 1mM added 1,25D . In untreated 1,25D cultures, OSVDR osteoblasts had significantly increased calcium deposition compared to WT untreated osteoblast cells ($p<0.01$, Figure 4.5A and 4.5B). This is related to a reduction in Alp, Col1 and Ocn mRNA levels ($p<0.01$), but an increase in Dmp1 mRNA levels ($p<0.01$, Figure 4.5C). Treatment with either 0.1nM or 1nM

of 1,25D resulted in no mineral being detected in all cultures. When cells were cultured in the presence of 1nM 1,25D there was no statistically significant difference in Alp and Col1 expression between WT and OSVDR, whereas the expression of Ocn was suppressed in OSVDR compared to WT osteoblasts ($p<0.05$, Figure 4.5C). Dmp1 expression in both WT and OSVDR osteoblast cultures were more than 100-fold lower in untreated compared to the 1,25D treated cultures. Interestingly in culture of WT osteoblasts treated with 1,25D, the expression of Alp and Col1 expression were unchanged compared to the WT untreated osteoblasts, whereas OSVDR osteoblasts treated with 1,25D had significantly higher expression of Alp and Col1 compared to untreated ($p<0.01$, Figure 4.5C), indicating WT and OSVDR cultures are distinct from one another.

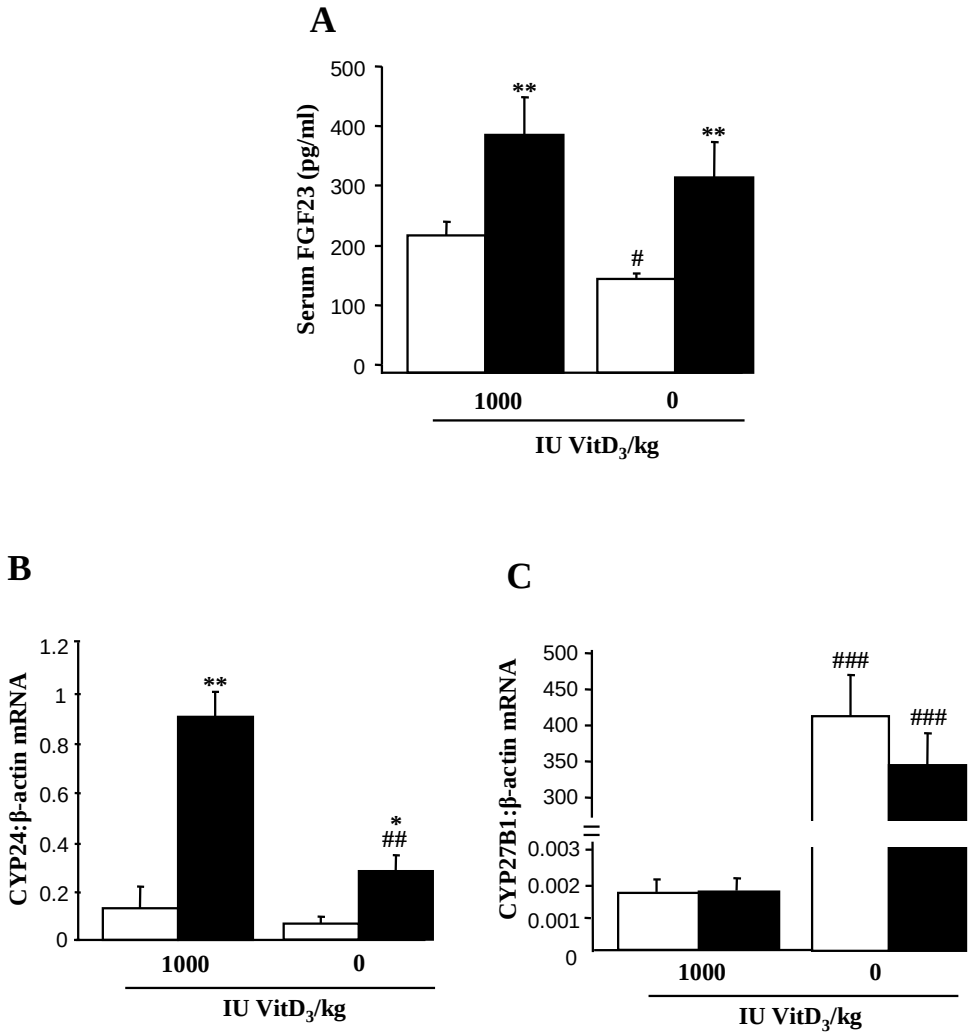

Figure 4.4: *The effect of vitamin D deficiency on serum FGF23 and renal vitamin D hydroxylase gene expression.* (**A**) Serum fibroblast growth factor 23 (FGF23) and (**B**) Renal 25 hydroxyvitamin D 24-hydroxylase *(Cyp24)* and (**C**) 25 hydroxyvitamin 1α-hydroxylase *(Cyp27b1)* mRNA levels in WT (white bar) and OSVDR animals (black bar) fed either 1000IU or 0IU $VitD_3$ per kg of diet. Serum FGF23 proteins were measured as described previously. Real-time RT-PCR results were expressed as relative expression with *β-actin* as a house-keeping gene using the formula: $2^{\wedge -(Ct\ [Gene\ of\ interest]-Ct\ [\beta\text{-actin}])}$. Values are mean ± SEM, n = 5; *p <0.05; **p <0.01 versus WT in the same dietary group; # p <0.05; ### p <0.001 versus 1000IU dietary group of the same genotype.

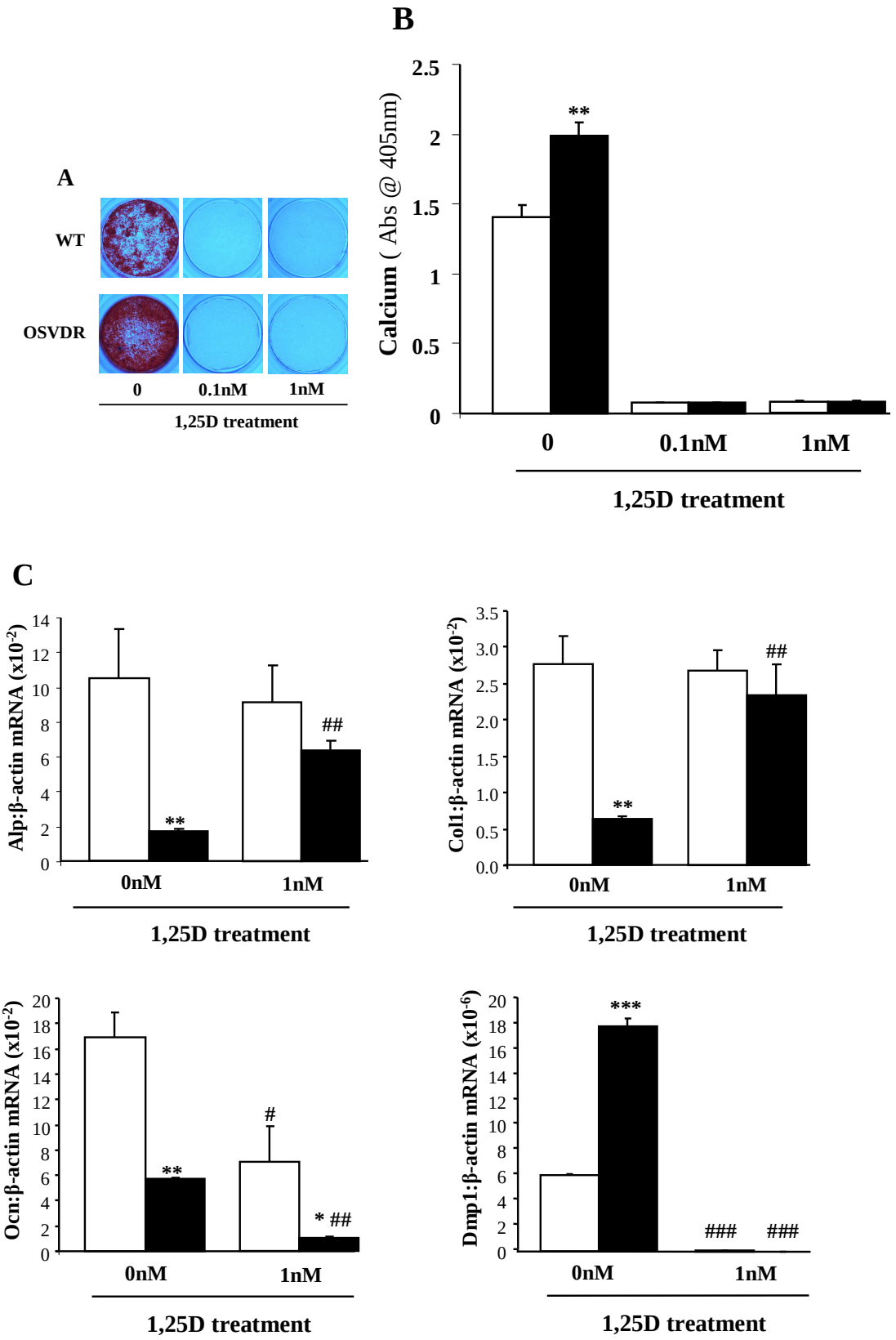
A
WT
OSVDR
0
0.1nM
1nM
1,25D treatment
B
Calcium (Abs @ 405nm)
2.5
2
1.5
1
0.5
0
**
0
0.1nM
1nM
1,25D treatment
C
Alp:β-actin mRNA (x10-2)
14
12
10
8
6
4
2
0
**
##
0nM
1nM
1,25D treatment
Col1:β-actin mRNA (x10-2)
3.5
3.0
2.5
2.0
1.5
1.0
0.5
0.0
**
##
0nM
1nM
1,25D treatment
Ocn:β-actin mRNA (x10-2)
20
18
16
14
12
10
8
6
4
2
0
**
#
* ##
0nM
1nM
1,25D treatment
Dmp1:β-actin mRNA (x10-6)
20
18
16
14
12
10
8
6
4
2
0
***
###
###
0nM
1nM
1,25D treatment

Figure 4.5: *The effect of 1,25D treatment on mineralisation in OSVDR osteoblasts.*

Long bones of 6-week old WT (white bar) and OSVDR hemizygous animals (black bar) were prepared for primary osteoblast cell cultures. Osteoblasts were cultured in osteogenic differentiation medium with either 0nM, 0.1nM or 1nM 1,25D for 18 days and examined for mineralisation by (**A**) Alizarin red staining, (**B**) calcium deposition by absorbance analysis and (**C**) mRNA levels for alkaline phosphatase (*Alp*), collagen 1 (*Col1*), osteocalcin (*Ocn*) and dentin matrix protein 1 (*Dmp1*). Real-time PCR results were expressed as relative expression with *β-actin* as a house-keeping gene using the formula: $2^{-(Ct\ [Gene\ of\ interest]-Ct\ [\beta\text{-actin}])}$. Values are mean ± SEM, n = 3, each animal was done in triplicate, experiment repeated 2x; *p <0.05; **p <0.01; ***p <0.001 versus WT in the same 1,25D treatment culture; # p <0.05; ## p <0.01; ### p <0.001 versus untreated culture of the same genotype.

4.4 DISCUSSION

4.4.1 OSVDR cortical bone effects and vitamin D deficiency

Consistent with previous findings (Baldock, et al., 2006; Gardiner, et al., 2000) we detected the transgene effect to be strongly apparent in the cortices as evidenced by increased cortical bone volume, cortical width and periosteal perimeter while there was no significant effect on endosteal surface, suggesting that the periosteal osteoblasts in the transgenic animals have a greater osteogenic response to extra-tissue stimulus such as that of mechanical loading, which is coordinated by the actions of osteocytes, which have also been reported to express the human VDR transgene in OSVDR model (Gardiner, et al., 2000).

Using Micro-Ct, our laboratory has previously detected changes in cortical bone rather than trabecular bone due to vitamin D depletion. This could possibly be due to the relative distribution of these structures in the region of interest (Lee et al., 2010). In our current study, WT animals with serum 25D level of approximately 25nmol/L had reduced cortical bone volume compared to WT animals with serum 25D levels above 140nmol/L. It appears that the lower cortical bone in WT animals was due to reduced periosteal apposition and was not due to increased osteoclastic responses as endosteal surface remained unaffected. Furthermore, since tibia length and body weights were unchanged, this suggests that in a growth model vitamin D deficiency impairs periosteal osteoblast activity, independent of the bone modelling/remodelling found on endosteal surfaces. While we observed moderately low serum calcium in WT animals fed 0 IU $VitD_3$/kg (D-) of vitamin D, no changes to serum PTH or serum 1,25D levels were recorded in this group suggesting that serum calcium levels were not markedly altered. The contribution of the moderately low serum calcium level to changes in cortical bone volume in this group is thus unclear. It would be of future interest to examine the urine calcium levels in these animals as it may be due to a greater excretion of calcium in the WT fed D- diet group. Furthermore, while vitamin D is important for active transport of calcium, passive absorption of calcium in the jejunum and ileum also plays a significant role

in determining total serum calcium level, however whether this has contributed to the differing of the calcium values in these animals remains unanswered.

In constrast to WT animals, OSVDR animals with serum 25D level of 25nml/L maintained their cortical bone volume to levels comparable with OSVDR animals with serum 25 level of above 150nmol/L. The over expression of VDR in OSVDR maintained cortical width and periosteal perimeter, suggesting a direct effect of vitamin D signalling on the periosteal osteoblast activity. It would be of great interest in the future to obtain actual measurements for periosteal mineral apposition, since a previous study (Gardiner, et al., 2000) indicated that the enhancement of periosteal perimeter in OSVDR mice was due to increased periosteal mineral apposition rate and not mineralising surface. Our current knowledge of periosteum biology is limited, although we know that it contains mesenchymal progenitor cells, osteoblasts and fibroblasts. These 'periosteal cells' respond uniquely to homeostatic regulators compared to other osteogenic cell populations (Allen, et al., 2004; Dwek, 2010). Compared to endosteal osteoblasts, periosteal osteoblasts exhibit greater mechanosensitivity (Guo and Cowin, 1992), a lower threshold of responsiveness to osteogenic compounds such as PTH (Midura, et al., 2003) and higher levels of proteins such as periostin, which is important for periosteal osteoblast proliferation and differentiation (Horiuchi, et al., 1999) and greater estrogen alpha receptors (Khosla, et al., 2006). These factors may all contribute to the differences in periosteal and endosteal surface responses in OSVDR mice to vitamin D signalling. Indeed, OSVDR animals have been shown to respond to mechanical loading by enhancing woven bone formation and cortical thickness compared to WT animals, suggesting that vitamin D may be required to mediate the sensitivity of periosteal osteoblasts to mechanosensing (Anderson, unpublished findings). More extensive data are needed to fully characterise and understand the reasons for the differences between OSVDR and WT periosteal osteoblasts in response to mechanical loading and to direct vitamin D activity in the bone.

Our laboratory has shown that 25D levels of less than 25nmol/L in rodents is substrate limiting for osteoblasts to induce bone CYP27B1 mRNA expression but not renal CYB27B1

mRNA (Anderson, et al., 2007; Anderson, et al., 2008). Our current study also presented serum 25D levels at approximately 25nmol/L in both WT and OSVDR animals fed the vitamin D deplete diet. Our data indicate that while a serum 25D level of 25nmol/L did not affect renal synthesis of 1,25D, it was not sufficient to maintain cortical bone in WT mice, suggesting substrate insufficiency for osteoblastic 1,25D production. The over-expression of VDR in OSVDR mice however appears to have lowered the osteoblastic requirement for circulating 25D, which is likely due to improved sensitivity to vitamin D. This further supports the proposed role of locally produced 1,25D within bone cells for the regulation of osteoblastic proliferation, differentiation and mineralisation for the maintenance of bone.

4.4.2 OSVDR trabecular bone effects and vitamin D deficiency

The increase in metaphyseal trabecular bone volume was due to an increase in bone formation as well as a decrease in osteoclastic bone resorption, which was also previously reported to be responsible for the OSVDR anabolic bone effects (Baldock, et al., 2006; Gardiner, et al., 2000). Our laboratory has previously shown that serum 25D levels are an important determinant of trabecular bone mineral volume in rodents when fed an adequate level of dietary calcium (Anderson, et al., 2007) and only when serum 25D levels were above 80nmol/L was the bone structural volume optimised. In this model, protection against bone loss was due to a reduction in bone resorption at higher levels of vitamin D status (Anderson, et al., 2008). In our current study, mice were fed vitamin D deficient diets for 4 months, achieving mean serum 25D levels of 25nmol/L. However, we were unable to demonstrate trabecular bone loss in the tibia or the vertebra in either WT and OSVDR animals in response to vitamin D depletion. We believe our study represents a young growing model where vitamin D is required to optimise bone mineral accumulation and that vitamin D-mediated trabecular bone loss in aged animals did not occur in our study. This may be attributed to the FVB/N genetic background, gender-specific differences in male versus females, as well as site-specific differences. Interestingly, the anabolic bone phenotype of the OSVDR animals

could be observed at 6-weeks of age (Figure 3.4), suggesting that vitamin D signalling in the mature osteoblast lineage cells can optimise processes of bone growth and modelling to favour enhanced mineralisation, which could be maintained even when vitamin D levels are reduced. Other studies in our laboratory are currently examining the OSVDR bone phenotype on the C57B6 genetic background in both male and female at varying ages. For these studies other sites such as the femur will also be examined.

4.4.3 Effects of increased osteoblastic VDR and FGF23 production

While much is known about the role of FGF23 with regard to its actions in the maintenance of serum phosphate and 1,25D production, the regulation of its production in the bone remains unclear. Studies have shown that 1,25D administration can dose-dependently increase FGF23 production in mice (Kolek, et al., 2005). Exposure of cultured osteoblasts to 1,25D can directly stimulate FGF23 transcription via a putative vitamin D response element (VDRE) in the FGF23 promoter (Liu, et al., 2006). Interestingly, VDR knockout mice have undetectable levels of FGF23 suggesting that the 1,25D-VDR system is important for FGF23 production (Inoue, et al., 2005). However, while phosphate is a regulator of FGF23 levels, it is unclear whether VDR plays a role in direct regulation of FGF23 production. These studies have therefore more completely characterised the mechanism of 1,25D-stimulated FGF23 production, but they have not demonstrated a direct role of osteoblastic/osteocytic VDR in vitamin D-mediated FGF23 production in the bone. For the first time, our study shows that OSVDR mice have greater FGF23 levels, suggesting that mature osteoblast/osteocyte VDR is a significant regulator of 1,25D-mediated FGF23 production. This could be due to 1,25D-VDR direct transcriptional regulation via the putative VDRE as suggested above or may be via an indirect mechanism involving suppression of the known FGF23 regulators PHEX and DMP1 activity in osteoblasts (Feng, et al., 2006; Liu, et al., 2007; Liu, et al., 2006). Notably, we observed no changes to serum phosphate as a result of increased FGF23, which coincides

with phosphate being the end product of multiple regulatory pathways, such as 1,25D/PTH and not just FGF23 alone [as recently reviewed by (Bergwitz and Juppner, 2010)].

FGF23 is a well known regulator of renal 1,25D production through inhibition of renal CYB27B1 and induction of renal CYP24 (Shimada, et al., 2004). Our data indicated that increased serum FGF23 levels in OSVDR animals was significantly associated with an up-regulation of renal CYP24 mRNA levels, however CYP27B1 levels remained unchanged. This may be because the regulation of CYP27B1 by 1,25D overrides the effects of FGF23. Interestingly, while the effect of FGF23 on PTH is still controversial, our data indicate that increased FGF23 levels have a significant physiological effect on PTH, which is independent of serum 1,25D. This suggests stimulation of FGF23 on the parathyroid gland to suppress PTH secretion as supported by other studies (Ben-Dov, et al., 2007; Krajisnik, et al., 2007) however whether this is a direct effect of FGF23 activity on PTH secretion requires to be elucidated.

4.4.4 Effects of increased osteoblastic VDR and 1,25D treatment on mineralisation

As previously discussed in Chapter 3, 1,25D can regulate osteoblastic proliferation, differentiation and mineralisation. We have in this study provided evidence to suggest increase 1,25D sensitivity in mature osteoblast (OSVDR) enhances their differentiation and mineralisation.

It has been well recognised that there are three principal stages of osteoblast phenotype development, these are proliferation, extracellular matrix development and maturation, and mineralization, which are tightly controlled by a vast array of genes (van Driel, et al., 2004). We have examined the expression of collagen type 1 (Col1), alkaline phosphatase (Alp) and osteocalcin (Ocn) mRNA to determine the stages of maturation in osteoblast cultures. Col1 is highly expressed during the proliferative period and is gradually down regulated as the osteoblast cells go through differentiation (Lynch, et al., 1995; Owen, et al., 1990). Alp however is expressed as the cultures progress through maturation to the mineralisation stage,

and then declines in heavily mineralised cultures (Lynch, et al., 1995; Owen, et al., 1990). Ocn on the other hand is expressed only in late osteoblast development, where its synthesis correlates strongly with calcium deposition *in vitro* (Aronow, et al., 1990; Barone, et al., 1991), although there is conflicting evidence to suggest osteocalcin *in vitro* is an inhibitor of mineralisation (Boskey, et al., 1985). Our data showed in untreated 1,25D culture of OSVDR osteoblasts, gene expression for Alp, Col1 and Ocn were all significantly lowered compared to WT untreated osteoblast cultures, indicating the OSVDR osteoblasts are more mature at 18 days of culture compared to WT osteoblasts, where these genes have been down regulated or perhaps no longer required in heavily mineralised cultures. The maturity of the OSVDR cultures is further supported by their higher expression of Dmp1 mRNA, a marker for late osteoblast/osteocyte development (Feng, et al., 2006; Maciejewska, et al., 2009). The role of DMP1 in regulating phosphate homeostasis and osteocyte health has been well studied (Qin, et al., 2007), however it's role in regulating mineralisation is not yet clear although there have been studies to suggest it's involvement in hydroxyapatite formation (Feng, et al., 2003; Narayanan, et al., 2003) as well as control of osteogenesis *in vitro* (Narayanan, et al., 2004; Narayanan, et al., 2001). Notably during the transition of osteoblast to osteocyte phase, DMP1 expression is markedly up-regulated and localizes to the extracellular matrix, where it functions to promote mineralization (Narayanan, et al., 2003; Narayanan, et al., 2004). Our laboratory [Anderson, unpublished data] and others (Feng, et al., 2003; Narayanan, et al., 2004) have shown strong DMP1 expression in late osteoblast/osteocyte cultures (of humans and mice) and an inverse relationship to Alp and Ocn gene expression (Narayanan, et al., 2003). Interestingly, deletion of DMP1 in mice leads to defects in osteoblast differentiation into osteocytes and is characterised by abnormally high expression of Alp and Col1 (Feng, et al., 2006). These results suggest a mechanism by which DMP1 may regulate the transition of osteoblasts into osteocytes.

In regard to the 1,25D treated cultures, our data suggest continuous treatment with 1,25D inhibits osteoblastic proliferation and maintains the cells in a 'quiescent' state, as evidenced

by a complete absence of mineralisation, unchanged Alp, Col1 and Ocn and undetectable Dmp1 levels. A recent report from (Wu, et al., 2007) demonstrated the 1,25D anti-tumorogenic properties in the human osteosarcoma SaOS-2 cell occurs via sustained upregulation of a c-jun/c-fos Ap-1/p[21] pathway and subsequent cell cycle arrest. Future studies to examine in detail expression of cell cycle genes such as cyclins, CDKs, histones and cell growth regulated genes such as c-myc, c-fos and c-jun in response to 1,25D continuous versus intermittent/acute treatment could prove useful to the understanding of 1,25D and cell growth. We do not exclude the possibility of cell apoptosis to explain the complete absence of mineralisation in our cultures, however it appeared unlikely since we did not observe extra cellular 'debris' in these cultures.

In summary, our data indicate that vitamin D deficiency causes impairment to bone mineralisation, which could be prevented by enhancing vitamin D signalling via the VDR in the mature cells of osteoblast lineage, possibly by the action of locally produced 1,25D. We further showed that direct vitamin D/VDR activity in the bone regulates renal feedback by FGF23 on 1,25D metabolism. Moreover, direct vitamin D signalling in osteoblasts plays an important role in the cell's growth, differentiation and mineralisation.

Chapter 5

THE ROLE OF VITAMIN D RECEPTOR IN OSTEOBLASTS DURING DIETARY CALCIUM RESTRICTION

5.1 INTRODUCTION

The levels of dietary calcium required to maintain calcium and phosphate homeostasis and adequate bone mineral volume is dependent on the stage of skeletal development as well as the presence of adequate vitamin D. Serum calcium and phosphate levels are regulated tightly by at least three mechanisms, which include intestinal absorption, renal reabsorption, and bone turnover. During the early stages of development when growth is vigorous, calcium and phosphate requirements are high as the skeleton accretes large amounts of mineral, and the net bone balance is positive (formation>resorption), this ensures healthy skeletal growth (Bailey, et al., 2000; Lu, et al., 1994). In the latter stages of life when bone growth ceases, the bone balance in healthy individuals becomes neutral (formation=resorption) and the calcium accrued can serve as a source of calcium if dietary calcium levels are inadequate for a prolonged period of time (Teegarden, et al., 1995; Weaver, et al., 1995).

The hormone, 1α,25-dihydroxyvitamin D3 (1,25D) is an important regulator of calcium and phosphorus homeostasis. In this context, 1,25D and the vitamin D receptor (VDR) are generally recognised as necessary for the maintenance of a healthy skeleton primarily through endocrine actions to stimulate intestinal calcium and phosphate absorption. The fact that the osteomalacia bone phenotype (under-mineralised bone) observed in the vitamin D receptor knockout (VDRKO) mouse can be prevented by feeding a diet containing high levels of calcium and phosphorus (Amling, et al., 1999) has led some researchers to suggest that VDR-mediated activities in the bone are redundant as long as dietary calcium and phosphate is provided in sufficient levels for passive diffusion in the intestine (Bouillon, et al., 2008). This suggestion however does not acknowledge the essential role of 1,25D stimulation of the calcium absorption genes, calcium-binding protein calbindin-9k (CaBP-9k) (Christakos, et al., 1992) and calcium channel Trvp6 mRNA (Peng, et al., 2003) which is significantly abrogated in VDRKO mice (Li, et al., 1998; Van Cromphaut, et al., 2001), demonstrating the central

role of VDR in regulation on these genes and active intestinal calcium transport. In deed, with a normal intake of calcium, the majority of dietary calcium intake is absorbed along the proximal small intestine which is under the control of the active 1,25D-dependent transport process (Bronner, 1987; Heaney, et al., 1975). Under these circumstances, 1,25D-dependent transport accounts for the majority of absorption and only 8 to 23% of overall calcium absorption is caused by passive diffusion.

Several years after the generation and initial published reports on the VDRKO mouse models, it was reported that adult VDRKO have only 50% of bone mineral volume despite being fed the calcium and phosphate diet that rescues osteomalacia. This is despite these adult VDRKO maintaining normocalcaemia without induction of PTH levels (Panda, et al., 2004). Furthermore, the bone loss that occurred in adult VDRKO mice was shown to be not due to increased osteoclastogenesis or bone resorption, as quantified by RANKL and TRAP staining intensity measures. In fact osteoclasts surface measures in VDRKO mice were significantly lower than in wild-type mice. The reason for the bone loss in VDRKO mice appeared to be due primarily to a reduction in mineral apposition, which was due to reduction in acid phosphatase and ALP positive staining for osteoblasts in bone surface, as well as reduced mineral apposition rate (Panda, et al., 2004). Thus the suggestion is that the age-related bone loss in these VDRKO mice occurred due to a failure of bone formation, a failure of RANKL signalling to maintain bone turnover, and not due to increase bone resorption. An appropriate interpretation of this finding is that direct vitamin D activity in bone cells plays a critical role or roles in regulating bone cell activities to maintain optimal bone mineralisation, at least during the aging process.

In chapter 4, we showed that enhanced vitamin D activity in osteoblasts not only increased bone volume in the OSVDR mouse model but allowed for optimal cortical bone formation in young mice despite being exposed to deficient dietary vitamin D during the period of rapid

growth. These mice were fed a diet which contained adequate levels of dietary calcium (1%) which is sufficient for adequate mineralisation of the rapidly growing skeleton. It is well established that vitamin D and dietary calcium play an essential interaction to prevent bone loss and reduce the incidence of hip fractures (Dawson-Hughes and Bischoff-Ferrari, 2007). Thus, it is of considerable interest that the trabecular bone phenotype of the OSVDR mouse is diminished to WT levels when mice are fed a low (0.1%) calcium diet (Baldock, et al., 2006). The low trabecular bone volume in OSVDR fed 0.1% calcium was due to reduction in bone formation and without changes to osteoclastic resorption or apparently calcium homeostatic regulators, suggesting the interaction between dietary calcium and direct vitamin D activity in osteoblasts is positive only when dietary calcium is adequate. However, a complete understanding of the molecular, cellular and biochemical mechanisms which give rise to the interaction of dietary calcium and enhanced vitamin D activity in osteoblasts on the bone phenotype of the OSVDR mouse model is currently lacking.

Thus, the study in this chapter, aims to characterise the biochemical, cellular and molecular mechanisms which underpin the influences of dietary calcium in determining the OSVDR anabolic bone phenotype. We hypothesised that vitamin D activity in the bone, including the osteoblasts, mediates bone turnover, which is independent of the effects of vitamin D in the intestine for calcium homeostasis.

5.2 METHODS

5.2.1 Mice and dietary calcium restriction

Age matched female FVB/N wild-type and hemizygous OSVDR animals were randomly allocated into groups of 6 animals/cage. Hemizygous OSVDR animals were bred by mating homozygous males to FVB/N wild-type females. All FVB/N animals studied were bought age-matched from Animal Resources Centre (ARC, Perth, Australia). All animals were fed a semi-synthetic diet beginning at 6 weeks of age, for 12 weeks, which contained either 1% calcium or low 0.1% calcium (recommended by the American Institute of Nutrition, AIN) and 1000 IU $VitD_3$ per kg of diet, plus 0.65% phosphorus. We have chosen to feed the animals these dietary calcium levels to replicate the study of Baldock et al., 2006, who also fed the animals with 1% and 0.1% dietary calcium amounts. Female hemizygous OSVDR animals at 6 weeks of age were selected for this study to replicate the study of Baldock et al., 2006, who also used the same age and sex of animals. Our previous data has shown that osteoclast surface is the most variable parameter. The average osteoclast surface we observed in control mice is 3% with a standard deviation of 0.8%. In order to detect a difference of 20% in osteoclast surface in our experimental mice at a significance level of = 0.05 with 80% power requires 6 mice per group. Animals were sacrificed at 18 weeks of age for analyses. These ages were chosen to represent growing (young) and non-growing (adult) groups of animals.

5.2.2 Micro-computed Tomography

The micro-architecture of the tibia was evaluated using a high resolution micro-CT system at 6.5µm/pixel. A 2mm diaphysis region and 3mm metaphysis region of the left proximal tibia was used for cortical bone volume and trabecular bone volume (BV/TV) analyses respectively as described in chapter 2.8. The same 2mm region of cortical bone volume was used cortical width, periosteal and endosteal surface perimeter.

5.2.3 Dynamic histomorphometry

Mice were injected with the fluorescent tetracycline compounds calcein and demeclocycline at 10mg/kg, 6 days and 2 days prior to sacrificed respectively. The proximal end of the right tibiae was used to prepare sections for the analysis of mineralizing surface, mineral apposition rate and for tartrate-resistant acid phosphatase (TRAP) activity as described in chapter 2.7.2 and 2.7.3. Images were captured microscopically and evaluated as described in chapter 2.7.

5.2.4 Serum Biochemistry

16-hour fasting blood samples were collected at time of death for analyses. Serum calcium and phosphate were measured using a chemistry analyser (chapter 2.6.2). Serum 1,25D levels were measured by a radioimmunoassay (RIA) (chapter 2.6.3). Serum PTH was measured using a rat-specific, two-site immunoradiometric assay (IRMA) (chapter 2.6.5). Serum FGF23 was measured using an Elisa-kit method (chapter 2.6.6).

5.2.5 Messenger RNA analyses

Total RNA was isolated from whole tissues (left femur, proximal intestine and kidney) using the Trizol extraction method as described in chapter 2.9.1. RNA was reverse transcribed from 1µg of total RNA from each sample using the Geneworks cDNA synthesis kit (Chapter 2.9.3). Human *VDR*, mouse *Vdr*, *Cyp27b1*, *Cyp24*, *Napi2a/2c*, *Trvp6*, *Cabp9k*, *Alp*, *Col1*, *Ocn*, *Runx2*, *Rankl*, *Nfatc1*, *E11*, *Fgf23*, *Dmp1*, *Phex*, *Sost* and *β-actin* mRNA expression were analyzed by real-time RT-PCR using the SYBR Green incorporation technique as previously described chapter 2.9.4. Relative gene expression was calculated using the comparative cycle threshold (ΔCT) method, using *β-actin* as a house keeping gene. Sequences of the oligonucleotide primers are shown in Table 2.3.

5.2.6 Calcium and osteoblast mineralization

Osteoblasts from long bones of 6-week old FVB/N wildtype and hemizygous OSVDR female mice were dissected out and defleshed as described in chapter 2.11.1, and seeded onto 24 well-plate at 40,000 cells/well in 500 uL of the media α-MEM+10% FBS (Chapter 2.11.1). Media was changed every 3rd day until 100% confluent. Fresh differentiated α-MEM media (2% FBS, 10 mM BGP and 0.1 nM of dexamethozone) (Chapter 2.11.1) was added containing either 1.8mM (basal amount in DMEM) or supplemented with 1mM (2.8mM) calcium concentration. The basis for considering 1.8mM calcium as a restricted level was based on our laboratory's observation of significantly greater mineralisation by osteoblasts when cultured with 2.8mM calcium compared to 1.8mM (Yang et al., unpublished). The same media was refreshed every 3rd day until day 18, the culture was ceased and cells were treated with alizarin red (chapter 2.11.3) and harvested on ice for messenger RNA analyses. Calcium quantification was performed as described in chapter 2.11.5.

5.2.7 Statistical analysis

The effects of dietary calcium and transgene were statistically analysed using a 2-way ANOVA, where the p-value significance was set at $P \leq 0.05$. If significance of the interaction between diet and genotype were found, then Tukey's post-hoc test was performed to determine where the significance occurred and values were reported under each figure and table where appropriate. If however the interaction p-value was >0.05 then no further statistical analysis was performed.

5.3 RESULTS

5.3.1 Serum biochemistry

Serum 1,25D levels in mice fed 0.1% Ca diet were significantly greater compared to 1% Ca fed mice, regardless of genotype ($p<0.05$, Table 5.1). However, OSVDR mice fed 0.1% diet had 40% lower serum 1,25D levels when compared to WT mice fed 0.1% Ca ($p<0.01$). Serum FGF23 levels in WT mice fed 0.1% Ca were significantly lower than levels in WT 1% Ca fed mice. In contrast, no differences in serum FGF23 levels occurred in OSVDR mice between 0.1 and 1% Ca fed groups. Thus, OSVDR mice fed 0.1% Ca had higher FGF23 levels than WT mice fed 0.1% Ca (Table 5.1). No statistical differences occurred for serum Ca, phosphate and PTH levels between OSVDR and WT mice fed either the 0.1% or 1% Ca diet.

5.3.2 Effects of calcium restriction on tibial bone volume and bone cell activities

In OSVDR 1% Ca fed mice, trabecular bone volume of the proximal tibia was 20% greater than levels in WT 1% Ca fed mice ($p<0.0001$). This was due to significantly greater trabecular thickness ($p<0.05$) and a trend towards increased trabecular number ($p=0.10$) (Table 5.2). Similarly the tibial cortical bone volume of 1% Ca fed OSVDR mice was 15% greater than the levels in WT mice ($p<0.001$). The high bone mass phenotype of OSVDR mice is consistent with a significantly higher BFR ($p<0.05$, Fig 5.1A), due to greater mineralised surface, and a trend for reduced Oc.N in metaphyseal trabecular bone of the tibia (Fig 5.1B, $p=0.12$)). While 0.1% Ca diet had no effects on WT cortical and trabecular bone parameters, OSVDR mice fed 0.1% Ca have significantly lowered cortical and trabecular bone volume when compared to OSVDR 1% Ca fed mice ($p<0.01$) (Table 5.3). Noticeably, OSVDR trabecular bone volume was equivalent to WT levels in the 0.1% Ca diet, which was due to a significant reduction in the trabecular thickness ($p<0.05$) (Table 5.2), reduction in BFR (comparable to WT levels) and markedly reduced Oc.N (Fig 5.1B, $p<0.01$). Calcium restriction had no effect on tibia length or body weight in both WT and OSVDR mice (Table 5.2), indicating the 0.1% Ca diet did not affect the growth of these mice.

Table 5.1: Serum 1,25D, calcium, phosphate, parathyroid hormone and FGF23 of WT and OSVDR animals at 18-week of age fed either 1% or 0.1% calcium diet.

		1% Ca	**0.1% Ca**
1,25D	WT	76 ± 23	291 ± 33#
pmol/L	OSVDR	92 ± 24	168 ± 25*#
Ca	WT	2.12 ± 0.10	2.17 ± 0.12
mmol/L	OSVDR	2.24 ± 0.07	2.20 ± 0.07
Pho	WT	2.04 ± 0.26	1.85 ± 0.10
mmol/L	OSVDR	2.15 ± 0.22	1.96 ± 0.10
PTH	WT	10.9 ± 1.3	12.0 ± 1.9
pmol/L	OSVDR	15.2 ± 1.8	15.2 ± 1.6
FGF23	WT	187 ± 9	132 ± 11#
pg/ml	OSVDR	172 ± 14	189 ± 13*

Values are mean ± SEM, n = 5; *p <0.05 versus WT in the same dietary calcium group; # p <0.05 versus 1% dietary calcium of the same genotype.

Table 5.2: Tibial cortical (Cort.BV) and trabecular (BV/TV) bone morphometric analyses and body weights of WT and OSVDR animals at 18-week of age fed either 1% and 0.1% calcium diet.

		1% Ca	**0.1% Ca**
Cort.BV	WT	1.68 ± 0.03	1.65 ± 0.02
mm^3	OSVDR	1.92 ± 0.04*	1.79 ± 0.03*#
BV/TV	WT	7.00 ± 0.33	7.19 ± 0.20
%	OSVDR	8.50 ± 0.57*	7.48 ± 0.14#
Tb.Th	WT	56.9 ± 0.8	56.2 ± 0.7
µm	OSVDR	62.6 ± 0.9*	58.3 ± 0.1*#
Tb.N	WT	1.23 ± 0.06	1.28 ± 0.03
#/mm	OSVDR	1.35 ± 0.07	1.27 ± 0.03
Length	WT	17.6 ± 0.3	17.5 ± 0.4
mm	OSVDR	17.4 ± 0.2	17.4 ± 0.3
Weight	WT	22.9 ± 1.2	23.6 ± 0.7
grams	OSVDR	21.9 ± 1.4	21.6 ± 1.6

Values are mean ± SEM, n = 5; *p <0.05 versus WT in the same dietary calcium group; # p <0.05 versus 1% dietary calcium of the same genotype.

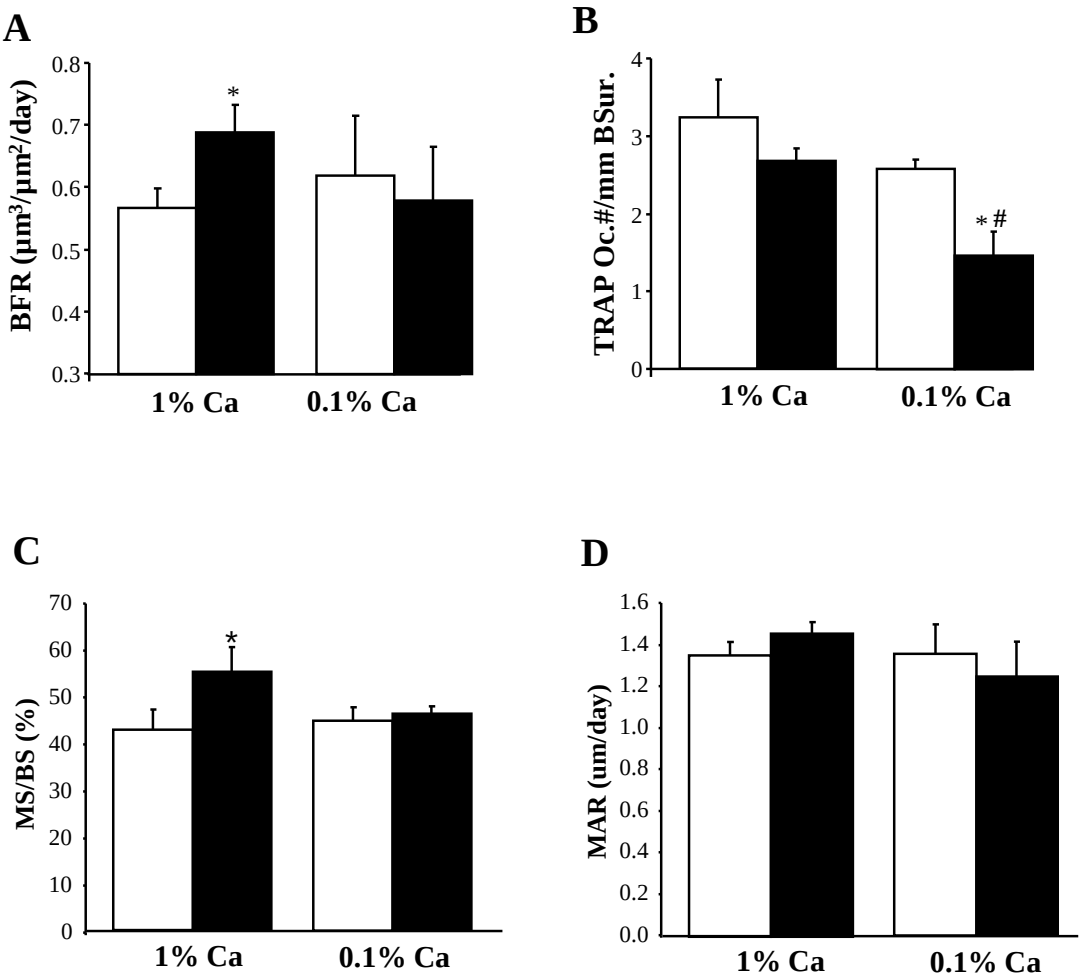

Figure 5.1 *The effect of low calcium on bone cell activities in OSVDR animals*. (**A**) Bone formation rate, (**B**) Tartrate resistance acid phosphatase (TRAP) positive osteoclast surface number per millimetre of bone surface, (**C**) Mineralised bone surface percentages over total bone surface, and (**D**) Mineral apposition rate measured in the tibial proximal trabecular bone of WT (white bar) and OSVDR (black bar) mice fed either 0.1% or 1% dietary calcium. Values are ± SEM. n=6; * $p<0.05$ versus WT of the same dietary group.

5.3.3 Effects of calcium restriction on kidney gene expression and the contribution of osteoblastic VDR and circulating FGF23

5.3.3.1 *Cyp27b1 mRNA*

Kidney *Cyp27b1* mRNA levels were 5-fold greater in WT fed 0.1% Ca compared to 1% Ca fed WT mice ($p<0.001$) (Fig 5.2A) which corresponded with the highest mean level of serum 1,25D (Table 5.1) in the same group. The levels of kidney *Cyp27b1* mRNA were 2-fold higher in OSVDR 0.1% Ca mice compared to OSVDR 1% Ca fed mice ($p<0.05$) (Fig 5.2A). OSVDR mice fed 1% Ca demonstrated a significantly higher kidney *Cyp27b1* mRNA levels when compared to WT mice ($p<0.05$) which also corresponded with the trend for greater mean level in serum 1,25D and lower mean serum FGF23 level in the OSVDR mice fed 1% Ca (Table 5.1). In contrast, kidney *Cyp27b1* mRNA level was significantly lower in OSVDR fed 0.1% Ca than that the levels in kidneys of WT mice fed 0.1% Ca ($p<0.05$). Interestingly, the lower kidney *Cyp27b1* mRNA levels in OSVDR mice fed 0.1% Ca was associated with significantly lower serum 1,25D and higher FGF23 levels (Table 5.1).

5.3.3.2 *Cyp24 mRNA*

In WT mice fed 0.1% Ca, kidney *Cyp24* mRNA was induced (2-fold, $p<0.05$) when compared to WT mice fed 1% Ca (Fig 5.2B). Kidney *Cyp24* levels in OSVDR mice fed 0.1% Ca was also greater that levels in OSVDR mice fed 1% Ca, however the effects did not reach statistical significance. Kidney *Cyp24* mRNA levels were not different in OSVDR and WT mice fed either 1% or 0.1% Ca diets.

5.3.3.3 *Napi2a and Napi2c mRNA*

To determine the physiological effects of circulating FGF23, kidney *Napi2a* and *Napi2c* mRNA were measured (Fig 5.3). In both WT and OSVDR mice fed 0.1% Ca, *Napi2a* and *Napi2c* mRNA levels were markedly enhanced relative to 1% Ca fed mice ($p<0.01$). However, the rise in *Napi2a* and *Napi2c* mRNA levels in 0.1% Ca fed OSVDR mice was

significantly lower ($p<0.05$) than the levels in WT mice fed 0.1% Ca. This is consistent with the higher mean serum FGF23 levels in the 0.1% Ca fed OSVDR mice compared to WT (Table 5.1). Although the levels of *Napi2a* and Napi2c mRNA levels were lower in 1% Ca fed mice, OSVDR fed 1% Ca exhibited significantly higher levels of each gene compared to WT fed 1 % Ca mice ($p<0.05$).

5.3.4 Effects of calcium restriction on intestinal calcium binding protein (Cabp9k) and Transient receptor potential vanilloid type 6 (Trvp6) gene expression

To determine the physiological changes to serum 1,25D, intestinal calcium regulatory genes of *Cabp9k* and *Trvp6* mRNA levels were measured. In WT mice fed 0.1% diet, both *Cabp9k* and *Trvp6* intestinal mRNA levels were markedly increased when compared to levels in 1% Ca fed WT mice ($p<0.01$). In contrast, when OSVDR mice were fed 0.1% Ca diet, no change in the levels of these mRNA species were observed (Fig 5.4). Furthermore, *Trpv6* mRNA levels in OSVDR mice fed 1% Ca were significantly lower than levels in WT mice fed 1% Ca diet ($p<0.05$).

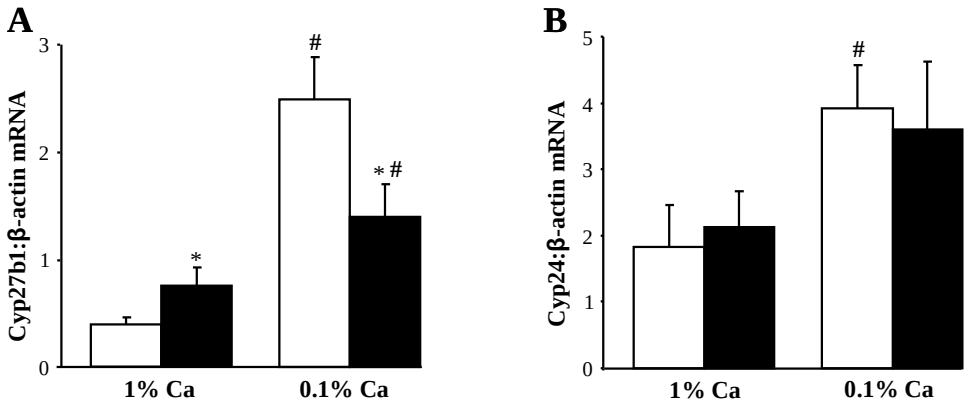

Figure 5.2 *The effect of low calcium on renal hydroxylase gene expression in OSVDR animals*. (**A**) Renal 25 hydroxyvitamin 1α-hydroxylase (*Cyp27b1)* mRNA and (**B**) 25 hydroxyvitamin D 24-hydroxylase *(Cyp24)* mRNA levels in WT (white bar) and OSVDR animals (black bar) fed 0.1% calcium compared to 1% calcium fed animals. Real-time PCR results were expressed as relative to *β-actin* mRNA as house keeping gene, calculated using the formula $2^{\wedge-(Ct[Gene\ of\ interest]-Ct[\beta\text{-actin}])}$. Values are ± SEM. n=6, * $p<0.05$ versus WT of the same dietary group; # $p<0.05$ versus 1% calcium fed animals of the same genetic background.

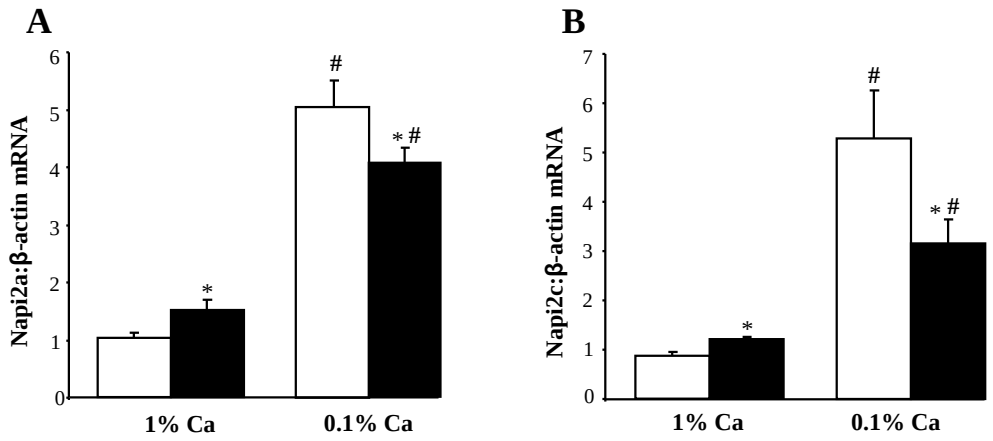

Figure 5.3 *The effect of low calcium on renal Napi2 gene expression..* (**A**) Renal *Napi2a* mRNA and (**B**) *Napi2c* mRNA levels in WT (white bar) and OSVDR animals (black bar) fed 0.1% calcium compared to 1% calcium fed animals. Real-time PCR results were expressed as relative to *β-actin* mRNA as house keeping gene, calculated using the formula $2^{\wedge-(Ct[Gene\ of\ interest]-Ct[\beta\text{-actin}])}$. Values are ± SEM. n=6; * $p<0.05$ versus WT of the same dietary group; # $p<0.05$ versus 1% calcium fed animals of the same genetic background.

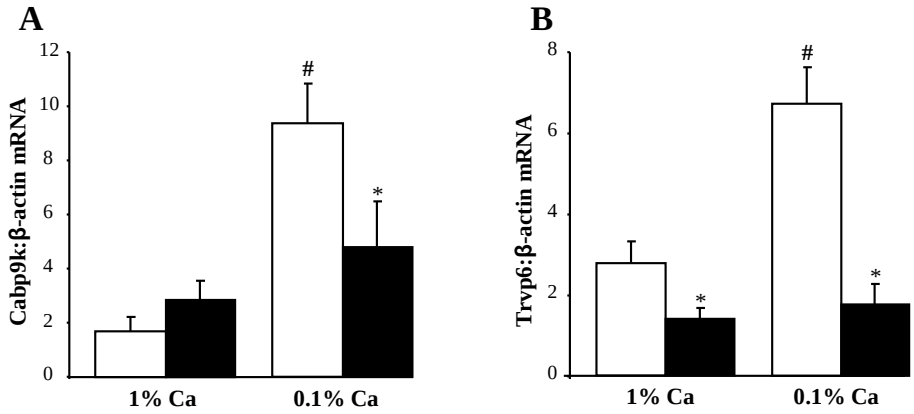

Figure 5.4 *The effect of low calcium on intestinal calcium transporters gene expression.* (**A**) Intestinal Calbindin-9k (*Cabd-9k*) mRNA and (**B**) Transient receptor potential vanilloid 6 (*Trvp6*) mRNA levels in WT (white bar) and OSVDR animals (black bar) fed 0.1% calcium compared to 1% calcium fed animals. Real-time PCR results were expressed as relative to *β-actin* mRNA as house keeping gene, calculated using the formula $2^{\wedge-(Ct[Gene\ of\ interest]-Ct[\beta\text{-}actin])}$. Values are ± SEM. n=6, * $p<0.05$ versus WT of the same dietary group; # $p<0.05$ versus 1% calcium fed animals of the same genetic background.

5.3.5 Effects of calcium restriction and the contribution of osteoblastic VDR on bone cell activities as measured by qRT-PCR

5.3.5.1 *Bone VDR mRNA*

To determine whether dietary calcium restriction had an effect on bone VDR levels, bone *mVdr* (mouse) and *hVDR* (human) mRNA was measured. Although the bone *mVdr* levels were lower in both OSVDR and WT mice fed 0.1% Ca when compared to the 1% Ca fed groups ($p<0.05$, Fig 5.5A), the *mVdr* levels in OSVDR's bones were comparable to WT levels (Fig 5.5A). Furthermore, a change in dietary calcium did not alter the expression of *hVDR* mRNA levels compared to OSVDR mice fed 1% Ca (Fig 5.5B). Messenger RNA for *hVDR* was expectedly undetectable in WT bones.

5.3.5.2 *Osteoblastic genes*

In WT bones, the osteoblastic marker, *Runx2* mRNA level was not altered as result of changed dietary calcium. In contrast, bone *Runx2* mRNA levels were 2-fold lower in OSVDR mice fed 0.1% Ca when compared to 1% Ca fed OSVDR mice ($p<0.001$, Fig 5.6A). *Runx2* mRNA levels in these 0.1% Ca fed OSVDR mice was also 2.5-fold lower than levels in WT mice fed 0.1% diet ($p<0.01$, Fig 5.6A). Unlike the *Runx2* mRNA levels, *Alp, Ocn* and *Col1* mRNA levels were all significantly higher in WT mice fed 0.1% Ca when compared to WT mice fed 1% Ca ($p<0.05$, Fig 5.6B, C, D). In stark contrast, OSVDR mice fed 0.1% Ca reported significantly lower *Ocn* and *Col1* mRNA levels ($p<0.05$) compared to levels in OSVDR fed 1% Ca mice. Furthermore, *Alp* mRNA levels were maintained in 0.l% Ca fed OSVDR mice which is in contrast to the increases observed to 0.1% Ca fed WT mice (Fig 5.6B, C, and D). The reduction in the osteoblast-related genes in 0.1% Ca fed OSVDR mice is consistent with reduced bone formation rate described earlier (Fig 5.1A). Similarly, the greater *Ocn* and *Alp* mRNA levels in 1% Ca fed OSVDR mice compared to WT miceconsistent with the higher bone formation rate in these 1% Ca fed OSVDR mice (Fig 5.1A).

5.3.5.3 *Osteoclastic genes*

The osteoclastic marker, *NFatc1* and *Rankl* mRNA levels were not significantly different between WT mice fed 1% or 0.1% Ca diet. In contrast, *NFatc1* and *Rankl* mRNA levels were significantly lower in OSVDR mice fed 0.1% Ca compared to both 1% Ca OSVDR mice and WT mice fed 0.1% Ca ($p<0.01$, Fig 5.7), consistent with the low osteoclast surface number in 0.1% Ca fed OSVDR mice (Fig 5.1B)

5.3.5.4 *Osteocytic genes*

To determine whether the OSVDR transgene affected osteocytic formation and activities, the mRNA levels for the early osteocytic marker *E11*, and mature osteocytic markers and functional genes such as *Dmp-1*, *Sost* and *Phex* were all measured. The results showed a similar pattern regardless of which gene was measured. No statistical difference was observed in the levels of any of these four mRNA species between WT mice fed either 0.1% or 1% Ca diet. In contrast, in OSVDR mice fed 0.1% Ca the levels of mRNA for *Dmp-1*, *Sost* and *Phex* were all markedly reduced when compared to OSVDR fed 1% Ca mice ($p<0.05$, Fig 5.8). In the 1% Ca fed mice, except for *E11*, *Dmp-1 Sost* and *Phex* mRNA levels were all significantly greater in OSVDR compared to WT mice ($p<0.05$). Furthermore, OSVDR mice fed 0.1% Ca demonstrated reduced levels of mRNA for *E11*, *Dmp-1*, *Sost* and *Phex* mRNA levels when compared to WT mice fed the same diet ($p<0.01$) (Fig 5.8). These data suggest that osteocytic formation activity is impaired in these OSVDR mice fed 0.1% Ca diet. However, despite the changes to serum FGF23 levels in OSVDR mice fed 0.1% Ca (Table 5.2), the levels of bone *Fgf23* mRNA were unchanged as result of either dietary calcium variation or OSVDR transgene (Fig 5.8E).

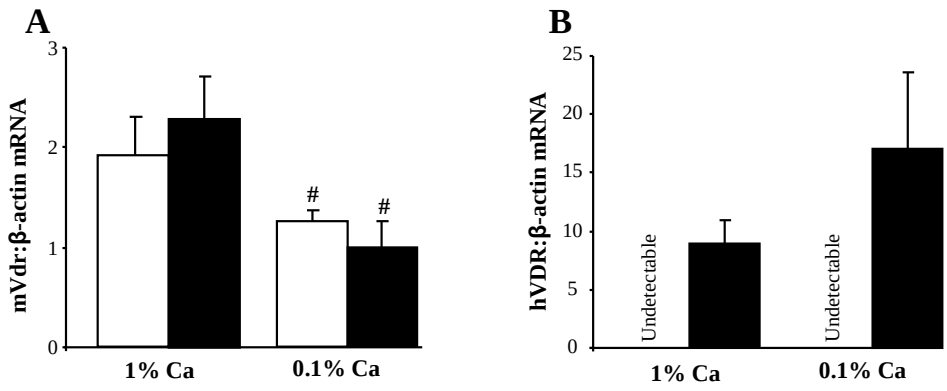

Figure 5.5 *The effect of low calcium on bone VDR gene expression.* (**A**) Mouse bone *Vdr* mRNA and (**B**) human bone VDR mRNA levels in WT (white bar) and OSVDR animals (black bar) fed 0.1% calcium compared to 1% calcium fed animals. Real-time PCR results were expressed as relative to *β-actin* mRNA as house keeping gene, calculated using the formula $2^{\wedge-(Ct[Gene\ of\ interest]-Ct[\beta\text{-}actin])}$. Values are ± SEM. n=6, # $p<0.05$ versus 1% calcium fed animals of the same genetic background.

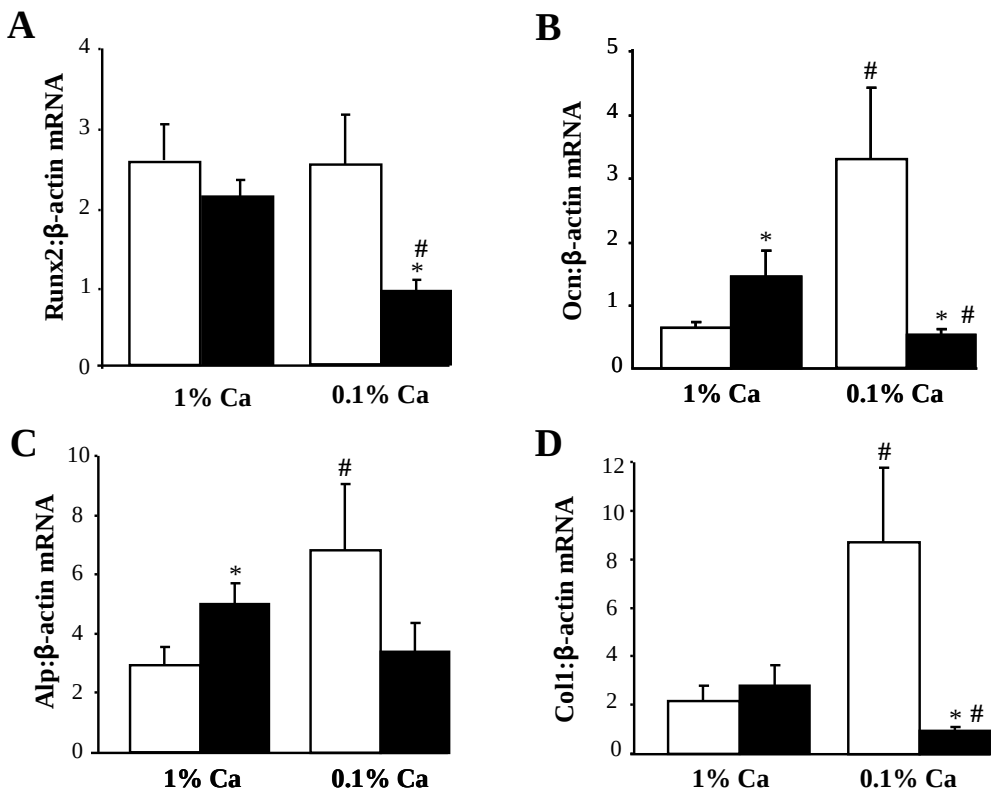

Figure 5.6 *The effect of low calcium on osteoblastic differentiation and functional genes.* (**A**) Bone Runt-related transcription factor 2 (*Runx2*), (**B**) osteocalcin (*Ocn*), (**C**) alkaline phosphatase (*Alp*) and (**D**) collagen 1 (*Col1*) mRNA levels in WT animals (white bar) and OSVDR animals (black bar) fed 0.1% calcium compared 1% calcium diet. Real-time PCR results were expressed as relative to *β-actin* mRNA as house keeping gene, calculated using the formula $2^{\wedge-(Ct[Gene\ of\ interest]-Ct[\beta\text{-}actin]}$). Values are ± SEM. n=6; * $p<0.05$ versus WT of the same dietary group; # $p<0.05$ versus 1% calcium fed animals of the same genetic background.

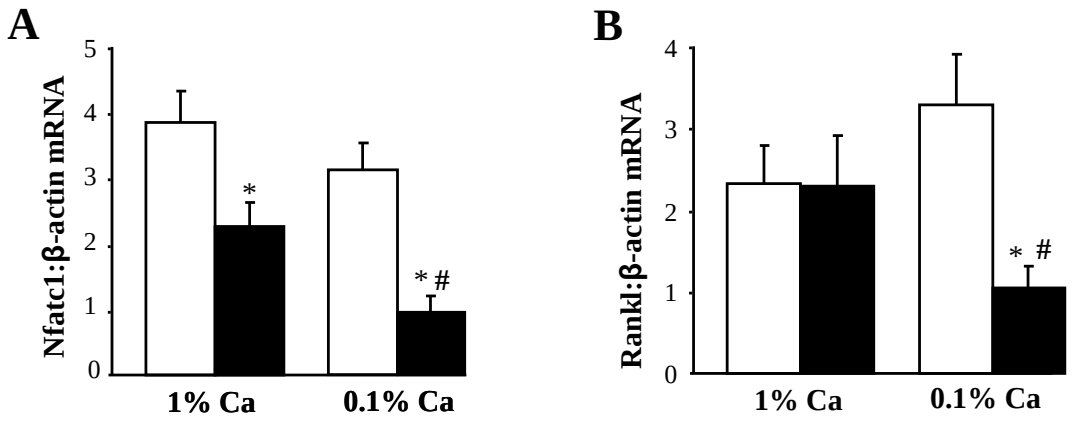

Figure 5.7 *The effect of low calcium on osteoclastic differentiation and activation genes.* (**A**) Bone nuclear factor activated T-cell cytoplasmic 1 (*Nfatc1*) and (**B**) receptor activator nuclear factor κB ligand (*Rankl*) mRNA levels in WT animals (white bar) and OSVDR animals (black bar) fed 0.1% compared to 1% calcium diet. Real-time PCR results were expressed as relative to *β-actin* mRNA as house keeping gene, calculated using the formula $2^{\wedge-(Ct[Gene\ of\ interest]-Ct[\beta-actin])}$. Values are ± SEM. n=6; * $p<0.05$ versus WT of the same dietary group; # $p<0.05$ versus 1% calcium fed animals of the same genetic background.

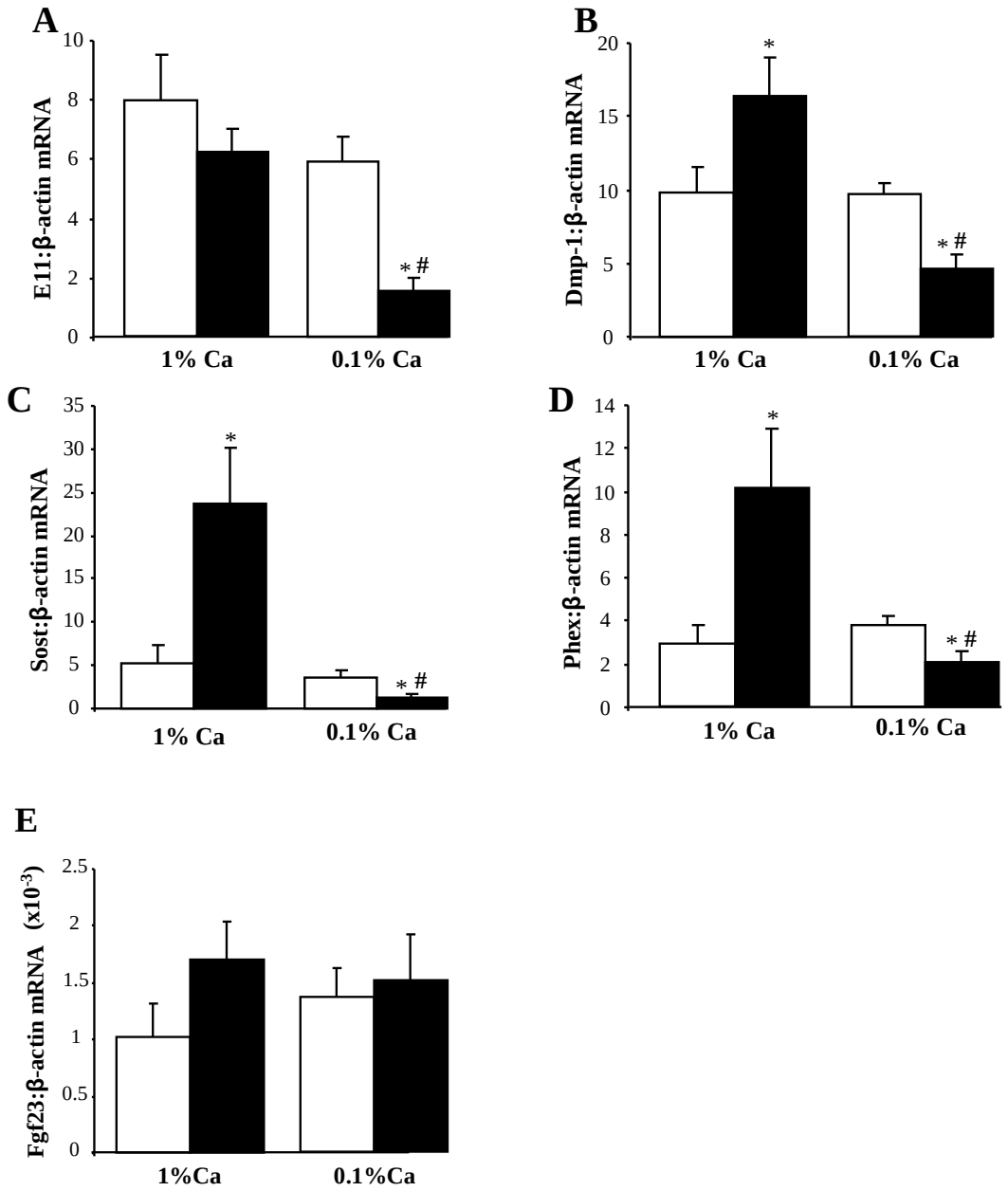

Figure 5.8 *The effect of low calcium on osteocytic differentiation and functional genes.* (**A**) Bone Early osteocytic marker *E11*, (**B**) Slerostin encoded gene (*Sost*), (**C**) Dentin matrix protein 1 (*Dmp-1*) and (**D**) Phosphate-regulating gene with homologies to endopeptidases on the X-chromosome (*Phex*) and (**E**) Fibroblast growth factor 23 (*Fgf23*) mRNA levels in WT animals (white bar) and OSVDR animals (black bar) fed 0.1% compared to 1% calcium diet. Real-time PCR results were expressed as relative to *β-actin* mRNA as house keeping gene, calculated using the formula $2^{\wedge-(Ct[Gene\ of\ interest]-Ct[\beta\text{-actin}])}$. Values are ± SEM. n=6; * $p<0.05$ versus WT of the same dietary group; # $p<0.05$ versus 1% calcium fed animals of the same genetic background.

5.3.6 Effects of increased osteoblastic VDR and calcium on mineralisation in vitro

To determine the direct effects of changes to extracellular calcium in OSVDR and WT osteoblastic functions, osteoblasts of WT and hemizygous OSVDR mice were isolated from long bones and cultured in pro-differentiated media containing either 1.8mM which represented low/basal level of calcium or 2.8mM, which represented high/supplement calcium (as described in chapter 5.2.6). Cultures were allowed to mineralise for 18 days. Both WT and OSVDR osteoblasts cultured with 2.8mM calcium had significantly greater mineral deposition compared to the levels in cultures treated with 1.8mM calcium ($p<0.001$, Fig 5.9A and B). Primary osteoblasts from OSVDR bones treated with 1.8mM calcium demonstrated significantly greater mineralisation compared to WT osteoblasts cultures ($p<0.001$, Fig 5.9A and B). However, there was no difference in the level of mineralisation between OSVDR and WT osteoblasts cultured with 2.8mM calcium.

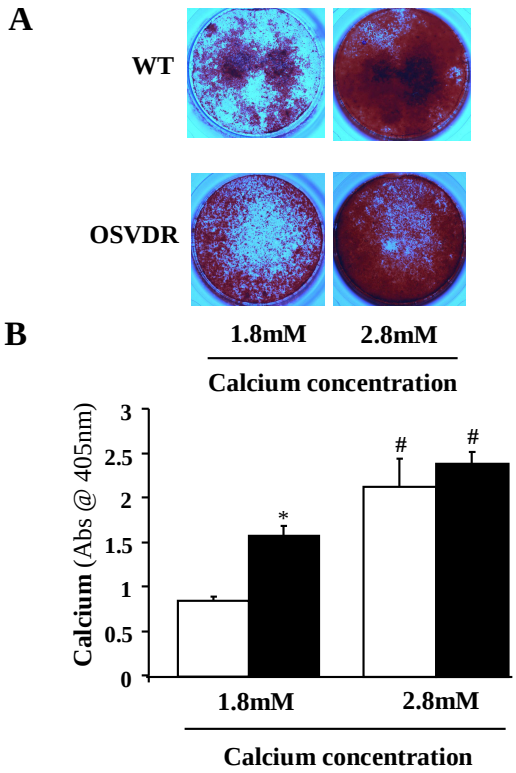

Figure 5.9 *The effect of low calcium on in vitro mineralisation.* Osteoblasts from long bones of 6-week old WT (white bar) and OSVDR hemizygous animals (black bar) were cultured in osteogenic differentiation medium for 18 days with either 1.8mM or 2.8mM calcium concentration. Osteoblasts were examined for ability to mineralise by (**A**) Alizarin red stains and (**B**) calcium quantification by absorbance analysis. Values are the mean ± SEM, n=3 animals of each genotypes, each animal done in triplicate, experiment repeated 2x; * $p<0.05$ versus WT of the same calcium grou;, # $p<0.05$ versus 2.8mM calcium of the same genetic background.

5.4 DISCUSSION

5.4.1 VDR activity in osteoblasts is important for bone remodelling

This study has provided novel *in vivo* evidence regarding the function of VDR activity in the bone for the regulation of bone cell activities and bone remodelling. We have demonstrated that OSVDR mice maintained on a diet containing sufficient vitamin D and calcium (1%) have enhanced osteoblastic activity as evidenced by the greater bone formation rate, associated with greater expression of the bone formation markers genes, *Ocn* and *Alp*. Furthermore, osteoclast number was reduced, which was associated with a reduction in the gene expression of osteoclast formation genes, *Nfatc1* and *Rankl*. Together these activities lead to greater bone mass in at least the metaphyseal trabecular and cortical bone volume of the tibia in the OSVDR mice, findings supported by previous reports (Baldock, et al., 2006; Gardiner, et al., 2000). While we observed no adverse effects of the mild calcium restriction of 0.1% on WT animal bone structure when compared to mice who received the more than adequate 1% Ca, OSVDR bone structure was markedly affected by this level of calcium restriction, with the trabecular and cortical bone volume of OSVDR mice diminished to bone levels of WT mice. While this finding is consistent with other observations (Baldock, et al., 2006), in the current experiment when OSVDR mice fed the calcium restricted diet, although we showed no difference in BFR, OSVDR mice have reduced mRNA levels for *Ocn*, *Alp* *Col1* and *Runx2*, all major markers of osteoblastogenesis and functions. Furthermore osteoclastic formation was also interrupted as represented by low *Rankl* and markedly reduced *Nfatc1* mRNA levels, leading to a reduction of osteoclastogenesis in these low calcium fed OSVDR mice. These data indicate that increased VDR activity in osteoblasts mediates significant effects on both osteoblastic and osteoclastic formation and is somewhat similar to what had previously been observed in the VDR knockout mice fed the rescue diet, where VDR activity was suggested to be playing an important role in optimising bone formation and resorption for normal bone remodelling (Panda, et al., 2004).

The question of whether the disruption of osteoblastic activity in OSVDR mice fed low calcium was due either to a direct effect of VDR mediated signalling of osteoblastic activity or to an indirect effect such as impaired osteoclastogenesis or other feed-back signalling is unclear in this *in vivo* study. Thus, in an attempt to understand the intrinsic features of the OSVDR osteoblasts in response to low calcium, we used long bones primary osteoblasts *in vitro* cultures to investigate the effect of a low calcium environment on cell activity and mineralisation. When treated with either calcium at the concentration of 1.8 or 2.8 mM, which is an approximation of insufficient and sufficient serum calcium levels respectively, no impairment of mineralisation relative to WT primary cells at either concentration of Ca was observed (Fig 5.9). This suggests that the involvement of regulatory mechanisms, other than a low calcium environment contribute to the disruption of bone turnover in OSVDR mice fed low dietary calcium. Moreover, the reason for reduced osteoblast activities in OSVDR animal fed the calcium restricted diet was also not due to loss of transgene VDR expression in the bone (Fig 5.5). Of considerable interest is the marked reduction in the expression of a number of osteocyte specific genes, including the early osteocytic marker E11, osteocytic maturation and functional genes Sost, Dmp1 and Phex in OSVDR mice fed 0.1% Ca. Thus, under conditions of low dietary stress, in addition to a disruption of normal osteoblast activity in OSVDR mice, it is possible that osteocyte formation and/or maturation may also have been impaired. Such a declined in osteocyte activity may have been due to a reduction on osteoblast transition into osteocytes or due to direct VDR signalling within osteocytes themselves by virtue of the fact that osteocalcin-driven transgene expression of VDR is likely to occur within osteocytes (Bilic-Curcic, et al., 2005). While no formal measures of osteocyte density where undertaken in this study, it is possible that a reduction in osteocyte activity or density in OSVDR mice may have impaired osteocyte-mediated signalling is the reason for failed bone turnover (Schaffler, 2003). The investigation of the role of osteocytes in this model is a worthy proposal requiring future exploration.

5.4.2 VDR activity in osteoblasts mediate feedback for renal 1,25D synthesis by FGF23, impacting on intestinal calcium absorption

In OSVDR mice fed the calcium restricted diet, the synthesis of vitamin D by the renal Cyp27b1 was reduced as evidenced by the lower serum 1,25D levels in 0.1% Ca fed OSVDR mice when compared to levels in WT mice. The most likely reason for this reduction in serum 1,25 levels is a significant increase in serum FGF23 levels of OSVDR mice. FGF23, which is produced mainly by cells of the osteoblast lineage (Liu, et al., 2007) is a potent suppressor of renal 1,25D levels by inhibiting Cyp27b1 and activating Cyp24 mRNA levels (Shimada, et al., 2004). Higher serum FGF23 levels in 0.1% Ca fed OSVDR mice not only had reduced renal Cyp27b1 mRNA levels and reduced serum 1,25D levels, but also Napi2a and Napi2c mRNA levels, targets of FGF23 suppressive activity were both significantly reduced. The rise in serum FGF23 level was not due to the direct increase in transcriptional regulation of FGF23 mRNA, suggesting that post-translational regulation of FGF23 is the reason for changes in serum FGF23 levels. Of some relevance to the current study, recently serum FGF23 levels were strongly associated with levels of bone turnover (Samadfam, et al., 2009). In this study, exogenous administration of the anti-resorptive agent OPG to male and female mice caused a profound suppression of bone turnover, represented by reduced serum osteocalcin and the osteoclast marker TRAP5b serum levels, which also resulted in markedly increased serum FGF23 levels. The opposite effect was observed after PTH administration with increased bone turnover and reduced serum FGF23 levels (Samadfam, et al., 2009). In the current study, OSVDR mice fed the calcium restricted diet demonstrated reduced bone turnover as measured by marked reduction in osteoblasts and osteoclasts formation, which was associated with higher serum FGF23 level and consistent with the reports of Samadfam and colleagues. This suggests that the modification of bone turnover in OSVDR mice plays an important role for FGF23 production.

While the full understanding of the mechanism for the effect of bone turnover on FGF23 production is unclear, there have been several lines of evidence to implicate DMP-1 and PHEX as potential candidates in the regulation of FGF23 production in the bone. PHEX and FGF23 co-localised in osteocytes and inactivating PHEX mutation leads to increased FGF23 circulating levels (Liu, et al., 2006). Furthermore, studies have suggested PHEX to be a putative inhibitor of mineralisation that may contribute to direct mineralisation defects in osteoblasts independent of hypophosphatemia (Xiao, et al., 1998). In regard to DMP-1, firstly, DMP-1 is expressed only in mature, mineralising osteoblasts and deletion of *Dmp-1* in mice results in markedly induced FGF23 circulating levels, although the mechanism is not clear (Feng, et al., 2006; Lorenz-Depiereux, et al., 2006). Secondly, PTH administration increases bone turnover associated with increased *Dmp-1* mRNA expression and inturn decreased FGF23 levels (Samadfam, et al., 2009). Furthermore, extracellular DMP-1 has been shown to inhibit vitamin D-induced *Ffg23* gene expression *in vitro,* implying a direct role for DMP-1 in modulating FGF23 production, however this is yet to be confirmed *in vivo* (Samadfam, et al., 2009). We have shown in our study that reduction in *Dmp-1* and *Phex* mRNA levels in OSVDR mice fed the calcium restricted diet correlated strongly with higher circulating FGF23 levels. Although the question as to why disruption of osteocyte formation and/or activity in OSVDR mice fed the calcium restricted diet lead to greater FGF23 production requires further investigation, our data support the essential regulation of FGF23 production by DMP-1 and PHEX and importantly the effects of VDR on mineralisation.

Published data showed using the quantitative backscattered electron microscopy technique that OSVDR femora contained 3.43% and 1.84% greater calcium content (Ca_{peak}) in the trabecular and cortical bone respectively compared to matched WT mice (Misof, et al., 2003), indicating higher calcium requirement per unit of bone in these OSVDR mice. It appeared that the active intestinal transport of calcium was altered in the OSVDR mice fed calcium restricted diet as evidence by the reduction in active intestinal calcium absorption genes of calbindin-9k and Trvp6. The likely consequence of this is reduced calcium available for

mineralisation which therefore may contribute to reduced bone phenotype that occurs in OSVDR fed the calcium restricted diet.

In conclusion, this study demonstrates direct VDR activity in osteoblasts, mediates the regulation of osteoblast, osteoclast and possibly osteocyte activities, impacting on bone turnover and bone homeostasis. Furthermore, VDR activity in osteoblasts is able to provide feedback for renal 1,25D synthesis, impacting on active calcium absorption and bone mineralisation. While the mechanisms remain to be completely elucidated our data provide further evidence to support the autocrine and paracrine roles of 1,25D in bone homeostasis.

Chapter 6

SUMMARY AND CONCLUSION

6.1 Introduction

This thesis was undertaken to investigate the actions of vitamin D acting via mature osteoblastic VDR activity to regulate skeletal homeostasis. More specifically, the studies described in this thesis were designed to assess the role of direct activity of vitamin D in osteoblasts via the VDR during the physiological challenges of vitamin D and calcium deficiency. We have utilised the mature osteoblast-specific VDR over-expression (OSVDR) transgenic mouse model for this investigation. Previously, the OSVDR mouse model was reported to have a high bone mass phenotype which was specifically located to cortical bone and vertebral trabecular bone. However, no previous investigation sought to describe the extent of the bone phenotype of the OSVDR mouse model using the more sensitive and descriptive techniques of micro-computed tomography. Although the reported increase in bone mass of the OSVDR mouse model was shown to be due to a combination of increased bone formation and reduced bone resorption (Baldock, et al., 2006), much less was understood regarding the direct *in vivo* role of vitamin D activity in osteoblasts. In particular, the question of whether direct activity of vitamin D in osteoblasts is altered during known physiological stressors of bone metabolism remains to be answered. Thus, my studies sought to answer whether enhanced vitamin D activity in osteoblasts alters osteoblastic activity in response to the physiological challenges to bone health of vitamin D and calcium deficiency. Furthermore, I have sought to address the question of whether the role for vitamin D activity within osteoblasts is entirely mediated locally or at least within the bone micro-environment or whether vitamin D activity in osteoblasts is also involved in signalling indirect endocrine mechanisms of bone homeostasis.

6.2 Extent of the bone phenotype of the OSVDR mouse model.

While the initial reports characterised cortical bone and vertebral trabecular bone as the primary sites for increased bone mass in the OSVDR mouse model, we were able to show using the 3D micro-CT analyses, that tibial and femoral metaphyseal bone was significantly greater in OSVDR mice when compared to WT mice. Furthermore, we confirmed that inhibition of bone resorption also occurred in the tibial and vertebral trabecular bone of both young (6-week) and aged (18-week) female mice, suggesting that the reduced RANKL expression and reduced osteoclastogenesis occured widespread throughout the skeleton and not limited to specific sites. In addition, the increased bone formation rate observed in OSVDR mice was confirmed in these metaphyseal regions. Thus the effect of vitamin D activity in mature osteoblasts can be observed both in cortical and trabecular bone, and appears to be independent of the region investigated.

6.3 Evidence for direct local effect of osteoblast-specific vitamin D activity

Our study on the effect of vitamin D deficiency and osteoblastic activities revealed that in young growing animals, mild 25D deficiency of 25nmol/L was insufficient to provide optimal bone accumulation, leading to a reduction in periosteal osteoblastic activities and thinner cortices in adult life. While renal synthesis of 1,25D was unaffected by the substrate 25D level of 25nmol/L, we speculated that osteoblastic synthesis of 1,25D may have been impaired and that increased sensitivity to locally produced 1,25D by the enhanced VDR prevented the impairment of periosteal osteoblastic activities. These data imply that the reason for low bone volume during low 25D deficiency is at least in part due to impaired vitamin D activity with osteoblasts and possibly points to the essential role of local 1,25D synthesis within bone. This has clinical implications as these data suggests that bone loss that occurs due to vitamin D depletion, is at least partially due to reduced vitamin D activity in osteoblasts and thus must be considered in addition to the effects of vitamin D deficiency on intestinal calcium absorption.

Our *in vitro* studies support the findings of vitamin D activity directly inhibiting osteoblastic differentiation, but stimulate matures osteoblasts to mineralise. Treatment of primary WT osteoblastic cells with 1,25D completely inhibited osteoblastic activities, possibly due to inhibition of cell differentiation, resulting in the absence of mineralisation. Conversely, primary osteoblasts derived from OSVDR bones resulted in the stimulation of mineralisation. This is consistent with the increase in bone formation rate observed *in vivo* in OSVDR mice. It is also consistent with some reports that reduced mineralisation occurs in osteoblasts derived from VDRKO mice. The concept that VDR in mature osteoblasts mediated bone formation processes is also supported by unpublished findings that OSVDR animals exhibit greater sensitivity to mechanical loading in terms of inducing woven bone formation when compared to wild-type mice receiving an equivalent microstrain (Anderson, unpublished findings). This periosteal mineral deposition is due to osteoblastic activity which may also involve osteocyte activity as the mechanosensing cell of the bone. Given that the VDR transgene is likely to be expressed in osteocytes as well, this suggests that enhanced vitamin D activity within osteocytes may mediate anabolic activities under the conditions of increased mechanical loading. It is also plausible that enhancing vitamin D activity in mature osteoblasts promotes greater mineralisation as well as differentiation of mature osteoblasts into osteocytes, leading to increased sensitivity to mechanical loading and bone formation. Such a role for VDR is suggested in this thesis but would need to be explored with studies that specifically examine this proposal.

Earlier studies have demonstrated that OSVDR long bones have increased calcium concentration in the mineralised matrix, suggesting a role for osteoblastic VDR in calcium homeostasis. We have confirmed the role of osteoblastic VDR and enhanced mineralisation effect of calcium on OSVDR osteoblast mineralisation *in vitro*. However, it appears that during the physiological challenges of low dietary calcium, vitamin D-mediated osteoblastic

mineralisation is secondary to essential role of maintaining serum calcium and phosphate within the physiological levels. Therefore the greater demand of calcium in OSVDR bones was not satisfied under low calcium condition, possibly contributing to disruption in osteoblastic activities, best demonstrated by a reduction of osteoblastic-specific mineralisation markers and bone formation rate. Moreover these data suggest that the osteoblast response to changes in extracellular calcium level is mediated through VDR signalling. One hypothesis is that this may occur via the VDRE present in the calcium sensing receptor genes. Such a novel proposal would suggest that vitamin D signalling and calcium homeostasis occur locally in osteoblasts, the result of which may be to directly modify the bone microenvironment.

Given that a major effect of increased VDR levels in osteoblasts is the reduced signalling of osteoclastogenesis, the lowered of osteoblastic activities under a low dietary calcium stress in OSVDR animals may be primarily due to a failure to promote appropriate osteoclastogenesis and the resultant increased bone turnover. Such a proposal would suggest that the OSVDR model is primarily a model of inhibition of bone resorption which, under conditions of adequate nutrition, is beneficial for bone mass. However, under circumstances of poor calcium nutrition, result in inappropriately low bone resorption leading to downstream pathology. In addition to failed bone formation, osteocyte activities appeared to also be affected as evidence by the marked reduction in various osteocyte-specific marker gene expressions. While the data confirm the role of vitamin D signalling to regulate bone remodelling processes, further studies utilising other appropriate mouse models may need to be performed to further elucidate the VDR role under the circumstance of calcium deprivation. Nonetheless, our data support the hypothesis that under physiological low calcium stress, the interactions of vitamin D signalling in osteoblasts is involved to directly modify cellular processes.

6.4 Endocrine effect of osteoblast-specific vitamin D activity

Previous reports on the OSVDR mouse model highlight the local effects of vitamin D activity in osteoblasts. Any suggestions of other changes to activities were dismissed as no significant changes were observed in measures of calciotropic hormones. Our studies have shed new light on the role for vitamin D activity in osteoblasts in as much as vitamin D signalling in osteoblasts was able to mediate renal feedback signalling via FGF23, leading to significant changes to renal vitamin D hydroxylase activities and circulating 1,25D levels. Our data suggested that *in vivo* osteoblastic VDR does not play a direct transcriptional role on *Fgf23* gene expression, suggesting that either an indirect mechanism or post-translational modification of FGF23 protein is involved. While we are unable to definitively show why FGF23 levels were higher in OSVDR mice when fed low dietary calcium, it was likely that altered osteocyte activity played a role. For instance, the expression of Dmp1 and Phex, which are known negative regulators of FGF23 production, were markedly reduced in OSVDR mice and thus could have been responsible for the higher FGF23 levels in these mice. Although we can suggest that the OSVDR bone phenotype was determined at least in part by changes to osteocyte activities, further studies will be required to specifically investigate the role of vitamin D activity in osteocytes.

To specifically identify the role of VDR in mature osteoblasts as well as osteocytes, future experiments could involve genetically altered mouse models to exclusively delete VDR in each of these cell types using Cre-Lox systems. Alternatively, a model whereby VDR is restored in osteoblasts in the genetic background of the VDRKO mouse could also prove useful to determine the necessity of VDR to maintain normal osteoblastic and osteocytic functions under circumstances of physiological stress, such as when fed low dietary calcium.

6.5 Limitations

The primary model used in my studies is that of the OSVDR mouse, which was designed to target the overexpression of VDR in osteocalcin expressing osteoblasts. While this model is useful to investigate the role of VDR-mediated activities in osteoblast, there are limitations as to its interpretation as well. The main reason for the limitation is that the activity of the osteocalcin promoter is not limited to osteoblast. Firstly, osteocalcin is expressed in osteocytes. Thus the likely over-expression of VDR in osteocytes as well as osteoblasts prohibits the decisive demonstration of the effects of VDR over-expression solely in osteoblasts. Similarly, a potential limitation of this mouse model is that osteocalcin driven VDR transgene was also expressed in non-osseous tissues, including the kidney and the intestine, which are involved with vitamin D and calcium homeostasis. However, there were no differences in the protein levels of VDR in these tissues between OSVDR and WT animals (Figure 3.5), nor effects on serum levels of calcium and phosphate in OSVDR animals when fed a standard diet, nor effects in intestinal genes Calbindin 9k and Trvp6, suggesting that any low level of transgene expression in either kidney and intestine may be insufficient to alter homeostatic mechanisms. However, greater expression of kidney Napi2a/c levels was observed in OSVDR animals, which would need to be further investigated to determine if there are potential effects of extra VDR in kidney.

Other limitations to the interpretation of data include the fact that design of each study varied sufficiently so as to not be able to directly compare results between studies. The variation between studies include: age, dietary duration/regime and the genotype of the OSVDR. Previous studies in rats showed calcium balance and the true calcium absorption decrease rapidly with age, especially greater in 12-15 weeks of age compared to 6-9 weeks of age (O'Loughlin and Morris, 1994). Our study used mice that were 4 weeks and 6 weeks old, as well as differences in the duration of the dietary feeding may have led to differences in the biochemical measures, making inter-study comparisons difficult to do. One such example of

this is the value obtained for serum 1,25D levels for the wild-type vitamin D replete mice. Serum 1,25D levels were comparable to the wild-type values in chapter 3 and 4, however, the 1,25D values for OSVDR mice fed replete diet between chapter 3 and 4 were different. The explanations for why this difference in 1,25D occurs between chapters are not immediately clear. However, as described above, the duration of feeding and the age of the mice between the two studies differed. Since the serum 1,25D levels are regulated by changes in the serum calcium and phosphate levels which are mediated by PTH and FGF23, the likely explanation in the divergent results for OSVDR's 1,25D levels is related to the feeding regimen, and/or the age of mice. Differences in the age and dietary regimen between studies may have resulted in differences in the bio-absorption of calcium and phosphate which were pronounced in OSVDR mice. Furthermore, as the mice were fed ad libitum rather than meal fed it is possible that the amount of diet consumed by each mouse differed. Since I was unable to directly compare biochemical measures for PTH between chapters (see discussion below), I am unable to provide direct evidence to establish reasons for the marked differences between 1,25D measures between assays. A study using metabolic cages where individual mice could be monitored for dietary consumption would be able to provide such data regarding precise consumption of vitamin D and calcium in relation to genotype and age of mice, however that was beyond the capacity of my studies. It is worth noting that the differences in 1,25D levels between chapter 3 and 4 may also partly based on the observed divergent response of OSVDR mice to a low calcium diet when compared to wild-type mice in chapter 5. In this chapter it is clear that, serum 1,25D levels can be lower than wild-types due to a difference in FGF23 levels between genotypes.

With respect to measurement for FGF23 levels, we observed a doubling of FGF23 levels in the OSVDR mice in chapter 5 compared to those in chapter 4. These may be explained by the difference in the age of the mice and the duration of the diet in these studies. However previous studies have shown that a diet containing 2% calcium, 200ng VitD3/animal/day significantly increases circulating FGF23 levels 10-fold, the same effect also occurred in

VDR-KO mice, indicating that calcium regulation of FGF23 production is independent of VDR {Shimada, et. al., 2005}. To our knowledge no studies have examined the effect of low (0.1%) calcium on FGF23 expression, therefore we did not know what to expect with 0.1% calcium diet in chapter 5. The data also showed that WT fed 0.1% calcium have reduced FGF23 levels and dramatically elevated 1,25D levels compared to WT fed 1% calcium diet. No effect of 0.1% calcium diet was observed in OSVDR mice. Due to the complexity of OSVDR mice and the control of FGF23 production (VDR-dependent vs. independent), I believe the effect of calcium in OSVDR mice may be very different to WT mice and further studies are needed to investigate these mechanisms.

My studies were also limited by a reliable PTH analysis between different assays and studies. While the immunoradiometric assay (IRMA) of PTH assay contains standards, it does not contain QC's, which, if included, could have been used to establish inter-assay variability. While the PTH IRMA assays performed well from the point of view of the standard curve, such that we can make comparison between groups within the assay, we are unable to make reliable comparisons of blood samples between different assays. Moreover, serum PTH values can be altered by technical issues such as where the blood sample are collected from (i.e. peripheral blood verses cardiac blood), as well as specimen stability (i.e. freeze-thaw degradation and instability). PTH also has a strong diurnal pattern of release related to fasting. While we did what we could to limit the variation due to these technical issues, variability in the measures between studies remains between the values in different studies. Moreover, we were not able to repeat measures of experimental samples due to only one aliquot of frozen serum being collected for PTH analysis per animal.

Another limitation is our *in vitro* studies have only one time point, we would endeavour for future experiments to include multiple time points to observe the cellular changes with culture condition over time and responses of the cells to treatment of 1,25D and calcium, as well as to include measures of osteoblastic proliferation and matrix composition. Furthermore, the

osteogenic potential of OSVDR's primary osteoblasts isolated from long bones versus calvaria bones were not examined in this thesis. Previous studies have shown significance differences in the cellular and matrix composition of bones from the skull and long bones (Van den Bos, et al., 2008; Vatsa, et al., 2008), therefore we would expect that differences would exist between the cells derived from calvaria and long bones.

6.6 Conclusion

The findings of this thesis indicate that the 1,25D/VDR-regulated pathways in mature osteoblastic cells are involved in local activities of bone mineral homeostasis as well as influencing feedback of the FGF23 endocrine pathway. We have provided compelling evidence that activation of VDR in mature osteoblasts plays an essential role in bone turnover, directly regulating osteoblasts, osteoclasts and possibly osteocyte activities. Importantly, 1,25D/VDR actions within osteoblasts are able to mediate renal 1,25D feedback, indirectly impacting on calcium homeostasis and possibly bone mineralisation. The findings from this thesis have provide further understanding to the activities of vitamin D within the skeleton and challenge the viewpoint that 1,25D is solely an endocrine regulator of bone and mineral metabolism.

BIBLIOGRAPHY

Abzhanov, A., *et al.* (2007) Regulation of skeletogenic differentiation in cranial dermal bone, *Development*, **134**, 3133-3144.

Allen, M.R., Hock, J.M. and Burr, D.B. (2004) Periosteum: biology, regulation, and response to osteoporosis therapies, *Bone*, **35**, 1003-1012.

Ames, S.K., *et al.* (1999) Vitamin D receptor gene Fok1 polymorphism predicts calcium absorption and bone mineral density in children, *J Bone Miner Res*, **14**, 740-746.

Amling, M., *et al.* (1999) Rescue of the skeletal phenotype of vitamin D receptor-ablated mice in the setting of normal mineral ion homeostasis: formal histomorphometric and biomechanical analyses, *Endocrinology*, **140**, 4982-4987.

Anderson, P.H. and Atkins, G.J. (2008) The skeleton as an intracrine organ for vitamin D metabolism, *Mol Aspects Med*, **29**, 397-406.

Anderson, P.H., *et al.* (2007) RNAi-mediated silencing of CYP27B1 abolishes 1,25(OH)2D3 synthesis and reduces osteocalcin and CYP24 mRNA expression in human osteosarcoma (HOS) cells, *J Steroid Biochem Mol Biol*, **103**, 601-605.

Anderson, P.H., *et al.* (2010) Bone CYP27B1 gene expression is increased with high dietary calcium and in mineralising osteoblasts, *J Steroid Biochem Mol Biol*, **121**, 71-75.

Anderson, P.H., *et al.* (2005) Modulation of CYP27B1 and CYP24 mRNA expression in bone is independent of circulating 1,25(OH)2D3 levels, *Bone*, **36**, 654-662.

Anderson, P.H., *et al.* (2007) 25-Hydroxyvitamin D requirement for maintaining skeletal health utilising a Sprague-Dawley rat model, *J Steroid Biochem Mol Biol*, **103**, 592-595.

Anderson, P.H., *et al.* (2008) Vitamin D depletion induces RANKL-mediated osteoclastogenesis and bone loss in a rodent model, *J Bone Miner Res*, **23**, 1789-1797.

Andersson, G. and Johansson, E.K. (1996) Adhesion of human myelomonocytic (HL-60) cells induced by 1,25-dihydroxyvitamin D3 and phorbol myristate acetate is dependent on osteopontin synthesis and the alpha v beta 3 integrin, *Connect Tissue Res*, **35**, 163-171.

Arai, F., *et al.* (2009) Niche regulation of hematopoietic stem cells in the endosteum, *Ann N Y Acad Sci*, **1176**, 36-46.

Arai, H., *et al.* (1997) A vitamin D receptor gene polymorphism in the translation initiation codon: effect on protein activity and relation to bone mineral density in Japanese women, *J Bone Miner Res*, **12**, 915-921.

Arai, H., *et al.* (2001) The polymorphism in the caudal-related homeodomain protein Cdx-2 binding element in the human vitamin D receptor gene, *J Bone Miner Res*, **16**, 1256-1264.

Arnala, I., *et al.* (1997) Analysis of 245 consecutive hip fracture patients with special reference to bone metabolism, *Ann Chir Gynaecol*, **86**, 343-347.

Aronow, M.A., *et al.* (1990) Factors that promote progressive development of the osteoblast phenotype in cultured fetal rat calvaria cells, *J Cell Physiol*, **143**, 213-221.

Asagiri, M. and Takayanagi, H. (2007) The molecular understanding of osteoclast differentiation, *Bone*, **40**, 251-264.

Atkins, G.J., *et al.* (2007) Metabolism of vitamin D3 in human osteoblasts: evidence for autocrine and paracrine activities of 1 alpha,25-dihydroxyvitamin D3, *Bone*, **40**, 1517-1528.

Atkins, G.J., *et al.* (2003) RANKL expression is related to the differentiation state of human osteoblasts, *J Bone Miner Res*, **18**, 1088-1098.

Aubin, J.E. (1998) Bone stem cells, *J Cell Biochem Suppl*, **30-31**, 73-82.

Bai, X.Y., *et al.* (2003) The autosomal dominant hypophosphatemic rickets R176Q mutation in fibroblast growth factor 23 resists proteolytic cleavage and enhances in vivo biological potency, *J Biol Chem*, **278**, 9843-9849.

Bailey, D.A., *et al.* (2000) Calcium accretion in girls and boys during puberty: a longitudinal analysis, *J Bone Miner Res*, **15**, 2245-2250.

Baker, A.R., *et al.* (1988) Cloning and expression of full-length cDNA encoding human vitamin D receptor, *Proc Natl Acad Sci U S A*, **85**, 3294-3298.

Bakker, A.D., *et al.* (2002) [The response of bone cells to shear stress], *Ned Tijdschr Tandheelkd*, **109**, 383-386.

Bakker. A., et al. (2003) Osteoblast isolation from murine calvariae and long bones. *Methods Mol Med*, **80**, 19–28

Baldock, P.A., *et al.* (2006) Vitamin D action and regulation of bone remodeling: suppression of osteoclastogenesis by the mature osteoblast, *J Bone Miner Res*, **21**, 1618-1626.

Balemans, W., *et al.* (2002) Identification of a 52 kb deletion downstream of the SOST gene in patients with van Buchem disease, *J Med Genet*, **39**, 91-97.

Barone, L.M., *et al.* (1991) Developmental expression and hormonal regulation of the rat matrix Gla protein (MGP) gene in chondrogenesis and osteogenesis, *J Cell Biochem*, **46**, 351-365.

Barragan-Adjemian, C., *et al.* (2006) Mechanism by which MLO-A5 late osteoblasts/early osteocytes mineralize in culture: similarities with mineralization of lamellar bone, *Calcif Tissue Int*, **79**, 340-353.

Baudino, T.A., *et al.* (1998) Isolation and characterization of a novel coactivator protein, NCoA-62, involved in vitamin D-mediated transcription, *J Biol Chem*, **273**, 16434-16441.

Bell, K.L., *et al.* (1999) Intracapsular hip fracture: increased cortical remodeling in the thinned and porous anterior region of the femoral neck, *Osteoporos Int*, **10**, 248-257.

Bellido, T. (2006) Downregulation of SOST/sclerostin by PTH: a novel mechanism of hormonal control of bone formation mediated by osteocytes, *J Musculoskelet Neuronal Interact*, **6**, 358-359.

Ben-Dov, I.Z., *et al.* (2007) The parathyroid is a target organ for FGF23 in rats, *J Clin Invest*, **117**, 4003-4008.

Benet-Pages, A., *et al.* (2005) An FGF23 missense mutation causes familial tumoral calcinosis with hyperphosphatemia, *Hum Mol Genet*, **14**, 385-390.

Beresford, J.N., Gallagher, J.A. and Russell, R.G. (1986) 1,25-Dihydroxyvitamin D3 and human bone-derived cells in vitro: effects on alkaline phosphatase, type I collagen and proliferation, *Endocrinology*, **119**, 1776-1785.

Bergwitz, C. and Juppner, H. (2010) Regulation of phosphate homeostasis by PTH, vitamin D, and FGF23, *Annu Rev Med*, **61**, 91-104.

Bikle, D.D. (2004) Vitamin D regulated keratinocyte differentiation, *J Cell Biochem*, **92**, 436-444.

Bilic-Curcic, I., *et al.* (2005) Visualizing levels of osteoblast differentiation by a two-color promoter-GFP strategy: Type I collagen-GFPcyan and osteocalcin-GFPtpz, *Genesis*, **43**, 87-98.

Bischoff-Ferrari, H.A. (2008) Optimal serum 25-hydroxyvitamin D levels for multiple health outcomes, *Adv Exp Med Biol*, **624**, 55-71.

Bischoff-Ferrari, H.A., *et al.* (2005) Fracture prevention with vitamin D supplementation: a meta-analysis of randomized controlled trials, *JAMA*, **293**, 2257-2264.

Boivin, G., *et al.* (1987) Ultrastructural immunocytochemical localization of endogenous 1,25-dihydroxyvitamin D3 and its receptors in osteoblasts and osteocytes from neonatal mouse and rat calvaria, *Bone Miner*, **3**, 125-136.

Bonewald, L.F. (2006) Mechanosensation and Transduction in Osteocytes, *Bonekey Osteovision*, **3**, 7-15.

Bonewald, L.F. (2011) The amazing osteocyte, *J Bone Miner Res*, **26**, 229-238.

Borou, O., et al. (2002) High-resolution three-dimensional micro-computed tomography detects bone loss and changes in trabecular architecture early: comparison with DEXA and bone histomorphometry in a rat model of disuse osteoporosis, *Invest Radiol*, **37**, 40-6.

Boskey, A.L., Wians, F.H., Jr. and Hauschka, P.V. (1985) The effect of osteocalcin on in vitro lipid-induced hydroxyapatite formation and seeded hydroxyapatite growth, *Calcif Tissue Int*, **37**, 57-62.

Bouillon, R., *et al.* (2008) Vitamin D and human health: lessons from vitamin D receptor null mice, *Endocr Rev*, **29**, 726-776.

Bouillon, R., *et al.* (2005) Mechanisms for the selective action of Vitamin D analogs, *J Steroid Biochem Mol Biol*, **97**, 21-30.

Boyle, I.T., *et al.* (1972) The response of intestinal calcium transport to 25-hydroxy and 1,25-dihydroxy vitamin D in nephrectomized rats, *Endocrinology*, **90**, 605-608.

Boyle, W.J., Simonet, W.S. and Lacey, D.L. (2003) Osteoclast differentiation and activation, *Nature*, **423**, 337-342.

Brenza, H.L. and DeLuca, H.F. (2000) Regulation of 25-hydroxyvitamin D3 1alpha-hydroxylase gene expression by parathyroid hormone and 1,25-dihydroxyvitamin D3, *Arch Biochem Biophys*, **381**, 143-152.

Brenza, H.L., *et al.* (1998) Parathyroid hormone activation of the 25-hydroxyvitamin D3-1alpha-hydroxylase gene promoter, *Proc Natl Acad Sci U S A*, **95**, 1387-1391.

Bronner, F. (1976) Vitamin D deficiency and rickets, *Am J Clin Nutr*, **29**, 1307-1314.

Bronner, F. (1987) Intestinal calcium absorption: mechanisms and applications, *J Nutr*, **117**, 1347-1352.

Brown, A.J., *et al.* (1996) Rat calcium-sensing receptor is regulated by vitamin D but not by calcium, *Am J Physiol*, **270**, F454-460.

Brumbaugh, P.F. and Haussler, M.R. (1973) 1Alpha,25-dihydroxyvitamin D3 receptor: competitive binding of vitamin D analogs, *Life Sci*, **13**, 1737-1746.

Buckwalter, J.A., *et al.* (1996) Bone biology. I: Structure, blood supply, cells, matrix, and mineralization, *Instr Course Lect*, **45**, 371-386.

Burr, D.B., Robling, A.G. and Turner, C.H. (2002) Effects of biomechanical stress on bones in animals, *Bone*, **30**, 781-786.

Canaff, L. and Hendy, G.N. (2002) Human calcium-sensing receptor gene. Vitamin D response elements in promoters P1 and P2 confer transcriptional responsiveness to 1,25-dihydroxyvitamin D, *J Biol Chem*, **277**, 30337-30350.

Canalis, E. (2009) Growth factor control of bone mass, *J Cell Biochem*, **108**, 769-777.

Castillo, A.I., *et al.* (1999) Synergistic activation of the prolactin promoter by vitamin D receptor and GHF-1: role of the coactivators, CREB-binding protein and steroid hormone receptor coactivator-1 (SRC-1), *Mol Endocrinol*, **13**, 1141-1154.

Chapuy, M.C., *et al.* (1992) Vitamin D3 and calcium to prevent hip fractures in the elderly women, *N Engl J Med*, **327**, 1637-1642.

Christakos, S., *et al.* (2010) Vitamin D: metabolism, *Endocrinol Metab Clin North Am*, **39**, 243-253, table of contents.

Christakos, S., *et al.* (2006) New insights into the mechanisms involved in the pleiotropic actions of 1,25dihydroxyvitamin D3, *Ann N Y Acad Sci*, **1068**, 194-203.

Christakos, S., *et al.* (1992) Molecular aspects of the calbindins, *J Nutr*, **122**, 678-682.

Cooper, G.S. and Umbach, D.M. (1996) Are vitamin D receptor polymorphisms associated with bone mineral density? A meta-analysis, *J Bone Miner Res*, **11**, 1841-1849.

Cowin, S.C. (1990) Deviatoric and hydrostatic mode interaction in hard and soft tissue, *J Biomech*, **23**, 11-14.

Currey, J.D. (2003) The many adaptations of bone, *J Biomech*, **36**, 1487-1495.

Dallas, S.L. and Bonewald, L.F. (2010) Dynamics of the transition from osteoblast to osteocyte, *Ann N Y Acad Sci*, **1192**, 437-443.

Dardenne, O., *et al.* (2001) Targeted inactivation of the 25-hydroxyvitamin D(3)-1(alpha)-hydroxylase gene (CYP27B1) creates an animal model of pseudovitamin D-deficiency rickets, *Endocrinology*, **142**, 3135-3141.

Dardenne, O., *et al.* (2004) Rescue of the phenotype of CYP27B1 (1alpha-hydroxylase)-deficient mice, *J Steroid Biochem Mol Biol*, **89-90**, 327-330.

Darwish, H.M. and DeLuca, H.F. (1996) Analysis of binding of the 1,25-dihydroxyvitamin D3 receptor to positive and negative vitamin D response elements, *Arch Biochem Biophys*, **334**, 223-234.

Dawson-Hughes, B. and Bischoff-Ferrari, H.A. (2007) Therapy of osteoporosis with calcium and vitamin D, *J Bone Miner Res*, **22 Suppl 2**, V59-63.

Demay, M.B. (2006) Mechanism of vitamin D receptor action, *Ann N Y Acad Sci*, **1068**, 204-213.

Dhawan, P., *et al.* (2005) Functional cooperation between CCAAT/enhancer-binding proteins and the vitamin D receptor in regulation of 25-hydroxyvitamin D3 24-hydroxylase, *Mol Cell Biol*, **25**, 472-487.

Doty, S.B. (1981) Morphological evidence of gap junctions between bone cells, *Calcif Tissue Int*, **33**, 509-512.

Downey, P.A. and Siegel, M.I. (2006) Bone biology and the clinical implications for osteoporosis, *Phys Ther*, **86**, 77-91.

Drake, F.H., *et al.* (1996) Cathepsin K, but not cathepsins B, L, or S, is abundantly expressed in human osteoclasts, *J Biol Chem*, **271**, 12511-12516.

Ducy, P., *et al.* (1997) Osf2/Cbfa1: a transcriptional activator of osteoblast differentiation, *Cell*, **89**, 747-754.

Dwek, J.R. (2010) The periosteum: what is it, where is it, and what mimics it in its absence?, *Skeletal Radiol*, **39**, 319-323.

Eisman, J.A. (1999) Genetics of osteoporosis, *Endocr Rev*, **20**, 788-804.

Erben, R.G., *et al.* (2002) Deletion of deoxyribonucleic acid binding domain of the vitamin D receptor abrogates genomic and nongenomic functions of vitamin D, *Mol Endocrinol*, **16**, 1524-1537.

Epker, B. N. et al. (1965) A histological study of remodeling at the periosteal. Haversian canal, cortical endosteal, and trabecularendosteal surfaces in human rib. *Anat Rec* **152**:129–136.

Fang, Y., *et al.* (2006) Vitamin D receptor gene BsmI and TaqI polymorphisms and fracture risk: a meta-analysis, *Bone*, **39**, 938-945.

Fang, Y., *et al.* (2003) Cdx-2 polymorphism in the promoter region of the human vitamin D receptor gene determines susceptibility to fracture in the elderly, *J Bone Miner Res*, **18**, 1632-1641.

Fang, Y., *et al.* (2005) Promoter and 3'-untranslated-region haplotypes in the vitamin d receptor gene predispose to osteoporotic fracture: the rotterdam study, *Am J Hum Genet*, **77**, 807-823.

Feng, J.Q., *et al.* (2003) The Dentin matrix protein 1 (Dmp1) is specifically expressed in mineralized, but not soft, tissues during development, *J Dent Res*, **82**, 776-780.

Feng, J.Q., *et al.* (2006) Loss of DMP1 causes rickets and osteomalacia and identifies a role for osteocytes in mineral metabolism, *Nat Genet*, **38**, 1310-1315.

Feng, W., *et al.* (1998) Hormone-dependent coactivator binding to a hydrophobic cleft on nuclear receptors, *Science*, **280**, 1747-1749.

Fermor, B. and Skerry, T.M. (1995) PTH/PTHrP receptor expression on osteoblasts and osteocytes but not resorbing bone surfaces in growing rats, *J Bone Miner Res*, **10**, 1935-1943.

Ferrari, S., *et al.* (1998) Vitamin D receptor gene start codon polymorphisms (FokI) and bone mineral density: interaction with age, dietary calcium, and 3'-end region polymorphisms, *J Bone Miner Res*, **13**, 925-930.

Fleet, J.C., *et al.* (1995) The BsmI vitamin D receptor restriction fragment length polymorphism (BB) predicts low bone density in premenopausal black and white women, *J Bone Miner Res*, **10**, 985-990.

Franz-Odendaal, T.A., Hall, B.K. and Witten, P.E. (2006) Buried alive: how osteoblasts become osteocytes, *Dev Dyn*, **235**, 176-190.

Fraser, D., *et al.* (1973) Pathogenesis of hereditary vitamin-D-dependent rickets. An inborn error of vitamin D metabolism involving defective conversion of 25-hydroxyvitamin D to 1 alpha,25-dihydroxyvitamin D, *N Engl J Med*, **289**, 817-822.

Freedman, L.P. (1992) Anatomy of the steroid receptor zinc finger region, *Endocr Rev*, **13**, 129-145.

Freedman, L.P. and Towers, T.L. (1991) DNA binding properties of the vitamin D3 receptor zinc finger region, *Mol Endocrinol*, **5**, 1815-1826.

Friedman, P.A. and Gesek, F.A. (1993) Vitamin D3 accelerates PTH-dependent calcium transport in distal convoluted tubule cells, *Am J Physiol*, **265**, F300-308.

Gallagher, J.C. (1990) The pathogenesis of osteoporosis, *Bone Miner*, **9**, 215-227.

Gardiner, E.M., *et al.* (2000) Increased formation and decreased resorption of bone in mice with elevated vitamin D receptor in mature cells of the osteoblastic lineage, *FASEB J*, **14**, 1908-1916.

Garnero, P., *et al.* (1995) Vitamin D receptor gene polymorphisms do not predict bone turnover and bone mass in healthy premenopausal women, *J Bone Miner Res*, **10**, 1283-1288.

Gill, R.K., *et al.* (1998) Mapping the domains of the interaction of the vitamin D receptor and steroid receptor coactivator-1, *Mol Endocrinol*, **12**, 57-65.

Glass, C.K. and Rosenfeld, M.G. (2000) The coregulator exchange in transcriptional functions of nuclear receptors, *Genes Dev*, **14**, 121-141.

Gluhak-Heinrich, J., *et al.* (2003) Mechanical loading stimulates dentin matrix protein 1 (DMP1) expression in osteocytes in vivo, *J Bone Miner Res*, **18**, 807-817.

Gomez Alonso, C., *et al.* (1998) Vitamin D receptor gene (VDR) polymorphisms: effect on bone mass, bone loss and parathyroid hormone regulation, *Nephrol Dial Transplant*, **13 Suppl 3**, 73-77.

Gong, J.K. (1978) Endosteal marrow: a rich source of hematopoietic stem cells, *Science*, **199**, 1443-1445.

Gowen, L.C., *et al.* (2003) Targeted disruption of the osteoblast/osteocyte factor 45 gene (OF45) results in increased bone formation and bone mass, *J Biol Chem*, **278**, 1998-2007.

Gross, C., *et al.* (1998) The vitamin D receptor gene start codon polymorphism: a functional analysis of FokI variants, *J Bone Miner Res*, **13**, 1691-1699.

Guo, X.D. and Cowin, S.C. (1992) Periosteal and endosteal control of bone remodeling under torsional loading, *J Biomech*, **25**, 645-650.

Haddad, J.G. (1995) Plasma vitamin D-binding protein (Gc-globulin): multiple tasks, *J Steroid Biochem Mol Biol*, **53**, 579-582.

Halleen, J.M., *et al.* (1999) Intracellular fragmentation of bone resorption products by reactive oxygen species generated by osteoclastic tartrate-resistant acid phosphatase, *J Biol Chem*, **274**, 22907-22910.

Harada, S. and Rodan, G.A. (2003) Control of osteoblast function and regulation of bone mass, *Nature*, **423**, 349-355.

Harris, S.S., *et al.* (1997) The vitamin D receptor start codon polymorphism (FokI) and bone mineral density in premenopausal American black and white women, *J Bone Miner Res*, **12**, 1043-1048.

Haussler, M.R., *et al.* (2008) Vitamin D receptor: molecular signaling and actions of nutritional ligands in disease prevention, *Nutr Rev*, **66**, S98-112.

Haussler, M.R., *et al.* (1998) The nuclear vitamin D receptor: biological and molecular regulatory properties revealed, *J Bone Miner Res*, **13**, 325-349.

He, G., *et al.* (2003) Dentin matrix protein 1 initiates hydroxyapatite formation in vitro, *Connect Tissue Res*, **44 Suppl 1**, 240-245.

Heaney, R.P., Saville, P.D. and Recker, R.R. (1975) Calcium absorption as a function of calcium intake, *J Lab Clin Med*, **85**, 881-890.

Heery, D.M., *et al.* (1997) A signature motif in transcriptional co-activators mediates binding to nuclear receptors, *Nature*, **387**, 733-736.

Heino, T.J., Hentunen, T.A. and Vaananen, H.K. (2002) Osteocytes inhibit osteoclastic bone resorption through transforming growth factor-beta: enhancement by estrogen, *J Cell Biochem*, **85**, 185-197.

Helfrich, M.H., *et al.* (1996) Beta 1 integrins and osteoclast function: involvement in collagen recognition and bone resorption, *Bone*, **19**, 317-328.

Henriksen, K., *et al.* (2009) Local communication on and within bone controls bone remodeling, *Bone*, **44**, 1026-1033.

Hoenderop, J.G., *et al.* (2001) Calcitriol controls the epithelial calcium channel in kidney, *J Am Soc Nephrol*, **12**, 1342-1349.

Hofbauer, L.C., Kuhne, C.A. and Viereck, V. (2004) The OPG/RANKL/RANK system in metabolic bone diseases, *J Musculoskelet Neuronal Interact*, **4**, 268-275.

Holick, M.F., *et al.* (2007) Vitamin D and skin physiology: a D-lightful story, *J Bone Miner Res*, **22 Suppl 2**, V28-33.

Holick, M.F., Garabedian, M. and DeLuca, H.F. (1972) 1,25-dihydroxycholecalciferol: metabolite of vitamin D3 active on bone in anephric rats, *Science*, **176**, 1146-1147.

Holick, M.F., *et al.* (1973) 1,24,25-Trihydroxyvitamin D3. A metabolite of vitamin D3 effective on intestine, *J Biol Chem*, **248**, 6691-6696.

Holick, M.F., *et al.* (1972) Isolation and identification of 24,25-dihydroxycholecalciferol, a metabolite of vitamin D made in the kidney, *Biochemistry*, **11**, 4251-4255.

Holmbeck, K., *et al.* (2005) The metalloproteinase MT1-MMP is required for normal development and maintenance of osteocyte processes in bone, *J Cell Sci*, **118**, 147-156.

Holtrop, M.E. (1975) The ultrastructure of bone, *Ann Clin Lab Sci*, **5**, 264-271.

Horiuchi, K., *et al.* (1999) Identification and characterization of a novel protein, periostin, with restricted expression to periosteum and periodontal ligament and increased expression by transforming growth factor beta, *J Bone Miner Res*, **14**, 1239-1249.

Horwood, N.J., *et al.* (1998) Osteotropic agents regulate the expression of osteoclast differentiation factor and osteoprotegerin in osteoblastic stromal cells, *Endocrinology*, **139**, 4743-4746.

Howard, G.A., *et al.* (1981) Human bone cells in culture metabolize 25-hydroxyvitamin D3 to 1,25-dihydroxyvitamin D3 and 24,25-dihydroxyvitamin D3, *J Biol Chem*, **256**, 7738-7740.

Hsieh, J.C., *et al.* (1998) Novel nuclear localization signal between the two DNA-binding zinc fingers in the human vitamin D receptor, *J Cell Biochem*, **70**, 94-109.

Hughes, M.R., *et al.* (1988) Point mutations in the human vitamin D receptor gene associated with hypocalcemic rickets, *Science*, **242**, 1702-1705.

Ingles, S.A., *et al.* (1997) Strength of linkage disequilibrium between two vitamin D receptor markers in five ethnic groups: implications for association studies, *Cancer Epidemiol Biomarkers Prev*, **6**, 93-98.

Inoue, Y., *et al.* (2005) Role of the vitamin D receptor in FGF23 action on phosphate metabolism, *Biochem J*, **390**, 325-331.

Javaid, K., et al. (2006) Maternal vitamin D status during pregnancy and childhood bone mass at age 9 years: a longitudinal study, *Lancet*, **367**, 36–43.

Jekir, M.G. and Donahue, H.J. (2009) Gap junctions and osteoblast-like cell gene expression in response to fluid flow, *J Biomech Eng*, **131**, 011005.

Jensen, E.D., Gopalakrishnan, R. and Westendorf, J.J. (2010) Regulation of gene expression in osteoblasts, *Biofactors*, **36**, 25-32.

Jenster, G., *et al.* (1997) Steroid receptor induction of gene transcription: a two-step model, *Proc Natl Acad Sci U S A*, **94**, 7879-7884.

Jilka, R.L., *et al.* (1998) Osteoblast programmed cell death (apoptosis): modulation by growth factors and cytokines, *J Bone Miner Res*, **13**, 793-802.

Jones, G., Strugnell, S.A. and DeLuca, H.F. (1998) Current understanding of the molecular actions of vitamin D, *Physiol Rev*, **78**, 1193-1231.

Jones, G., *et al.* (1987) Side-chain hydroxylation of vitamin D3 and its physiological implications, *Steroids*, **49**, 29-53.

Jurutka, P.W., *et al.* (1996) Human vitamin D receptor phosphorylation by casein kinase II at Ser-208 potentiates transcriptional activation, *Proc Natl Acad Sci U S A*, **93**, 3519-3524.

Jurutka, P.W., *et al.* (2000) Biochemical evidence for a 170-kilodalton, AF-2-dependent vitamin D receptor/retinoid X receptor coactivator that is highly expressed in osteoblasts, *Biochem Biophys Res Commun*, **267**, 813-819.

Jurutka, P.W., *et al.* (2001) Molecular nature of the vitamin D receptor and its role in regulation of gene expression, *Rev Endocr Metab Disord*, **2**, 203-216.

Karsenty, G., Kronenberg, H.M. and Settembre, C. (2009) Genetic control of bone formation, *Annu Rev Cell Dev Biol*, **25**, 629-648.

Kato, S., *et al.* (1998) The importance of 25-hydroxyvitamin D3 1 alpha-hydroxylase gene in vitamin D-dependent rickets, *Curr Opin Nephrol Hypertens*, **7**, 377-383.

Kearns, A.E., Khosla, S. and Kostenuik, P.J. (2008) Receptor activator of nuclear factor kappaB ligand and osteoprotegerin regulation of bone remodeling in health and disease, *Endocr Rev*, **29**, 155-192.

Khosla, S., Moedder, U.I. and Syed, F.A. (2006) Estrogen receptor beta: the antimechanostat?, *Bone*, **38**, 289; author reply 290.

Kido, S., *et al.* (2003) Expression of RANK is dependent upon differentiation into the macrophage/osteoclast lineage: induction by 1alpha,25-dihydroxyvitamin D3 and TPA in a human myelomonocytic cell line, HL60, *Bone*, **32**, 621-629.

Kim, M.S., *et al.* (2007) 1Alpha,25(OH)2D3-induced transrepression by vitamin D receptor through E-box-type elements in the human parathyroid hormone gene promoter, *Mol Endocrinol*, **21**, 334-342.

Kitanaka, S., *et al.* (1998) Inactivating mutations in the 25-hydroxyvitamin D3 1alpha-hydroxylase gene in patients with pseudovitamin D-deficiency rickets, *N Engl J Med*, **338**, 653-661.

Kitazawa, R., Kitazawa, S. and Maeda, S. (1999) Promoter structure of mouse RANKL/TRANCE/OPGL/ODF gene, *Biochim Biophys Acta*, **1445**, 134-141.

Klein-Nulend, J., Nijweide, P.J. and Burger, E.H. (2003) Osteocyte and bone structure, *Curr Osteoporos Rep*, **1**, 5-10.

Kogawa, M., *et al.* (2010) The metabolism of 25-(OH)vitamin D3 by osteoclasts and their precursors regulates the differentiation of osteoclasts, *J Steroid Biochem Mol Biol*, **121**, 277-280.

Kogawa, M., *et al.* (2010) Osteoclastic metabolism of 25(OH)-vitamin D3: a potential mechanism for optimization of bone resorption, *Endocrinology*, **151**, 4613-4625.

Kolek, O.I., *et al.* (2005) 1alpha,25-Dihydroxyvitamin D3 upregulates FGF23 gene expression in bone: the final link in a renal-gastrointestinal-skeletal axis that controls phosphate transport, *Am J Physiol Gastrointest Liver Physiol*, **289**, G1036-1042.

Komori, T., *et al.* (1997) Targeted disruption of Cbfa1 results in a complete lack of bone formation owing to maturational arrest of osteoblasts, *Cell*, **89**, 755-764.

Kong, Y.Y., *et al.* (1999) OPGL is a key regulator of osteoclastogenesis, lymphocyte development and lymph-node organogenesis, *Nature*, **397**, 315-323.

Kostner, K., *et al.* (2009) The relevance of vitamin D receptor (VDR) gene polymorphisms for cancer: a review of the literature, *Anticancer Res*, **29**, 3511-3536.

Krajisnik, T., *et al.* (2007) Fibroblast growth factor-23 regulates parathyroid hormone and 1alpha-hydroxylase expression in cultured bovine parathyroid cells, *J Endocrinol*, **195**, 125-131.

Kuhn, J.L., *et al.* (1990) Evaluation of a microcomputed tomography system to study trabecular bone structure, *J Orthop Res*, **8**, 833-842.

Kumar, R. and Thompson, E.B. (1999) The structure of the nuclear hormone receptors, *Steroids*, **64**, 310-319.

Kusu, N., *et al.* (2003) Sclerostin is a novel secreted osteoclast-derived bone morphogenetic protein antagonist with unique ligand specificity, *J Biol Chem*, **278**, 24113-24117.

Larsson, T., *et al.* (2005) A novel recessive mutation in fibroblast growth factor-23 causes familial tumoral calcinosis, *J Clin Endocrinol Metab*, **90**, 2424-2427.

Lee, M., *et al.* (2010) Discordant effects of vitamin D deficiency in trabecular and cortical bone architecture and strength in growing rodents, *J Steroid Biochem Mol Biol*, **121**, 284-7.

Leong, G.M., *et al.* (2004) Ski-interacting protein, a bifunctional nuclear receptor coregulator that interacts with N-CoR/SMRT and p300, *Biochem Biophys Res Commun*, **315**, 1070-1076.

Li, X., *et al.* (2008) Targeted deletion of the sclerostin gene in mice results in increased bone formation and bone strength, *J Bone Miner Res*, **23**, 860-869.

Li, X., *et al.* (2007) Parathyroid hormone stimulates osteoblastic expression of MCP-1 to recruit and increase the fusion of pre/osteoclasts, *J Biol Chem*, **282**, 33098-33106.

Li, X., *et al.* (2005) Sclerostin binds to LRP5/6 and antagonizes canonical Wnt signaling, *J Biol Chem*, **280**, 19883-19887.

Li, Y.C., *et al.* (1998) Normalization of mineral ion homeostasis by dietary means prevents hyperparathyroidism, rickets, and osteomalacia, but not alopecia in vitamin D receptor-ablated mice, *Endocrinology*, **139**, 4391-4396.

Li, Y.C., *et al.* (1997) Targeted ablation of the vitamin D receptor: an animal model of vitamin D-dependent rickets type II with alopecia, *Proc Natl Acad Sci U S A*, **94**, 9831-9835.

Lian, J.B., *et al.* (1998) Osteocalcin gene promoter: unlocking the secrets for regulation of osteoblast growth and differentiation, *J Cell Biochem Suppl*, **30-31**, 62-72.

Lidor, C., *et al.* (1993) Decrease in bone levels of 1,25-dihydroxyvitamin D in women with subcapital fracture of the femur, *Calcif Tissue Int*, **52**, 146-148.

Lin, C., *et al.* (2009) Sclerostin mediates bone response to mechanical unloading through antagonizing Wnt/beta-catenin signaling, *J Bone Miner Res*, **24**, 1651-1661.

Liu, F., Malaval, L. and Aubin, J.E. (1997) The mature osteoblast phenotype is characterised by extensive plasticity, *Exp Cell Res*, **232**, 97-105.

Liu, S., Gupta, A. and Quarles, L.D. (2007) Emerging role of fibroblast growth factor 23 in a bone-kidney axis regulating systemic phosphate homeostasis and extracellular matrix mineralization, *Curr Opin Nephrol Hypertens*, **16**, 329-335.

Liu, S. and Quarles, L.D. (2007) How fibroblast growth factor 23 works, *J Am Soc Nephrol*, **18**, 1637-1647.

Liu, S., *et al.* (2007) Phosphorylated acidic serine-aspartate-rich MEPE-associated motif peptide from matrix extracellular phosphoglycoprotein inhibits phosphate regulating gene with homologies to endopeptidases on the X-chromosome enzyme activity, *J Endocrinol*, **192**, 261-267.

Liu, S., *et al.* (2006) Fibroblast growth factor 23 is a counter-regulatory phosphaturic hormone for vitamin D, *J Am Soc Nephrol*, **17**, 1305-1315.

Liu, S., *et al.* (2006) Pathogenic role of Fgf23 in Hyp mice, *Am J Physiol Endocrinol Metab*, **291**, E38-49.

Liu, S.M., *et al.* (1996) Characterization of a response element in the 5'-flanking region of the avian (chicken) PTH gene that mediates negative regulation of gene transcription by 1,25-dihydroxyvitamin D3 and binds the vitamin D3 receptor, *Mol Endocrinol*, **10**, 206-215.

Lore, F., *et al.* (1981) Serum levels of 25-hydroxyvitamin D in postmenopausal osteoporosis, *Calcif Tissue Int*, **33**, 467-470.

Lorenz-Depiereux, B., *et al.* (2006) DMP1 mutations in autosomal recessive hypophosphatemia implicate a bone matrix protein in the regulation of phosphate homeostasis, *Nat Genet*, **38**, 1248-1250.

Lozupone, E. (1985) The structure of the trabeculae of cancellous bone. 1. The calcaneus, *Anat Anz*, **159**, 211-229.

Lu, P.W., *et al.* (1994) Bone mineral density of total body, spine, and femoral neck in children and young adults: a cross-sectional and longitudinal study, *J Bone Miner Res*, **9**, 1451-1458.

Lynch, M.P., *et al.* (1995) The influence of type I collagen on the development and maintenance of the osteoblast phenotype in primary and passaged rat calvarial osteoblasts: modification of expression of genes supporting cell growth, adhesion, and extracellular matrix mineralization, *Exp Cell Res*, **216**, 35-45.

Ma, Y.L., *et al.* (2001) Catabolic effects of continuous human PTH (1--38) in vivo is associated with sustained stimulation of RANKL and inhibition of osteoprotegerin and gene-associated bone formation, *Endocrinology*, **142**, 4047-4054.

MacDonald, P.N., *et al.* (2001) Vitamin D receptor and nuclear receptor coactivators: crucial interactions in vitamin D-mediated transcription, *Steroids*, **66**, 171-176.

Maciejewska, I., *et al.* (2009) Distinct compartmentalization of dentin matrix protein 1 fragments in mineralized tissues and cells, *Cells Tissues Organs*, **189**, 186-191.

Makin, G., *et al.* (1989) Target cell metabolism of 1,25-dihydroxyvitamin D3 to calcitroic acid. Evidence for a pathway in kidney and bone involving 24-oxidation, *Biochem J*, **262**, 173-180.

Mahon, P., et al. (2009) Low maternal vitamin D status and fetal bone development: cohort study, *J Bone Miner Res*, **25**, 14–19.

Malloy, P.J., Pike, J.W. and Feldman, D. (1999) The vitamin D receptor and the syndrome of hereditary 1,25-dihydroxyvitamin D-resistant rickets, *Endocr Rev*, **20**, 156-188.

Mangelsdorf, D.J. and Evans, R.M. (1995) The RXR heterodimers and orphan receptors, *Cell*, **83**, 841-850.

Mangelsdorf, D.J., *et al.* (1995) The nuclear receptor superfamily: the second decade, *Cell*, **83**, 835-839.

Marino, R. (2011) Growth plate biology: new insights, *Curr Opin Endocrinol Diabetes Obes*, **18**, 9-13.

Martin, T.J., *et al.* (2006) Mechanisms involved in skeletal anabolic therapies, *Ann N Y Acad Sci*, **1068**, 458-470.

Marwan, N., *et al.* (2009) Three-dimensional quantification of structures in trabecular bone using measures of complexity, *Phys Rev E Stat Nonlin Soft Matter Phys*, **79**, 021903.

Masumoto, O., Ohyama, Y. and Okuda, K. (1988) Purification and characterization of vitamin D 25-hydroxylase from rat liver mitochondria, *J Biol Chem*, **263**, 14256-14260.

Matsumoto, T., *et al.* (1991) Stimulation by 1,25-dihydroxyvitamin D3 of in vitro mineralization induced by osteoblast-like MC3T3-E1 cells, *Bone*, **12**, 27-32.

McKenna, N.J. and O'Malley, B.W. (2002) Combinatorial control of gene expression by nuclear receptors and coregulators, *Cell*, **108**, 465-474.

Meller, Y., *et al.* (1985) Parathormone, calcitonin, and vitamin D metabolites during normal fracture healing in geriatric patients, *Clin Orthop Relat Res*, 272-279.

Midura, R.J., *et al.* (2003) Parathyroid hormone rapidly stimulates hyaluronan synthesis by periosteal osteoblasts in the tibial diaphysis of the growing rat, *J Biol Chem*, **278**, 51462-51468.

Mimura, H., *et al.* (1994) 1,25-Dihydroxyvitamin D3 transcriptionally activates the beta 3-integrin subunit gene in avian osteoclast precursors, *Endocrinology*, **134**, 1061-1066.

Misof, B.M., *et al.* (2003) Targeted overexpression of vitamin D receptor in osteoblasts increases calcium concentration without affecting structural properties of bone mineral crystals, *Calcif Tissue Int*, **73**, 251-257.

Mithal, A., *et al.* (2009) Global vitamin D status and determinants of hypovitaminosis D, *Osteoporos Int*, **20**, 1807-1820.

Moester, M.J., *et al.* (2010) Sclerostin: current knowledge and future perspectives, *Calcif Tissue Int*, **87**, 99-107.

Moorehead, W.R. and Biggs, H.G. (1974) 2-Amino-2-methyl-1-propanol as the alkalizing agent in an improved continuous-flow cresolphthalein complexone procedure for calcium in serum, *Clin Chem*, **20**, 1458-1460.

Morris, H.A., *et al.* (1984) Vitamin D and femoral neck fractures in elderly South Australian women, *Med J Aust*, **140**, 519-521.

Müller, R. & Rüegsegger, P. (1997) Micro-tomographic imaging for the nondestructive evaluation of trabecular bone architecture, *Stud. Health Technol. Inform*. **40**, 61-79.

Murayama, A., *et al.* (1999) Positive and negative regulations of the renal 25-hydroxyvitamin D3 1alpha-hydroxylase gene by parathyroid hormone, calcitonin, and 1alpha,25(OH)2D3 in intact animals, *Endocrinology*, **140**, 2224-2231.

Nampei, A., *et al.* (2004) Matrix extracellular phosphoglycoprotein (MEPE) is highly expressed in osteocytes in human bone, *J Bone Miner Metab*, **22**, 176-184.

Naja, P., et al. (2009) Chondrocyte-specific modulation of Cyp27b1 expression supports a role for local synthesis of 1,25-dihydroxyvitamin D3 in growth plate development. *Endocrinology*, **150**, 4024–4032.

Narayanan, K., *et al.* (2003) Dual functional roles of dentin matrix protein 1. Implications in biomineralization and gene transcription by activation of intracellular Ca2+ store, *J Biol Chem*, **278**, 17500-17508.

Narayanan, K., *et al.* (2004) Transcriptional regulation of dentin matrix protein 1 by JunB and p300 during osteoblast differentiation, *J Biol Chem*, **279**, 44294-44302.

Narayanan, K., *et al.* (2001) Differentiation of embryonic mesenchymal cells to odontoblast-like cells by overexpression of dentin matrix protein 1, *Proc Natl Acad Sci U S A*, **98**, 4516-4521.

Need, A.G. (2006) Bone resorption markers in vitamin D insufficiency, *Clin Chim Acta*, **368**, 48-52.

Need, A.G. (2007) Seasonal variation in bone histomorphometry, *J Bone Miner Res*.

Need, A.G., *et al.* (2008) Vitamin D metabolites and calcium absorption in severe vitamin D deficiency, *J Bone Miner Res*, **23**, 1859-1863.

Omdahl, J.L., *et al.* (2001) Overview of regulatory cytochrome P450 enzymes of the vitamin D pathway, *Steroids*, **66**, 381-389.

Ordonez-Moran, P., et al. (2009) Nuclear receptors: genomic and non-genomic effects converge, *Cell Cycle*, **8**, 1675–1680.

Orwoll, E.S. (2003) Toward an expanded understanding of the role of the periosteum in skeletal health, *J Bone Miner Res*, **18**, 949-954.

Ott, S.M. (2005) Sclerostin and Wnt signaling--the pathway to bone strength, *J Clin Endocrinol Metab*, **90**, 6741-6743.

Otto, F., *et al.* (1997) Cbfa1, a candidate gene for cleidocranial dysplasia syndrome, is essential for osteoblast differentiation and bone development, *Cell*, **89**, 765-771.

Owen, T.A., *et al.* (1990) Progressive development of the rat osteoblast phenotype in vitro: reciprocal relationships in expression of genes associated with osteoblast proliferation and differentiation during formation of the bone extracellular matrix, *J Cell Physiol*, **143**, 420-430.

Owen, T.A., *et al.* (1991) Pleiotropic effects of vitamin D on osteoblast gene expression are related to the proliferative and differentiated state of the bone cell phenotype: dependency upon basal levels of gene expression, duration of exposure, and bone matrix competency in normal rat osteoblast cultures, *Endocrinology*, **128**, 1496-1504.

Oyajobi, B., et al. (1999) Isolation and characterization of human clonogenic osteoblast progenitors immunoselected from fetal bone marrow stroma using STRO-1 monoclonal antibody, *J Bone Miner Res*, **14**, 351-61.

Panda, D.K., *et al.* (2004) Inactivation of the 25-hydroxyvitamin D 1alpha-hydroxylase and vitamin D receptor demonstrates independent and interdependent effects of calcium and vitamin D on skeletal and mineral homeostasis, *J Biol Chem*, **279**, 16754-16766.

Panda, D.K., *et al.* (2001) Targeted ablation of the 25-hydroxyvitamin D 1alpha -hydroxylase enzyme: evidence for skeletal, reproductive, and immune dysfunction, *Proc Natl Acad Sci U S A*, **98**, 7498-7503.

Partridge, N.C., *et al.* (1987) Hormonal regulation of the production of collagenase and a collagenase inhibitor activity by rat osteogenic sarcoma cells, *Endocrinology*, **120**, 1956-1962.

Peacock, M., Heyburn, P.J. and Aaron, J. (1979) Plasma 1,25(OH)2 vitamin D concentrations in nutritional osteomalacia, *Lancet*, **2**, 195.

Pederson, L., *et al.* (2008) Regulation of bone formation by osteoclasts involves Wnt/BMP signaling and the chemokine sphingosine-1-phosphate, *Proc Natl Acad Sci U S A*, **105**, 20764-20769.

Peng, J.B., Brown, E.M. and Hediger, M.A. (2003) Epithelial Ca2+ entry channels: transcellular Ca2+ transport and beyond, *J Physiol*, **551**, 729-740.

Pierce, E.A., Dame, M.C. and DeLuca, H.F. (1987) Size and charge of the functional 1,25-dihydroxyvitamin D receptor in porcine intestine, *J Biol Chem*, **262**, 17092-17099.

Poole, K.E., *et al.* (2005) Sclerostin is a delayed secreted product of osteocytes that inhibits bone formation, *FASEB J*, **19**, 1842-1844.

Prosser, D.E. and Jones, G. (2004) Enzymes involved in the activation and inactivation of vitamin D, *Trends Biochem Sci*, **29**, 664-673.

Purpura, K., et al. (2003) Fluorescence activated cell sorting reveals heterogeneous and cell non-autonomous osteoprogenitor differentiation in fetal rat calvaria cell populations, *J Cell Biochem*, **90**, 109-20.

Qin, C., D'Souza, R. and Feng, J.Q. (2007) Dentin matrix protein 1 (DMP1): new and important roles for biomineralization and phosphate homeostasis, *J Dent Res*, **86**, 1134-1141.

Raab-Cullen, D.M., *et al.* (1994) Mechanical loading stimulates rapid changes in periosteal gene expression, *Calcif Tissue Int*, **55**, 473-478.

Rachez, C., *et al.* (2000) The DRIP complex and SRC-1/p160 coactivators share similar nuclear receptor binding determinants but constitute functionally distinct complexes, *Mol Cell Biol*, **20**, 2718-2726.

Rey, C., *et al.* (2009) Bone mineral: update on chemical composition and structure, *Osteoporos Int*, **20**, 1013-1021.

Ribeiro, R.C., Kushner, P.J. and Baxter, J.D. (1995) The nuclear hormone receptor gene superfamily, *Annu Rev Med*, **46**, 443-453.

Rickard, D.J., Kazhdan, I. and Leboy, P.S. (1995) Importance of 1,25-dihydroxyvitamin D3 and the nonadherent cells of marrow for osteoblast differentiation from rat marrow stromal cells, *Bone*, **16**, 671-678.

Rochel, N., et al. (2000) The crystal structure of the nuclear receptor for vitamin D bound to its natural ligand, *Molecular Cell*, **5**, 173–179.

Robling, A.G., *et al.* (2002) Shorter, more frequent mechanical loading sessions enhance bone mass, *Med Sci Sports Exerc*, **34**, 196-202.

Robling, A.G., *et al.* (2008) Mechanical stimulation of bone in vivo reduces osteocyte expression of Sost/sclerostin, *J Biol Chem*, **283**, 5866-5875.

Rochel, N., *et al.* (2007) Crystal structure of the vitamin D nuclear receptor ligand binding domain in complex with a locked side chain analog of calcitriol, *Arch Biochem Biophys*, **460**, 172-176.

Rochel, N. and Moras, D. (2006) Ligand binding domain of vitamin D receptors, *Curr Top Med Chem*, **6**, 1229-1241.

Salo, J., *et al.* (1997) Removal of osteoclast bone resorption products by transcytosis, *Science*, **276**, 270-273.

Samadfam, R., *et al.* (2009) Bone formation regulates circulating concentrations of fibroblast growth factor 23, *Endocrinology*, **150**, 4835-4845.

Santos, A., Bakker, A.D. and Klein-Nulend, J. (2009) The role of osteocytes in bone mechanotransduction, *Osteoporos Int*, **20**, 1027-1031.

Sawakami, K., *et al.* (2006) The Wnt co-receptor LRP5 is essential for skeletal mechanotransduction but not for the anabolic bone response to parathyroid hormone treatment, *J Biol Chem*, **281**, 23698-23711.

Schaffler, M.B. (2003) Role of bone turnover in microdamage, *Osteoporos Int*, **14 Suppl 5**, S73-77; discussion S77-80.

Schmidt, S., *et al.* (1997) The BsmI vitamin D-receptor polymorphism and secondary hyperparathyroidism, *Nephrol Dial Transplant*, **12**, 1771-1772.

Schulze, E., *et al.* (1999) Immunohistochemical investigations on the differentiation marker protein E11 in rat calvaria, calvaria cell culture and the osteoblastic cell line ROS 17/2.8, *Histochem Cell Biol*, **111**, 61-69.

Shi, Y.C., *et al.* (2007) Effects of continuous activation of vitamin D and Wnt response pathways on osteoblast proliferation and differentiation. *Bone*, **41**, 87–96.

Shimada, T., *et al.* (2004) FGF-23 is a potent regulator of vitamin D metabolism and phosphate homeostasis, *J Bone Miner Res*, **19**, 429-435.

Shimada, T., *et al.* (2004) Targeted ablation of Fgf23 demonstrates an essential physiological role of FGF23 in phosphate and vitamin D metabolism, *J Clin Invest*, **113**, 561-568.

Shimada, T., *et al.* (2001) Cloning and characterization of FGF23 as a causative factor of tumor-induced osteomalacia, *Proc Natl Acad Sci U S A*, **98**, 6500-6505.

Shimada, T., *et al.* (2005) Vitamin D receptor-independent FGF23 actions in regulating phosphate and vitamin D metabolism, *Am J Physiol Renal Physiol*, **289**, F1088-1095.

Shinkyo, R., *et al.* (2004) Metabolism of vitamin D by human microsomal CYP2R1, *Biochem Biophys Res Commun*, **324**, 451-457.

Simonet, W.S., *et al.* (1997) Osteoprotegerin: a novel secreted protein involved in the regulation of bone density, *Cell*, **89**, 309-319.

Sims, N.A., *et al.* (1997) Human and murine osteocalcin gene expression: conserved tissue restricted expression and divergent responses to 1,25-dihydroxyvitamin D3 in vivo, *Mol Endocrinol*, **11**, 1695-1708.

Sitara, D., *et al.* (2004) Homozygous ablation of fibroblast growth factor-23 results in hyperphosphatemia and impaired skeletogenesis, and reverses hypophosphatemia in Phex-deficient mice, *Matrix Biol*, **23**, 421-432.

Sitara, D., *et al.* (2006) Genetic ablation of vitamin D activation pathway reverses biochemical and skeletal anomalies in Fgf-23-null animals, *Am J Pathol*, **169**, 2161-2170.

Skerry, T.M., *et al.* (1989) Early strain-related changes in enzyme activity in osteocytes following bone loading in vivo, *J Bone Miner Res*, **4**, 783-788.

Sone, T., Kerner, S. and Pike, J.W. (1991) Vitamin D receptor interaction with specific DNA. Association as a 1,25-dihydroxyvitamin D3-modulated heterodimer, *J Biol Chem*, **266**, 23296-23305.

Song, Y., Kato, S. and Fleet, J.C. (2003) Vitamin D receptor (VDR) knockout mice reveal VDR-independent regulation of intestinal calcium absorption and ECaC2 and calbindin D9k mRNA, *J Nutr*, **133**, 374-380.

Song, Y., *et al.* (2003) Calcium transporter 1 and epithelial calcium channel messenger ribonucleic acid are differentially regulated by 1,25 dihydroxyvitamin D3 in the intestine and kidney of mice, *Endocrinology*, **144**, 3885-3894.

Sooy, K., Kohut, J. and Christakos, S. (2000) The role of calbindin and 1,25dihydroxyvitamin D3 in the kidney, *Curr Opin Nephrol Hypertens*, **9**, 341-347.

Sooy, K., Sabbagh, Y. and Demay, M.B. (2005) Osteoblasts lacking the vitamin D receptor display enhanced osteogenic potential in vitro, *J Cell Biochem*, **94**, 81-87.

St-Arnaud, R. (1999) Targeted inactivation of vitamin D hydroxylases in mice, *Bone*, **25**, 127-129.

St-Arnaud, R., *et al.* (2000) Deficient mineralization of intramembranous bone in vitamin D-24-hydroxylase-ablated mice is due to elevated 1,25-dihydroxyvitamin D and not to the absence of 24,25-dihydroxyvitamin D, *Endocrinology*, **141**, 2658-2666.

Stein, G.S., *et al.* (1996) Transcriptional control of osteoblast growth and differentiation, *Physiol Rev*, **76**, 593-629.

Suda, T., Takahashi, N. and Martin, T.J. (1992) Modulation of osteoclast differentiation, *Endocr Rev*, **13**, 66-80.

Suda, T., *et al.* (1999) Modulation of osteoclast differentiation and function by the new members of the tumor necrosis factor receptor and ligand families, *Endocr Rev*, **20**, 345-357.

Swarthout, J.T., *et al.* (2002) Parathyroid hormone-dependent signaling pathways regulating genes in bone cells, *Gene*, **282**, 1-17.

Szabo, A., *et al.* (1989) 1,25(OH)2 vitamin D3 inhibits parathyroid cell proliferation in experimental uremia, *Kidney Int*, **35**, 1049-1056.

Takayanagi, H. (2007) The role of NFAT in osteoclast formation, *Ann N Y Acad Sci*, **1116**, 227-237.

Takeda, S., *et al.* (1999) Stimulation of osteoclast formation by 1,25-dihydroxyvitamin D requires its binding to vitamin D receptor (VDR) in osteoblastic cells: studies using VDR knockout mice, *Endocrinology*, **140**, 1005-1008.

Tang, B.M., *et al.* (2007) Use of calcium or calcium in combination with vitamin D supplementation to prevent fractures and bone loss in people aged 50 years and older: a meta-analysis, *Lancet*, **370**, 657-666.

Tang, W.J., *et al.* (2010) Autocrine/paracrine action of vitamin D on FGF23 expression in cultured rat osteoblasts, *Calcif Tissue Int*, **86**, 404-410.

Tatsumi, S., *et al.* (2007) Targeted ablation of osteocytes induces osteoporosis with defective mechanotransduction, *Cell Metab*, **5**, 464-475.

Taylor, J.A., *et al.* (1996) Association of prostate cancer with vitamin D receptor gene polymorphism, *Cancer Res*, **56**, 4108-4110.

Teegarden, D., *et al.* (1995) Peak bone mass in young women, *J Bone Miner Res*, **10**, 711-715.

Tezuka, K., *et al.* (1994) Identification of matrix metalloproteinase 9 in rabbit osteoclasts, *J Biol Chem*, **269**, 15006-15009.

Thomas, G.P., *et al.* (2001) Changing RANKL/OPG mRNA expression in differentiating murine primary osteoblasts, *J Endocrinol*, **170**, 451-460.

Thompson, D.L., *et al.* (2002) Ontogeny of Phex/PHEX protein expression in mouse embryo and subcellular localization in osteoblasts, *J Bone Miner Res*, **17**, 311-320.

Thomsen, J., et al. (2005) Stereological measures of trabecular bone structure: comparison of 3D micro computed tomography with 2D histological sections in human proximal tibial bone biopsies, *J Microscopy*, **218**, 171–179.

Ubaidus, S., *et al.* (2009) FGF23 is mainly synthesized by osteocytes in the regularly distributed osteocytic lacunar canalicular system established after physiological bone remodeling, *J Electron Microsc (Tokyo)*, **58**, 381-392.

Uitterlinden, A.G., *et al.* (2004) Genetics and biology of vitamin D receptor polymorphisms, *Gene*, **338**, 143-156.

Uitterlinden, A.G., *et al.* (2004) Vitamin D receptor gene polymorphisms in relation to Vitamin D related disease states, *J Steroid Biochem Mol Biol*, **89-90**, 187-193.

Vaananen, H.K., *et al.* (1990) Evidence for the presence of a proton pump of the vacuolar H(+)-ATPase type in the ruffled borders of osteoclasts, *J Cell Biol*, **111**, 1305-1311.

Vaananen, H.K. and Laitala-Leinonen, T. (2008) Osteoclast lineage and function, *Arch Biochem Biophys*, **473**, 132-138.

Valdivielso, J.M. (2009) The physiology of vitamin D receptor activation, *Contrib Nephrol*, **163**, 206-212.

Van Cromphaut, S.J., *et al.* (2001) Duodenal calcium absorption in vitamin D receptor-knockout mice: functional and molecular aspects, *Proc Natl Acad Sci U S A*, **98**, 13324-13329.

Van den Bos, T., et al. (2008) Differences in matrix composition between calvaria and long bone in mice suggest differences in biomechanical properties and resorption: special emphasis on collagen, *Bone* **43**, 459–468.

van Driel, M., *et al.* (2006) Evidence for auto/paracrine actions of vitamin D in bone: 1alpha-hydroxylase expression and activity in human bone cells, *FASEB J*, **20**, 2417-2419.

van Driel, M., Pols, H.A. and van Leeuwen, J.P. (2004) Osteoblast differentiation and control by vitamin D and vitamin D metabolites, *Curr Pharm Des*, **10**, 2535-2555.

van Leeuwen, J.P., *et al.* (2001) Vitamin D control of osteoblast function and bone extracellular matrix mineralization, *Crit Rev Eukaryot Gene Expr*, **11**, 199-226.

Vanhooke, J.L., *et al.* (2004) Molecular structure of the rat vitamin D receptor ligand binding domain complexed with 2-carbon-substituted vitamin D3 hormone analogues and a LXXLL-containing coactivator peptide, *Biochemistry*, **43**, 4101-4110.

Vatsa, A., et al. (2008) Osteocyte morphology in fi bula and calvaria – is there a role for mechanosensing?, *Bone*, **43**, 452–458.

Villagra, A., *et al.* (2006) Chromatin remodeling and transcriptional activity of the bone-specific osteocalcin gene require CCAAT/enhancer-binding protein beta-dependent recruitment of SWI/SNF activity, *J Biol Chem*, **281**, 22695-22706.

Vincent, C., *et al.* (2009) The generation of osteoclasts from RAW 264.7 precursors in defined, serum-free conditions, *J Bone Miner Metab*, **27**, 114-119.

Wasserman, R.H., *et al.* (1992) Intestinal calcium transport and calcium extrusion processes at the basolateral membrane, *J Nutr*, **122**, 662-671.

Wasserman, R.H. and Fullmer, C.S. (1995) Vitamin D and intestinal calcium transport: facts, speculations and hypotheses, *J Nutr*, **125**, 1971S-1979S.

Weaver, C.M., *et al.* (1995) Differences in calcium metabolism between adolescent and adult females, *Am J Clin Nutr*, **61**, 577-581.

Weinbaum, S., Cowin, S.C. and Zeng, Y. (1994) A model for the excitation of osteocytes by mechanical loading-induced bone fluid shear stresses, *J Biomech*, **27**, 339-360.

Westbroek, I., *et al.* (2000) Differential stimulation of prostaglandin G/H synthase-2 in osteocytes and other osteogenic cells by pulsating fluid flow, *Biochem Biophys Res Commun*, **268**, 414-419.

Wetterwald, A., *et al.* (1996) Characterization and cloning of the E11 antigen, a marker expressed by rat osteoblasts and osteocytes, *Bone*, **18**, 125-132.

Wiktor-Jedrzejczak, W., *et al.* (1990) Total absence of colony-stimulating factor 1 in the macrophage-deficient osteopetrotic (op/op) mouse, *Proc Natl Acad Sci U S A*, **87**, 4828-4832.

Winwood, K., *et al.* (2006) The importance of the elastic and plastic components of strain in tensile and compressive fatigue of human cortical bone in relation to orthopaedic biomechanics, *J Musculoskelet Neuronal Interact*, **6**, 134-141.

Wood, R.J. and Fleet, J.C. (1998) The genetics of osteoporosis: vitamin D receptor polymorphisms, *Annu Rev Nutr*, **18**, 233-258.

Wu, W., Zhang, X. and Zanello, L.P. (2007) 1alpha,25-Dihydroxyvitamin D(3) antiproliferative actions involve vitamin D receptor-mediated activation of MAPK pathways and AP-1/p21(waf1) upregulation in human osteosarcoma, *Cancer Lett*, **254**, 75-86.

Xiao, Z., *et al.* (2006) Cilia-like structures and polycystin-1 in osteoblasts/osteocytes and associated abnormalities in skeletogenesis and Runx2 expression, *J Biol Chem*, **281**, 30884-30895.

Xiao, Z.S., *et al.* (1998) Intrinsic mineralization defect in Hyp mouse osteoblasts, *Am J Physiol*, **275**, E700-708.

Xiao, Z.S. and Quarles, L.D. (2010) Role of the polycytin-primary cilia complex in bone development and mechanosensing, *Ann N Y Acad Sci*, **1192**, 410-421.

Xue, Y. and Fleet, J.C. (2009) Intestinal vitamin D receptor is required for normal calcium and bone metabolism in mice, *Gastroenterology*, **136**, 1317-1327, e1311-1312.

Yang, C.M., *et al.* (2004) Mechanical strain induces collagenase-3 (MMP-13) expression in MC3T3-E1 osteoblastic cells, *J Biol Chem*, **279**, 22158-22165.

Yang, W., *et al.* (2005) Dentin matrix protein 1 gene cis-regulation: use in osteocytes to characterise local responses to mechanical loading in vitro and in vivo, *J Biol Chem*, **280**, 20680-20690.

Yoshizawa, T., *et al.* (1997) Mice lacking the vitamin D receptor exhibit impaired bone formation, uterine hypoplasia and growth retardation after weaning, *Nat Genet*, **16**, 391-396.

Zajac, J.D., *et al.* (1992) Regulation of gene transcription and proliferation by parathyroid hormone is blocked in mutant osteoblastic cells resistant to cyclic AMP, *Mol Cell Endocrinol*, **87**, 69-77.

Zanello, P., et al. (2004) Rapid modulation of osteoblast ion channel responses by 1alpha,25(OH)2-vitamin D3 requires the presence of a functional vitamin D nuclear receptor, *PNAS*, **101**, 1589–1594.

Zhang, K., *et al.* (2006) E11/gp38 selective expression in osteocytes: regulation by mechanical strain and role in dendrite elongation, *Mol Cell Biol*, **26**, 4539-4552.

Zhao, C., *et al.* (2006) Bidirectional ephrinB2-EphB4 signaling controls bone homeostasis, *Cell Metab*, **4**, 111-121.

Zhao, Q., *et al.* (2007) Osteoclast differentiation and gene regulation, *Front Biosci*, **12**, 2519-2529.

Zhao, Q., *et al.* (2010) NFATc1: functions in osteoclasts, *Int J Biochem Cell Biol*, **42**, 576-579.